UNIVERSITY OF CALIFORNIA
RIVERSIDE

Development of a Sorption Enhanced Steam Hydrogasification Process for In-situ Carbon Dioxide (CO_2) Removal and Enhanced Synthetic Fuel Production

A Dissertation submitted in partial satisfaction
of the requirements for the degree of

Doctor of Philosophy

in

Chemical and Environmental Engineering

by

Zhongzhe Liu

March 2014

Dissertation Committee:
Dr. Joseph M. Norbeck, Chairperson
Dr. David R. Cocker III
Dr. Akua Asa-Awuku

The Dissertation of Zhongzhe Liu is approved:

Committee Chairperson

University of California, Riverside

ACKNOWLEDGMENTS

I would like to express my deepest gratitude to my advisor, Professor Joseph M. Norbeck, who selected me as his student and introduced me to a brand new research field. He always conveys spirits of optimism and innovation to my daily life and research. He always shares his experience and installs confidence to help my future career development. I learned how to express my feeling including disagreement in a flower way from him. I found some essential characters to be a leader. I would like to thank him for his continued support and concern on my research and dissertation.

I would like to express my sincerest thanks to Dr. Chan Seung Park, my co-advisor, who is always giving me a hand. He is knowledgeable and modest. I learned many things from him, such as the essential software for a chemical research engineer. Without his contribution, I would not have completed my PhD.

I show my thanks to Junior Castillo. He trains me from a desk engineer to be a real engineer who can use various tools to build reactors to realize new concepts. Also, I need to thank all my colleagues and friends in the research group for their suggestions and assistance to my research work. They are Dr. Neal Richter, Dr. Arun Raju, Yoothana Thanmongkhon, Amornrat Suemanotham, Yang Li, Minyoung Yun, Noam Hart, Sean Franco, Dr. Xiaoming Lu, Dr. Qian Luo, Dr. Xin Fan and Dr. Wei He. Especially, I express my gratitude to Dr. Dalhee Bae and Dr. Suhyun Kim who shared their practical research experience with me on the fluidized bed design and SNG production. In addition, I thank my good friend, Dr. Jizhi Zhou, who helped me a lot on the characterization of my samples.

Also, I would like to thank my reading and advance to candidacy committee members, Professor David Cocker, Professor Akua Asa-Awuku, Professor Sharon Walker and Professor Pingyun Feng. I am grateful to the Center for Environmental Research and Technology to provide me such a good platform to carry out my work.

Last but not least, I owe my love to my dad, mom and my wife. They are always supporting me on the way of realizing my dreams. I know I need to work harder to reward the love they are giving me. This dissertation is also dedicated to my son, Ethan. I hope he can grow healthily and have a great future.

Riverside, California, USA

December, 2013

Zhongzhe Liu

ABSTRACT OF THE DISSERTATION

Development of a Sorption Enhanced Steam Hydrogasification Process
for In-situ Carbon Dioxide (CO_2) Removal and Enhanced Synthetic Fuel Production

by

Zhongzhe Liu

Doctor of Philosophy, Graduate Program in Chemical and Environmental Engineering
University of California, Riverside, March 2014
Dr. Joseph M. Norbeck, Chairperson

Energy security and climate change are two common challenges in the coming decades. The demand for energy is increasing. The CO_2 in the atmosphere has increased to almost 400ppm, and it is mainly from energy usage. How to deal with energy-related CO_2 emissions with the increasing demand for energy is becoming more crucial.

Carbon capture and sequestration during energy production is an efficient way to guarantee enough energy supply with a smaller carbon footprint. One unique technique is using in-situ CO_2 capture technology, which uses a sorbent to capture CO_2 directly in the reactor. CO_2 is removed quickly as it forms by the sorbent, which can change the equilibrium to promote more energetic production. This technology has great potential to lower CO_2 emissions and get higher energy production simultaneously.

A new concept of sorption enhanced steam hydrogasification reaction (SE-SHR) is the topic of this thesis. It combines sorption enhanced principles with the steam hydrogasification reaction (SHR). It was found that the addition of sorbent enhanced the CO_2 removal and increased the production of H_2 and CH_4. Particularly, the amount of H_2

was increased dramatically. It was found that the increase in H_2 was enough to recycle when the CaO/C molar ratio was over 0.29. The sorption enhanced performance was also evaluated by varying other parameters including H_2/C and Steam/C molar ratio, gasification temperature and sorbent particle size.

A study of the kinetics of the system showed that higher gasification temperature favored faster formation rates of CO_2, CO and CH_4 during both SHR and SE-SHR. The formation rates of CO_2 and CO at 650°C, 700°C and 750°C were much lower during SE-SHR.

Several configurations based on SE-SHR for the production of Fischer Tropsch fuel and synthetic natural gas were developed and evaluated. The optimum gasification condition (H_2/C-Steam/C) for Fischer Tropsch fuel production using SE-SHR based process was found to be 1.59-2.78. This process had lower total CO_2 emissions with higher fuel yield compared to the optimum SHR based process. SE-SHR-Methanation based process for SNG production with the optimum gasification condition (H_2/C-Steam/C) of 1.08-2.22 had the highest CH_4% and near zero CO_2% in the final gas product.

Table of Contents

List of Figures

List of Tables

1. Introduction

1.1 Energy-related CO_2 emissions issue

Almost all countries will face the common challenges of energy security and climate change in the coming decades. The demand for energy is increasing with population growth and industrial development. The International Energy Outlook predicts that world energy consumption will increase by 49 percent, or 1.4 percent per year, from 495 quadrillion Btu in 2007 to 739 quadrillion Btu in 2035. This is shown in Fig.1.1[1]. The concentration of carbon dioxide in the atmosphere has increased from 280ppm to almost 400ppm since the beginning of the industrial revolution. This is mainly attributed to the use of fossil fuels[2].

Fig.1.1 World marketed energy consumption, 1990-2035 (quadrillion Btu)[1]

Energy-related CO_2 emissions accounted for 80% the total U.S. greenhouse gas amount in 2009[3]. This is shown in Fig.1.2. Petroleum is the largest fossil fuel source

for energy-related CO_2 emissions, contributing 43% of the total as shown in Fig.1.3. Coal produces higher CO_2 per unit of energy produced compared to petroleum and natural gas (i.e. coal has a higher carbon intensity). Coal becomes the second-largest fossil fuel contributor, though it has least contribution to the energy consumption in the United States[3].

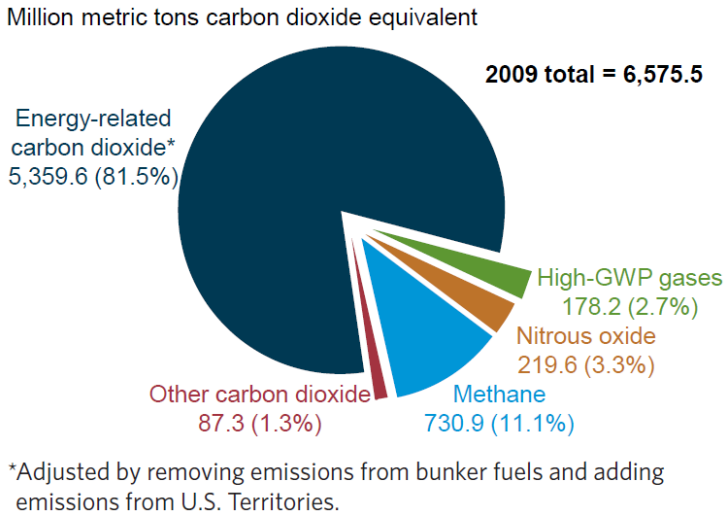

Fig.1.2 U.S. greenhouse gas emissions by gas, 2009[3]

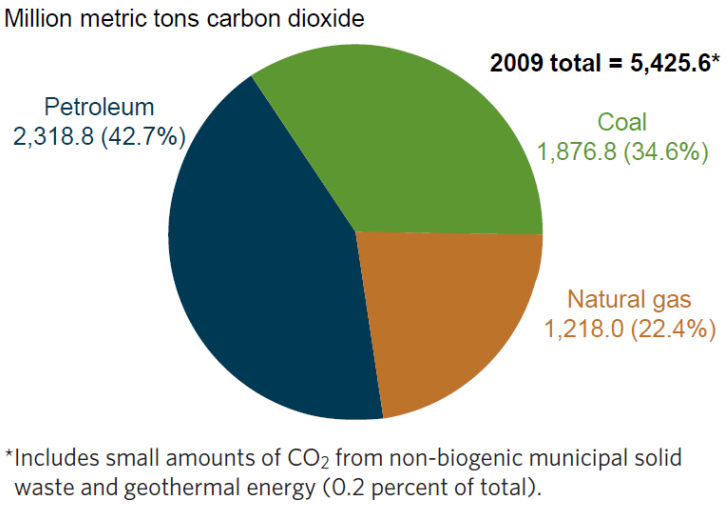

Fig.1.3 U.S. energy-related carbon dioxide emissions by major fuel, 2009[3]

Governments and research organizations should seriously respond to this synergetic issue which will shape the future of energy in the long term. How to deal with energy-related CO_2 emissions with the increasing demand for energy is becoming more crucial.

There are many existing and potential solutions to reduce energy-related CO_2 emissions: energy conservation; improving energy efficiency; carbon capture and sequestration (CCS) during fossil fuel conversion; using renewable power and renewable fuels; and CCS during renewable fuel production. CCS is a process of capturing CO_2 from large point sources, transporting it to a storage site, and depositing it where it will not enter the atmosphere, normally an underground geological formation[4].

The first two options are on the top of the energy hierarchy, which could reduce greenhouse gas emissions efficiently during usage. CCS in fossil fuel conversion is an efficient way to guarantee enough energy supply with a less carbon footprint. One method is to capture CO_2 for enhanced oil recovery (EOR) which is being used in many countries. Renewable power and fuels, like wind power and biofuel, are promising pathways to strengthening global energy security with carbon neutral[5]. The combination of CCS with renewable energy could be an ultimate solution to supply the world with enough energy and negative CO_2 emission, such as bio-energy with carbon capture and storage (BECCS) technology[6,7].

It can be seen that for either fossil fuel conversion or renewable fuel production, CCS plays an important role in reducing energy-related CO_2 emissions to a lower level. One key step of CCS is CO_2 capture. There are three major CO_2 capture systems and corresponding capture technologies applied to the energy production field. The following

sections will introduce the state of the art of CO_2 capture systems and technologies for CCS. The application to synthetic fuel production will be described in detail, which is the focus of this thesis.

1.2 CO_2 capture systems and technologies during fuel conversion

CO_2 capture systems for fuel conversion could be divided into three categories: post-combustion, pre-combustion, and oxy-combustion. Fig.1.4 illustrates those capture approaches, as well as established and developmental technologies in corresponding systems[8-16].

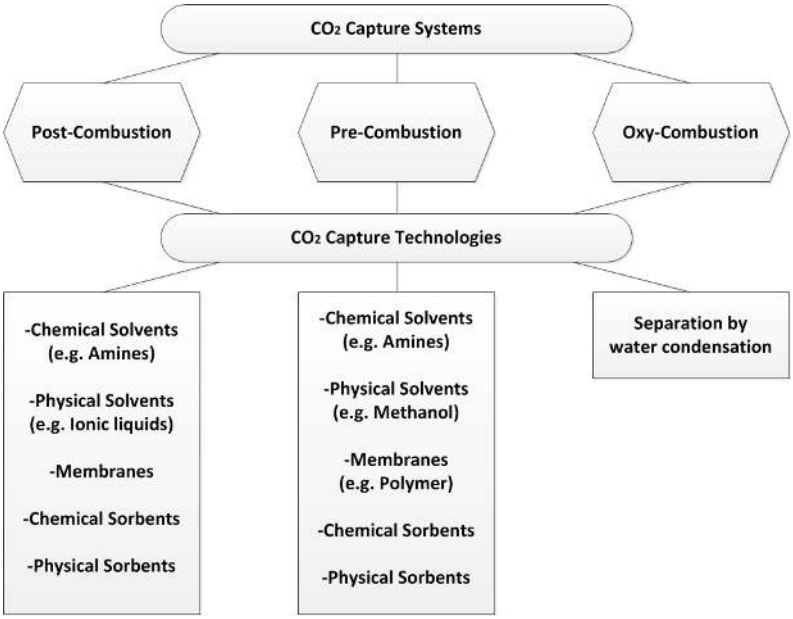

Fig.1.4 Schematic of CO_2 capture systems and technologies

1.2.1 Post-combustion CO_2 capture system

Post-combustion CO_2 capture is mainly applied to a conventional pulverized coal-fired power generation. The illustration of post-combustion is shown in Fig.1.5. The fuel,

such as coal, is burned with air in a boiler to produce steam. The steam is used to generate power via a steam turbine. The flue gas containing mostly N_2 and CO_2 is sent to the post-combustion CO_2 capture unit for separation, in which the most common method is using chemical solvents such as monoethanolamine (MEA) to capture CO_2.

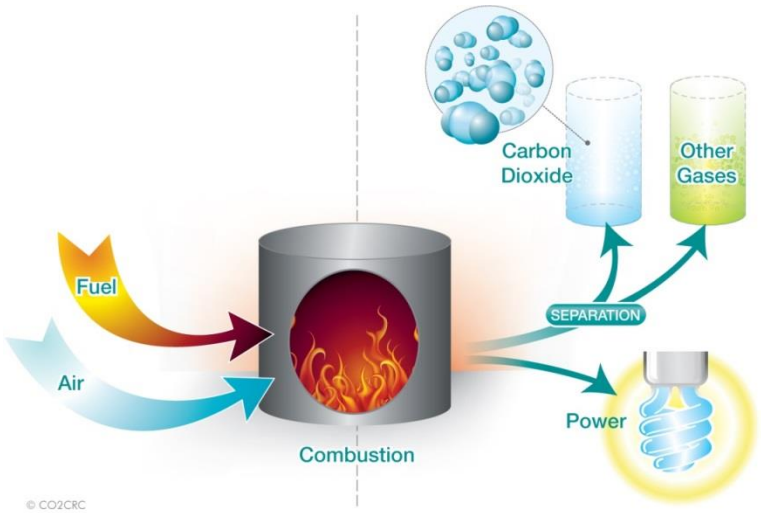

Fig.1.5 Illustration of post-combustion CO_2 capture[17]

1.2.2 Pre-combustion CO_2 capture system

Pre-combustion CO_2 capture is related to gasification technology. Gasification technologies are crucial to synthetic fuel production and this will be described in 1.3.

An illustration of pre-combustion is depicted in Fig.1.6. Pre-combustion here does not mean the final downstream step is only combustion. It can include any other parallel downstream processing steps such as fuel and chemical synthesis. The syngas from gasification is mainly composed of H_2, CO and minor amounts of other gas components. In order to get higher H_2 yield, CO is converted to CO_2 via a shift reaction, thus, more

CO_2 is produced. Before CO_2 goes to downstream processing such as gas turbine, it is first captured and separated from the gasification exhaust stream. Rectisol and Selexol, as physical solvents, are two widely used and commercialized technologies applied in the industrial field[18].

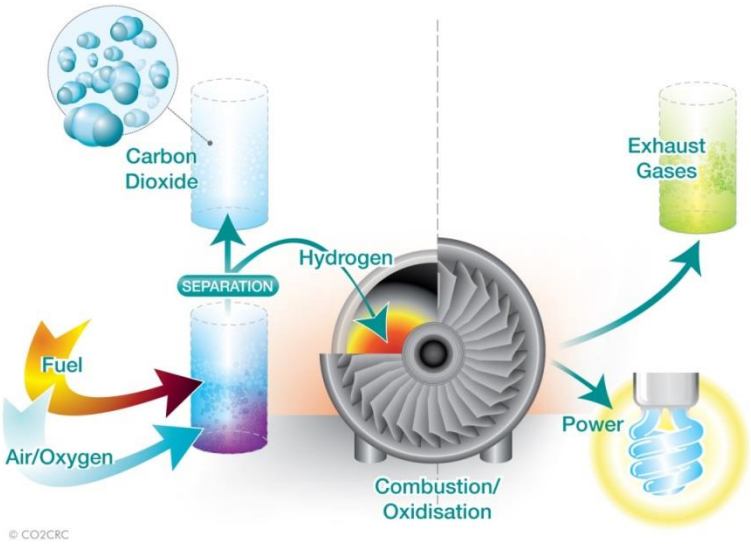

Fig.1.6 Illustration of pre-combustion CO_2 capture[17]

1.2.3 Oxy-combustion CO_2 capture system

Fuel is burned in pure oxygen instead of air in oxy-combustion capture. The resulting exhaust only contains CO_2 and steam, which can be easily separated by condensing the water. The diagram is shown in Fig.1.7. There are many additional benefits for oxy-combustion capture including the reduction in NOx emissions and improved mercury removal. However, due to high oxygen separation cost, oxy-combustion has not been commercialized yet.

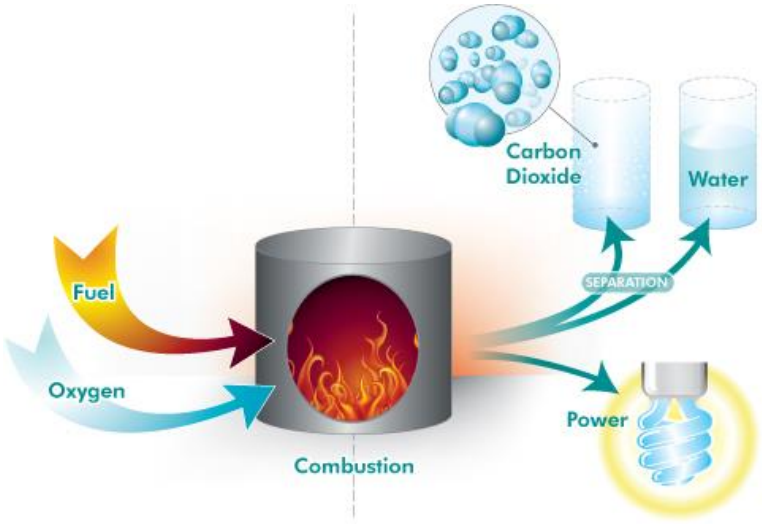

Fig.1.7 Illustration of oxy-combustion CO_2 capture[17]

1.3 CO_2 capture during synthetic fuel production based on gasification technology

Synthetic fuel or synfuel is a liquid or gaseous fuel converted from coal, natural gas, oil shale, or biomass[19]. Because of the increasing demand for fuel, the limited local crude oil reserve, and the higher cost of imported fuel, more and more countries have begun to produce synfuel domestically by fully utilizing other natural resources such as coal and biomass. This is also aimed to mitigate the dependence on imported fuels.

For general synfuel production, gasification is a pivotal step to start the whole process, providing synthetic gas for downstream catalytic synthesis use[20]. However, this step generates large amounts of CO_2 in the product gas which affects downstream processes.

In the following sections, the main stream gasification technologies will be introduced. Then the methods for CO_2 capture during liquid and gaseous synfuel productions will be described.

1.3.1 Gasification technologies

Gasification is a process that uses heat, pressure, steam, and often oxygen to convert any carbonaceous matters into synthesis gas (syngas). The syngas mainly contains H_2, CO, CH_4 and CO_2. The syngas can be burned directly in the combined cycle for electric power generation, and can also be converted to different kinds of chemicals and synthetic transportation fuels such as ammonia, fertilizer, Fischer Tropsch (FT) liquid fuel and synthetic natural gas or substitute natural gas (SNG). The most well-known industrial application of gasification technology is integrated gasification combined cycle (IGCC), which is used for polygeneration (i.e. power, fuels and chemicals) [21].

a. POX (partial oxidation) gasification

Gasification is commonly referred to the partial oxidation process using oxygen and steam as the gasification agent. The term “partial” means that the gasification processes operate in an oxygen-lean environment, compared to the oxygen requirement for complete combustion of the same amount of fuel[20].

The chemistry of POX gasification involves a series of physical transformations and chemical reactions within the gasifier. The carbonaceous feedstock, such as coal and biomass, undergoes several different processes and/or reactions: dehydration, pyrolysis, combustion and gasification[21]. Some major reactions are shown in Fig.1.8.

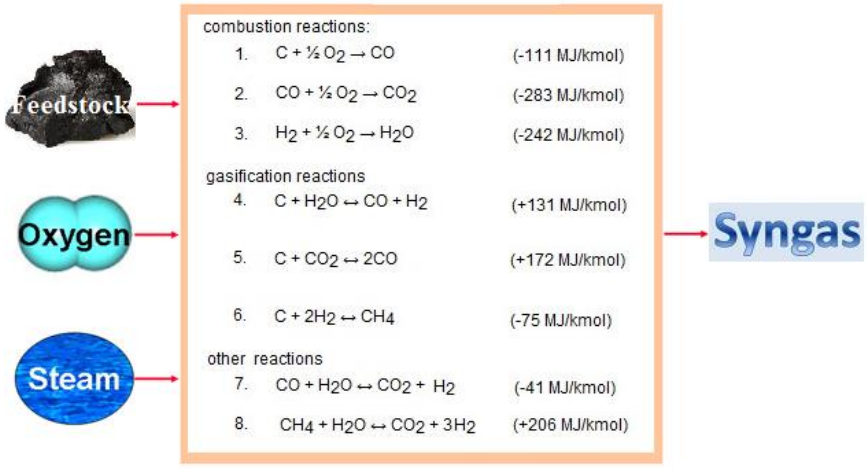

Fig.1.8 Thermochemical reactions involved in POX gasification[21]

The CO_2 amount in the syngas in general POX gasification is about 5-15%. However, CO_2 percentage is further increased to a higher level via the water gas shift (WGS) to convert CO and steam to H_2 and CO_2. This is because more H_2 is needed to meet the downstream requirement. Hence, the CO_2 percentage could be over 30% in the final producer gas. The capture of CO_2 before the ultimate use of syngas is necessary because CO_2 influences the turbine efficiency or catalytic conversion efficiency.

b. Hydrogasification and steam hydrogasification

Hydrogasification (HG) is a technology that uses H_2 as the gasification agent. It has been used for the production of SNG from coal or other feedstocks since the 1930s[21]. This is a direct process to produce SNG by hydrogenation of carbonaceous matters to CH_4. The primary reaction is shown below.

$C + 2H_2 \leftrightarrow CH_4$ -75MJ/kmol

The hydrogasification process was once developed to pilot plant scale[21]. However, with the increase of natural gas (NG) availability during that time, further developments were suspended before 1990[21]. Hydrogasification does not require an oxygen plant, which can save a substantial cost to a gasification facility. However, due to the comparatively lower reactivity between hydrogen and carbon[22], the reactants should be brought to a high temperature to increase the reaction rate, although the reaction is exothermic. A catalyst is needed sometimes to get an economically acceptable reaction rate. Additionally, how to integrate the production of H_2 into the whole process still requires further research.

In order to increase the reaction rate and improve the integration of H_2, several new processes based on steam hydrogasification reaction (SHR) were developed by the College of Engineering-Center for Environmental Research & Technology (CE-CERT) at University of California, Riverside. Some major reactions in SHR are shown in Fig.1.9.

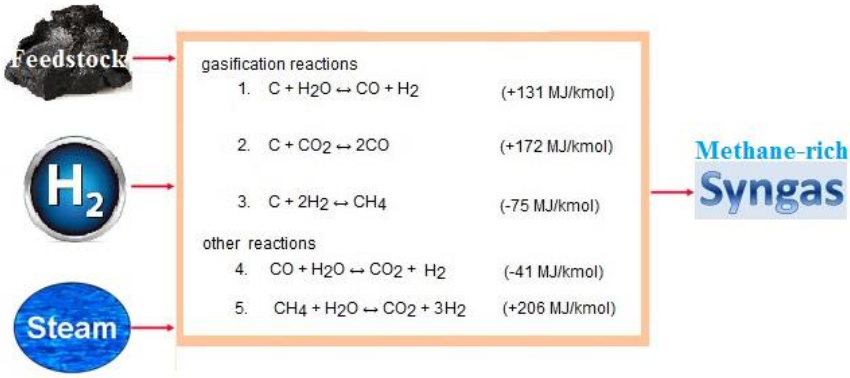

Fig.1.9 Thermochemical reactions involved in SHR gasification

SHR can generate a methane-rich syngas for versatile downstream operations. The details of SHR based processes will be described in section 1.3.3.

1.3.2 CO_2 capture during commercialized FT fuel and SNG production

The synthesis gas from gasification can be used to produce bulk products like ammonia, methanol, synthetic fuel and electricity via IGCC. The overall pathways of syngas utilization are shown in Fig.1.10.

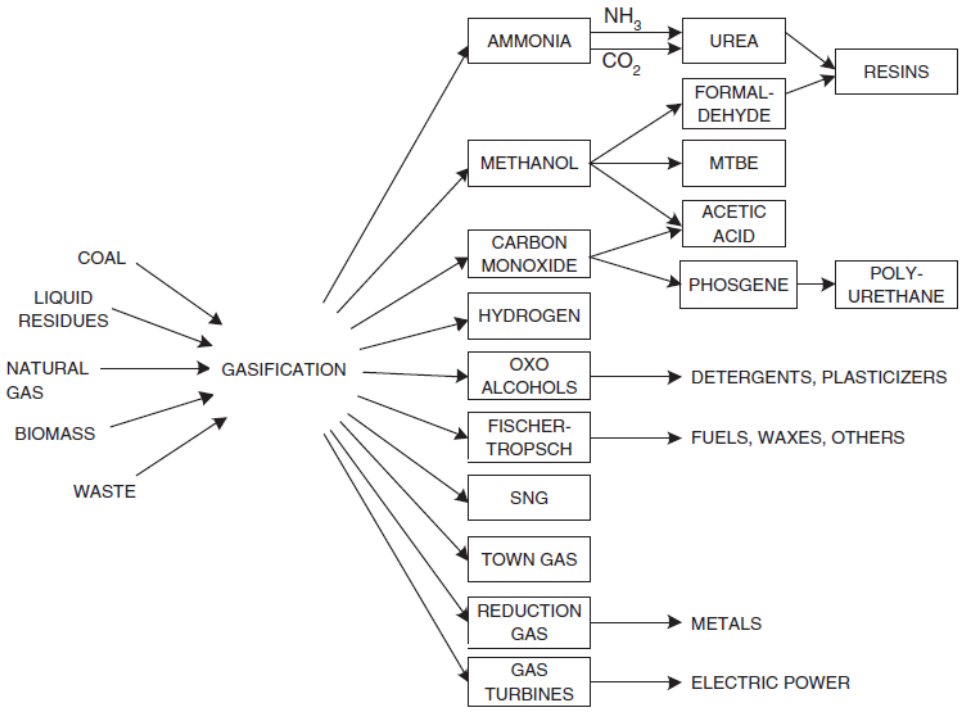

Fig.1.10 Applications for syngas[21]

In particular, the conversion of coal or biomass into synthetic fuels such as SNG and FT liquid fuel for transportation purpose has been widely studied and some processes have been commercialized[23-32]. The synthetic liquid fuel production from coal, biomass, and any feedstock (e.g. mixture) is referred to as CTL (Coal-to-Liquids), BTL

(Biomass-to-Liquids) and XTL (Feedstock-to-Liquids), respectively. The synthetic gaseous fuel production from coal, biomass, and any feedstock is referred to as CTG (Coal-to-Gas), BTG (Biomass-to-Gas) and XTG (Feedstock-to-Gas), respectively.

1.3.2.1. FT fuel production and CO_2 capture

FT liquid fuel generally represents synthetic diesel and gasoline via indirect conversion based on gasification. It was first developed by Franz Fischer and Hans Tropsch by converting coal-derived syngas into a series of hydrocarbons in 1923[33]. The process includes three key steps, which are syngas production, FT synthesis and refining[34]. Syngas is from gasfication of carbonaceous feedstock and is used for catalytic conversion to different hydrocarbons ranging mainly from C4 to C24. Iron and cobalt catalysts are commonly used for FT synthesis. The product distribution follows an Anderson–Schulz–Flory (ASF) distribution[35], the details of which will be given in Chapter 4. Liquid hydrocarbons are the major components in FT products other than some gas and solid products. These liquids are mostly composed of paraffins which can be refined to gasoline, kerosene and diesel. Long carbon chain product, wax, can further be converted to fuel range by hydrotreating[36]. These fuel products can easily fit into existing infrastructures and automobile engines because they are almost the same as fuels refined from crude oil.

Sasol (an international integrated energy and chemical company) has two successful commercial synfuel-from-coal plants in the world[37]. Sasol uses the FT indirect liquefaction method to convert coal into petrol and diesel fuels, and provides raw

materials for the petro-chemical and fertilizer industries. The detailed Sasol process is depicted in Fig.1.11.

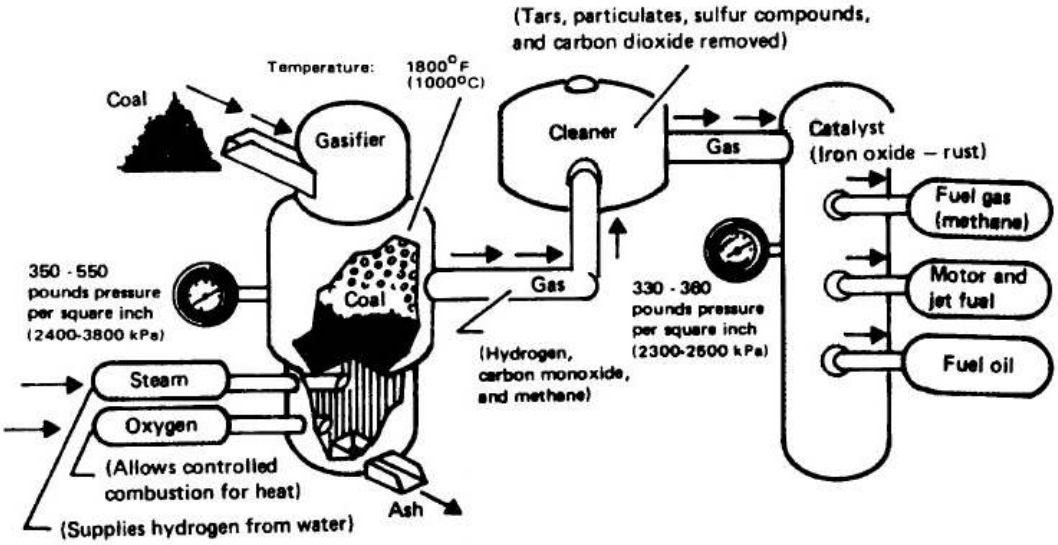

Fig.1.11 Block flow diagram of Sasol process[38]

Coal is first gasified in the Sasol-Lurgi gasifier and the synthesis gas undergoes cleanup steps in which 98% of the CO_2 is removed in addition to sulfur by using Rectisol method[39]. The purified syngas is then converted to synthetic diesel fuels with other valuable petrochemicals by Synthol process[37].

CO_2 must be reduced or removed from the syngas before entering the FT reactor, because it was found that CO_2 could influence the FT synthesis adversely[40,41]. First, CO_2 plays a diluting role during the synthesis. Second, the addition of CO_2 can increase water and overall oxygenate formation rates with slightly change on product distribution when using iron catalyst[42]. When using cobalt catalyst, dramatic alteration of product distribution can happen[43].

1.3.2.2. SNG production and CO_2 capture

SNG is a versatile energy carrier, which is interchangeable with natural gas and can be used in the existing gas distribution network and end use technologies, like CNG cars (compressed natural gas) and CHP (combined heat and power)[44,45]. SNG can be produced via biological treatment of bio-feedstock (e.g. anaerobic digestion) or thermochemical conversion of any carbonaceous feedstock. Thermochemical conversion contains several steps, including gasification, gas cleaning/conditioning, methanation and fuel upgrading.

CO_2 must be removed during SNG production due to the quality requirement with the consideration of compatibility with the distribution system and end use appliance. CO_2 should normally occupy about 1% in the final SNG product[46]. Therefore, the removal of CO_2 is mandatory.

Great Plains Synfuels Plant is the only commercialized SNG plant in the United States, which main product is pipeline-quality SNG, with other products such as carbon dioxide, anhydrous ammonia and phenol. The plant became one of the first commercial facilities to sequester carbon emissions. The plant delivers a 95% pure stream of CO_2 through a pipeline to an oilfield for EOR[47]. The Great Plains Synfuels process diagram is shown in Fig.1.12.

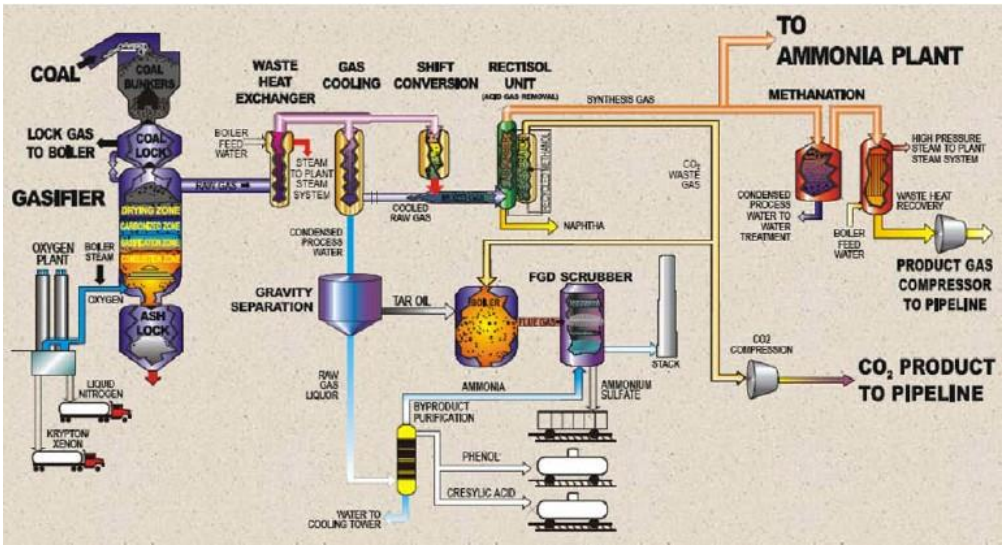

Fig.1.12 Block flow diagram of Great Plains synfuel process[47]

Sasol-Lurgi gasifier is used for the gasification of North Dakota lignite coal. The synthesis gas is conditioned via shift conversion (e.g. WGS) to increase the H_2 to CO ratio to 3 for later methantion step. Methanation is the reaction between H_2 and CO to generate CH_4 and steam. Acid gases including H_2S and CO_2 are removed via Rectisol process. CO_2 is then sent to the pipeline for EOR purpose. High quality SNG is finally obtained after upgrading and delivered to the existing gas distribution network.

1.3.3 CO_2 capture during CE-CERT processes for synthetic fuel production

1.3.3.1. Introduction to CE-CERT process and its advantages

The CE-CERT process is based on SHR technology by combining hydrogen and steam as the gasification agents. As mentioned above, this technology can significantly enhance the rate of methane formation[48]. Besides, it can utilize lower energy content and high moisture feedstock such as lignite, biomass waste, biosolids and microalgae.

Green waste and biosolids are common municipal waste which is usually disposed by a means of landfill. Micro-algal bloom resulted from eutrophication is a significant cause of water quality deterioration in some lakes and streams in United States (e.g. Salton Sea, California). CE-CERT process can convert these annoying waste streams to valuable fuels and chemicals without drying, which saves lots of energy on pretreatment.

SHR is coupled with steam methane reforming (SMR) or WGS in order to generate sufficient hydrogen to recycle back to SHR thus eliminating the need for an external source of hydrogen. The details of related research and patents have been published earlier[48-54].

The major advantages of CE-CERT process is summarized below:

a. The feed method of SHR is in terms of slurry. Thus, feedstock with high moisture content can be used directly, reducing the feedstock drying cost.

b. SHR does not need catalyst and can be operated at moderate temperature and pressure, which reduces the capital and operation cost. Also, the addition of steam dramatically increases the rate of CH_4 formation.

c. CE-CERT process is self-sustainable on H_2 supply with a closed-loop cycle, eliminating the need for external H_2.

d. The H_2 to CO ratio of the synthesis gas can be controlled by varying steam to feedstock ratio and H_2 to carbon ratio in the SHR gasifier.

e. CE-CERT process is feasible and economic for small and medium scale facilities using local feedstock resource, which can reduce the high transportation cost. Low rank coal, biosolids and municipal solid waste including green waste are suitable and favorable for this process[55]. By contrast, conventional gasification plant (POX based) is not economically viable on a small scale due to the expensive capital cost of oxygen separation.

In 2010, the National Energy Technology Laboratory (NETL) completed an independent technical and economic assessment of the CE-CERT process for co-production of power and FT fuel. The report concludes that CE-CERT process has 12% higher efficiency with 18% less capital costs compared to the most up-to-date mainstream gasification technologies[56].

1.3.3.2. CE-CERT process for FT liquid fuel production and CO_2 capture

In the case of FT synthetic fuel production, SHR is coupled with SMR. The flow diagram is shown in Fig.1.13. In this process, the wet feedstock is first pretreated under 220°C by the hydrothermal reaction to get a pumpable slurry[57,58]. Then it is gasified in the presence of steam and hydrogen to obtain a methane-rich output gas. The gasifier temperature is usually 750°C and the reactor type could be circulating fluidized bed using silica sand as bed material. Circulating fluidized bed can provide good mixing between feedstock and gasification agents, improving both heat and mass transfer. This kind of gasifier could operate at comparatively lower temperature, which is suitable for gasifying reactive feedstocks, like low-rank coals and biomass. The leftover char in the gasifier is

delivered to the combustor along with the sand for extra heat supply. The impurities such as sulfur species (H_2S, COS, etc) are removed from the product gas by warm gas cleanup at 350°C[59-62]. Also, the water can still be kept in the form of steam under this temperature for the SMR step. SMR is the reaction between steam and methane to generate H_2 and CO. SMR then converts most CH_4 to the mixture of H_2 and CO at 850°C, meanwhile, making the extra H_2 amount enough for recycle to the SHR gasifier. The H_2 to CO ratio is regulated by H_2 separation to 1 or 2 depending on iron catalyst or cobalt catalyst used in the FT reactor. The FT product includes crude naphtha, crude middle distillate and crude wax, which require further upgrading. The crude naphtha and middle distillate undergo hydrotreating to saturate the olefins. The wax is sent to a hydrocracking unit in which it is converted into hydrocarbon gases, naphtha and diesel[63].

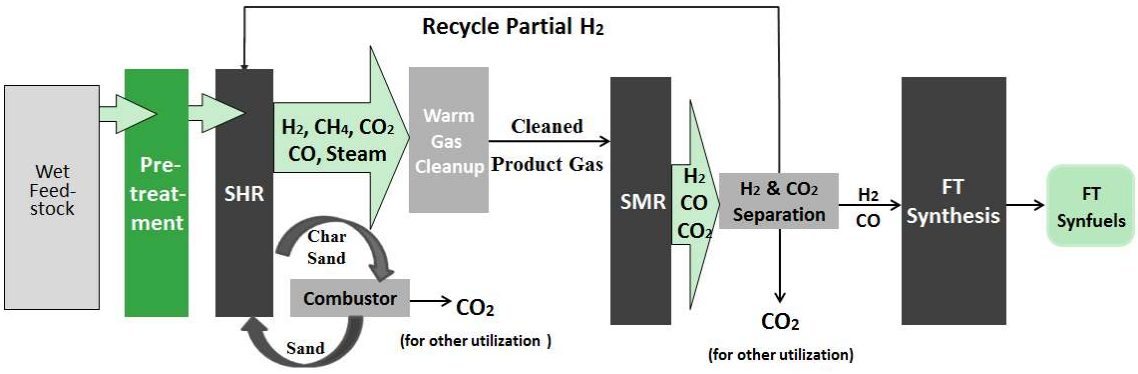

Fig.1.13 Block flow diagram of CE-CERT process for FT synthetic fuel production

CO_2 is from two main streams in this process, flue gas from regenerator and syngas from SMR. For example, when Utah bituminous coal is used for FT fuel production via CE-CERT process, the CO_2 in the regenerator flue gas and SMR syngas occupies 18% and 22% the carbon in the feeding coal, respectively. At least 90% of these CO_2

emissions are totally captured during the whole process. Based on the preliminary design, amine-based chemical absorber/stripper configuration is chosen for CO_2 removal in the syngas from SMR at high pressure, such as utilizing methyldiethanolamine (MDEA) solvent. The CO_2-lean syngas is then sent to the FT reactor. Fluor Economine FG Plus CO_2 recovery process is applied to the regenerator flue gas by using MEA[55].

1.3.3.3. CE-CERT process for SNG production and CO_2 capture

CE-CERT process for SNG production is based on the combination of SHR and WGS. The process also has sufficient hydrogen remaining to recycle to SHR. The process flow diagram is shown in Fig.1.14. Similar to the process for FT synfuel production, the wet feedstock is first converted to a pumpable slurry and then it is gasified in the SHR reactor. The remained char was burned in the combustor to provide heat for the gasifier. The warm gas cleanup step removes the impurities. The majority of CO in the synthesis gas is converted to H_2 and CO_2 via WGS using two shift reactors in tandem loaded with high temperature catalyst and low temperature catalyst, respectively. This step produces enough H_2 amount for cyclic use. Then, H_2 and CO_2 are separated from the main stream for recycle and other utilization such as EOR and algae growth. Finally, the output gas is SNG.

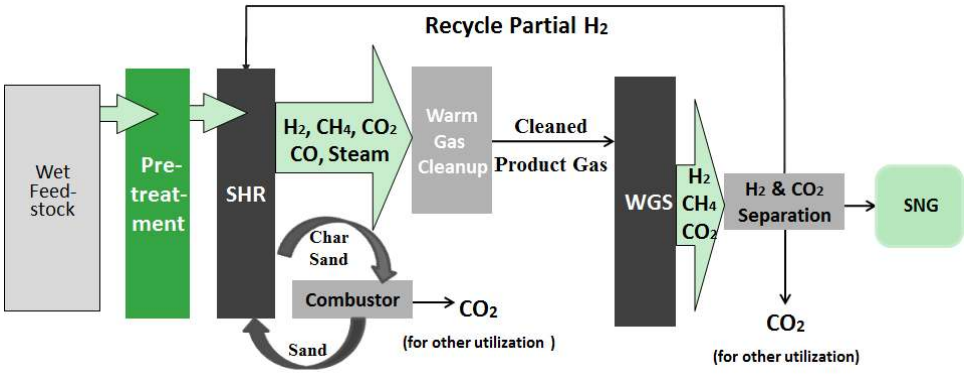

Fig.1.14 Block flow diagram of CE-CERT process for SNG production

The CO_2 during SNG production is derived from two main streams, flue gas from regenerator and raw SNG from WGS reactor. Similar to FT liquid fuel production, amine-based absorber/stripper configuration is used for CO_2 removal in the raw SNG at high pressure, and Fluor Econamine FG Plus CO_2 recovery process can be an option for regenerator flue gas.

1.4 Sorption enhanced CE-CERT processes using in-situ CO_2 capture technology

1.4.1 In-situ CO_2 capture technology

One unique technique in the pre-combustion system which attracts much attention in the past several years is in-situ CO_2 capture. The illustration is shown in Fig.1.15.

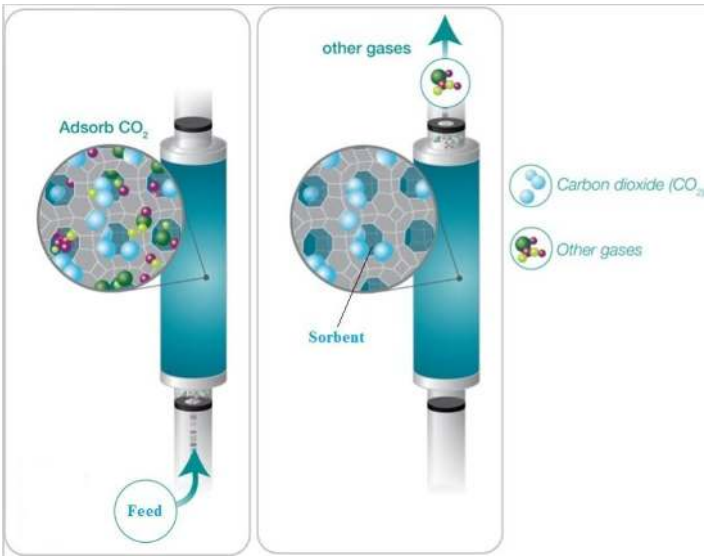

Fig.1.15 Illustration of in-situ CO_2 capture technique

This technique uses a chemical sorbent such as CaO to capture CO_2 directly in the reactor such as shift reactor or gasifier. CO_2 is removed quickly as it forms by the sorbent mixed with carrier materials or catalysts, which can change the equilibrium to promote even more energetic production than otherwise possible. This technology has great potential to have lower CO_2 emission and higher energy production simultaneously. It is corresponding to the mitigation of greenhouse gas effect and satisfying the ascending demand for energy. This process is also called sorption enhanced (SE) process. SE related studies are mainly focused on WGS, SMR, and gasification for simultaneous enhanced hydrogen production and CO_2 emission reduction[64-79].

Sorption enhanced steam gasification has been extensively studied over the past ten years. A remarkable enhancement of hydrogen production and a dramatic decrease of CO_2 were observed with addition of CaO containing sorbent using different types of feedstock such as coal, woody waste and oil waste[80-89]. Some researchers also showed

that the combined use of a commercial catalyst like nickel and calcium-based sorbent results in higher purity hydrogen[90-93]. The sorbent also contributed in tar reduction to some extent[94-98].

1.4.2 Sorption enhanced CE-CERT processes for synthetic fuel production

A new concept named sorption enhanced steam hydrogasification reaction (SE-SHR) is proposed here. SE-SHR combines sorption enhanced principles and steam hydrogasification reaction. The process for synthetic fuel production based on SE-SHR is called sorption enhanced CE-CERT process. The new block flow diagram for FT synthetic fuel production is shown in Fig.1.16.

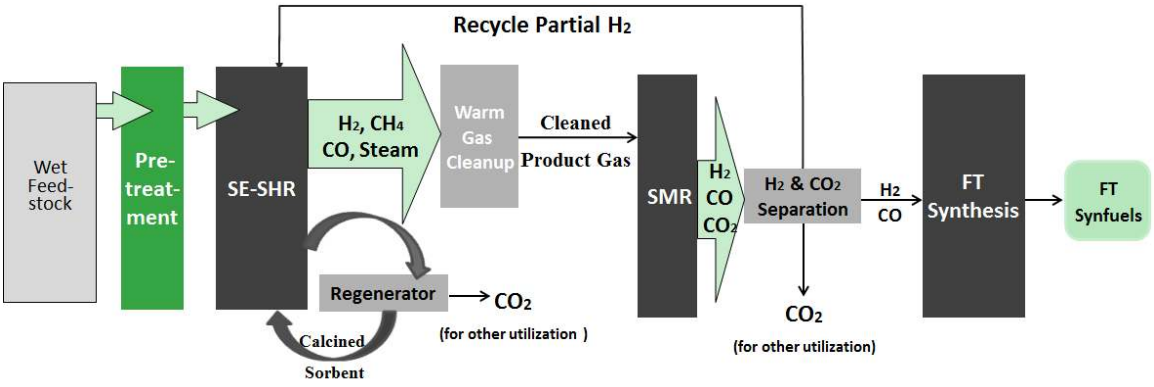

Fig.1.16 Block flow diagram of sorption enhanced CE-CERT process for FT synthetic fuel production

It was expected that SE-SHR could produce enough H_2 for recycle use and capture most of the CO_2. The process is similar to the conventional SHR-based process. Besides sand, sorbent (e.g. CaO) is used in the fluidized bed. Sorbent can be used singly or mixed with sand. CaO has similar density and heat capacity compared to silica sand. The used

sorbent is calcined in the regenerator and sent back to the gasifier for cyclic use. The released CO_2 stream is for other utilization. It was expected that sorption enhanced technology could generate more energetic gas such as H_2 and CH_4. Consequently, there is more CH_4 fed to the SMR, which most likely leads to more CO produced via SMR. This could improve the subsequent FT fuel yield due to increased carbon input. The new block flow diagrams of two sorption enhanced CE-CERT processes for SNG production are shown in Fig.1.17.

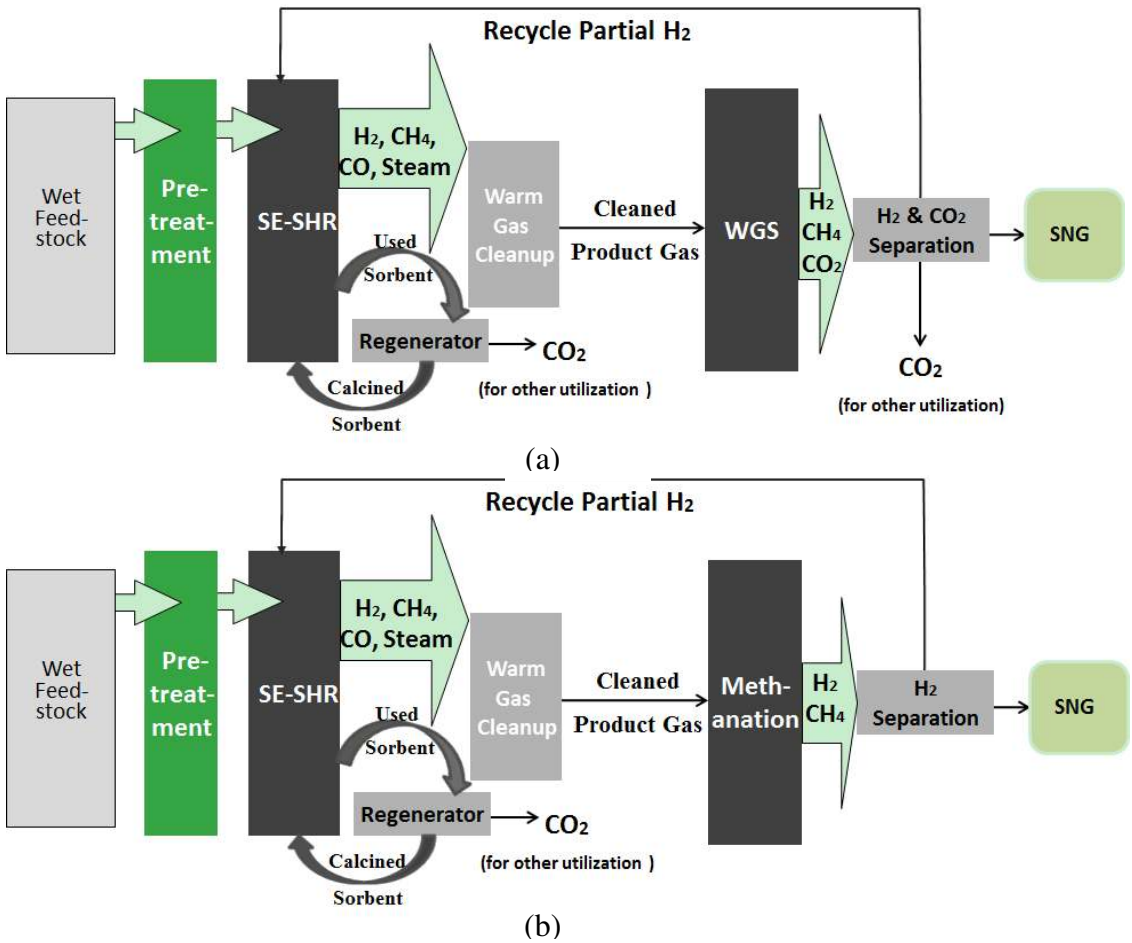

Fig.1.17 Block flow diagram of sorption enhanced CE-CERT process for SNG production (a) SE-SHR with WGS (b) SE-SHR with methanation

These two processes are SE-SHR coupled with WGS and SE-SHR coupled with methanation. High H_2 yield and low CO_2 concentration were expected from the SE-SHR gasifier. The sorbent from the gasifier is calcined in the regenerator and will be returned to the gasifier for cyclic use. The process of SE-SHR with WGS is shown in Fig.1.17(a). It is similar to the conventional process combining SHR with WGS. But, the process based on SE-SHR was expected to produce less CO_2 and higher CH_4. The process of SE-SHR with methanation is depicted in Fig.1.17(b). Since the process can produce more H_2 than the recycle amount needed for SHR, additional H_2 can be used to react with residual CO and CO_2 in the producer gas via methanation to maximize the CH_4 production.

1.5 Objectives

The objective of this research is to evaluate the overall SE-SHR performance and to investigate the optimum operation parameters of SE-SHR in different sorption enhanced CE-CERT processes. The research is aimed to minimize the CO_2 production in the syngas and to maximize the final synthetic fuel yield. The sorption enhanced process will be compared to the corresponding conventional CE-CERT process.

The first objective is focused on the evaluation of SE-SHR performance. Three different types of carbonaceous feedstock, biomass (pinewood sawdust and microalgae), biosolids (centrifuged sewage sludge), and coal are gasified in the presence of hydrogen and steam. The effect of the addition of calcium based sorbent on the gas production is studied by increasing the sorbent loading gradually. It is expected that the sorption enhanced performance could minimize CO_2 production and enhance the yield of

energetic gases with certain sorbent input. The relationship between captured CO_2 amount and the increase of energetic gas is obtained. The sample is also characterized before and after SE-SHR. Then, the effect of other factors such as temperature and sorbent particle size are investigated. In particular, steam to carbon molar ratio and hydrogen to carbon molar ratio determines the final syngas composition and production. The trend of gas production is studied by simultaneous variation of these two parameters. In the meantime, the leftover char amount under different gasification conditions is obtained. The amount will be used for further scale-up simulation to get the optimum SE-SHR condition for each sorption enhanced CE-CERT process.

The second goal is to investigate the kinetics of SE-SHR. This study will help to determine the specifications and operation parameters of the future gasifier. A new lab-scale mini reactor is designed and constructed for kinetics study. The new configuration can minimize the gas loss during the real time analysis of gas composition by using a specific capillary line. The study is focused on the formation rate of CO_2, CO and CH_4 in the first 150 seconds at three temperatures (650°C, 700°C and 750°C) with and without sorbent introduction. In addition, the effect of sorbent loading and feedstock-sorbent contact type on the CO_2 evolution is also determined. The activation energy of each gas is then obtained based on the temperature range from 650°C to 750°C. The kinetics data of SE-SHR will be compared to SHR.

The last objective is focused on the simulation of different sorption enhanced CE-CERT processes for FT liquid fuel and SNG production on a pilot scale basis. Aspen Plus

simulation software is applied to get the mass and energy balance of a 400 tonnes/day (dry basis) synfuel plant. The optimum parameters of SE-SHR are determined based on the maximum production of synthetic fuel and being with enough H_2 back to the gasifier. The comparison of overall energy efficiency and fuel conversion efficiency for SNG production will also be performed between sorption enhanced CE-CERT process and conventional CE-CERT process.

2. Performance of Sorption Enhanced Steam Hydrogasification Reaction

In this section, the effect of the addition of calcium based sorbent on steam hydrogasification is investigated. First, the preliminary SE-SHR performance is evaluated by using coal and another two commingled feedstock (biomass-biosolids and biomass-microalgae) with the increase of calcium oxide to carbon molar ratio (CaO/C). The relationship between the increase of energetic gas and captured CO_2 amount is then established. The characterization of both feedstock and gasification residue was also conducted. Second, the effect of temperature, sorbent particle size, and the combined effect of steam to carbon molar ratio (Steam/C) and hydrogen to carbon molar ratio (H_2/C) is evaluated. Besides, SE-SHR and sorption enhanced hydrogasification (SE-HG) is compared.

2.1 Experimental method

The experiments were carried out in a constantly stirred batch reactor. The reactor sketch and dimensions are shown in Fig.2.1. The system included a batch vessel with 230cc made of Inconel, a ceramic radiative heater, a magnetic driven impeller, a gas purge/release system, and a product gas collection system. Pressure and temperature in the vessel were measured by an Omega px303 pressure sensor and a K type thermocouple, respectively. All data were recorded and processed using LabView®.

Lignite, pinewood sawdust, microalgae and wastewater treatment sludge (biosolids) were selected as typical samples for this study, which characteristics can be seen in Table 2.1. Most feedstock has high moisture content suitable for SHR. Lignite is a low-rank

coal which is usually converted by gasification to high quality fuel. The lignite used in this study was from Nutratherm Australia. The pinewood sawdust is a typical green waste and F.M.BROWN'S pinewood sawdust was used. The specific microalgae genus used was Chlorella vulgaris, because it is one of the most notable bloom forming factors[99]. Chlorella vulgaris was purchased from NOW Foods. In addition, the disposal of biosolids is always an environmental issue in most countries. The sewage sludge selected was received from Riverside wastewater quality control plant.

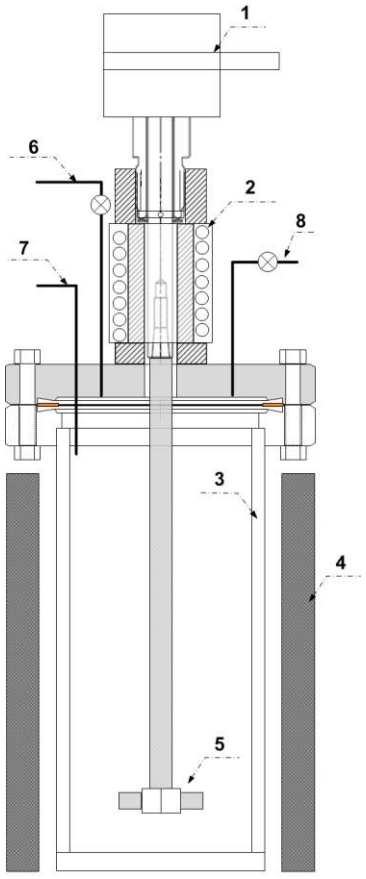

Fig.2.1 Schematic diagram of the stirred batch reactor system (1.Magnetic agitator driven by belt 2.Cooling coils 3.Inconel reactor 4.Radiative heater 5.Impeller coupled with agitator 6.Gas purge and release system 7.Thermocouple and pressure gauge linked with LabView® 8.Gas collection system)

Table 2.1 Composition analysis of feedstock

		Lignite	Pinewood	Algae	Sludge
Proximate Analysis (wt% dry basis)	Volatile Matter	50.2	86.4	79.53	69.01
	Fixed Carbon	42.4	13.33	15.88	8.45
	Ash	7.4	0.27	4.59	22.54
Ultimate Analysis (wt% dry basis)	Carbon	59.85	50.89	49.19	37.22
	Hydrogen	4.64	9.37	7.06	5.47
	Nitrogen	2.83	5.34	9.3	11.03
	Sulphur, Organic	1.5	0.01	0.61	1.3
	Oxygen	23.78	34.12	29.25	22.44
	Balance	7.4	0.27	4.59	22.54
Moisture in raw sample (wt% wet basis)	H_2O	60	10	90	92

All feedstock was dried and ground to pass the sieve of 150μm. A mass of 0.5g sample was used for all experiments. Water was mixed with dry feedstock first to simulate the wet feedstock slurry with desired moisture content in the reactor. In the case of SE-SHR experiment, sorbent was added and mixed with the feedstock in the vessel. Quicklime was used as the sorbent due to its widespread availability and low cost, which was obtained from ChemLime Co. (Fort Worth, TX). The CaO composition was over 98% (wt% dry basis). The sorbent was also grounded and sieved to the specific range.

It should be mentioned here that initial drying was only for the lab scale study to control the experimental accuracy. For large scale practical operation, the wet feedstock such as biosolids or microalgae is directly blended with wood waste by the optimum ratio to form a pumpable slurry via hydrothermal pretreatment[57,58]. The empirical moisture

content of pretreated feedstock slurry with acceptable viscosity is 66.7% (i.e. steam to feedstock mass ratio is 2).

Lignite, commingled biomass-biosolids and commingled biomass-microalgae was used for this study. The design of experiment is listed in Table 2.2.

The reactor was heated to the desired temperature with heating rate of 30°C/min. The reaction was not terminated until the inside pressure was stable. Then the reactor was cooled down very quickly to stop the reaction from proceeding via air convection to below 100°C. The dry product gas was collected in a Tedlar® bag for analysis. The molar concentrations of carbon monoxide, carbon dioxide, hydrogen and methane were obtained via a gas analyzer (Cirrus™ bench-top residual gas analyzer, MKS Instruments). The total molar amount of the dry product gas was estimated by the Virial equation at the collection temperature of 90°C[100]. The molar amount of each gas was the product of the percentage and the total amount. In order to calculate how much CO_2 was captured by the sorbent, the remainder was immersed in dilute hydrochloric acid to decompose the carbonate thoroughly. The absorbed CO_2 amount was then obtained by weight difference. The amount of char and sulfur was calculated based on the corresponding elemental analysis of the residue with CO_2 released. Sulfur retained percentage was obtained by dividing the residual sulfur amount by the initial sulfur amount. Some feedstock and residues were selected for characterization using a D8 Advance X-ray Diffractometer of GermanyBRUKER/AXSCo., Ltd. The crystalline compounds were determined through computer system aiding, which was presented by an intensity-2θ format.

Table 2.2 Design of experiment for SE-SHR performance evaluation

Feedstock	Item	Parameter Value	Steam/C (molar ratio)	H2/C (molar ratio)	CaO/C (molar ratio)	Temperature (°C)	Sorbent particle size (mm)
Pinewood & Sludge (83% & 17% dry wt basis)	Effect of CaO/C (molar ratio)	0, 0.88	2.74	1	/	750	0.075-0.15
Pinewood & Algae (80% & 20% dry wt basis)		0, 0.85	2.64	1	/	750	0.075-0.15
Lignite		0, 0.12, 0.29, 0.57, 0.86, 1.14	2.22	1.08	/	750	0.075-0.15
	Effect of Temperature	650, 700, 750, 800	2.22	1.08	0.57	/	0.075-0.15
	Effect of Sorbent particle size (mm)	<0.038, 0.075-0.15, 1.7-2	2.22	1.08	0.57	750	/
	Effect of Steam/C (molar ratio)	1.67, 2.22, 2.78	/	0.63, 1.08, 1.59	0.36	750	0.075-0.15
	Effect of H2/C (molar ratio)	0.63, 1.08, 1.59	1.67, 2.22, 2.78	/	0.36	750	0.075-0.15
	Reaction system	HG, SHR	for HG, 0 for SHR, 2.22	1.08	0.57	750	0.075-0.15

2.2 Results and discussion

2.2.1 Effect of CaO/C molar ratio

The preliminary effect of CaO addition on the steam hydrogasification of three aforementioned types of feedstock was evaluated first. A certain amount of sorbent (CaO/C≈0.86) was added into the reactor. The SE-SHR performance was compared to the conventional SHR without sorbent introduced, which is shown in Fig.2.2.

It can be seen that there was almost no CO_2 in the product gas when sorbent was added. In addition, H_2 was increased dramatically with the sorbent introduced. The initial H_2 input for lignite, pinewood-sludge (pwd-slg) and pinewood-microalgae (pwd-alg) was 0.027mol, 0.02mol and 0.021mol, respectively, which is shown in terms of "H_2 recycle baseline" in the figure. H_2 yield was beyond corresponding baseline in SE-SHR and already enough back to gasifier for these feedstocks. However, the H_2 amount in the conventional SHR was lower than the baseline. Moreover, CH_4 was increased and CO was decreased in SE-SHR.

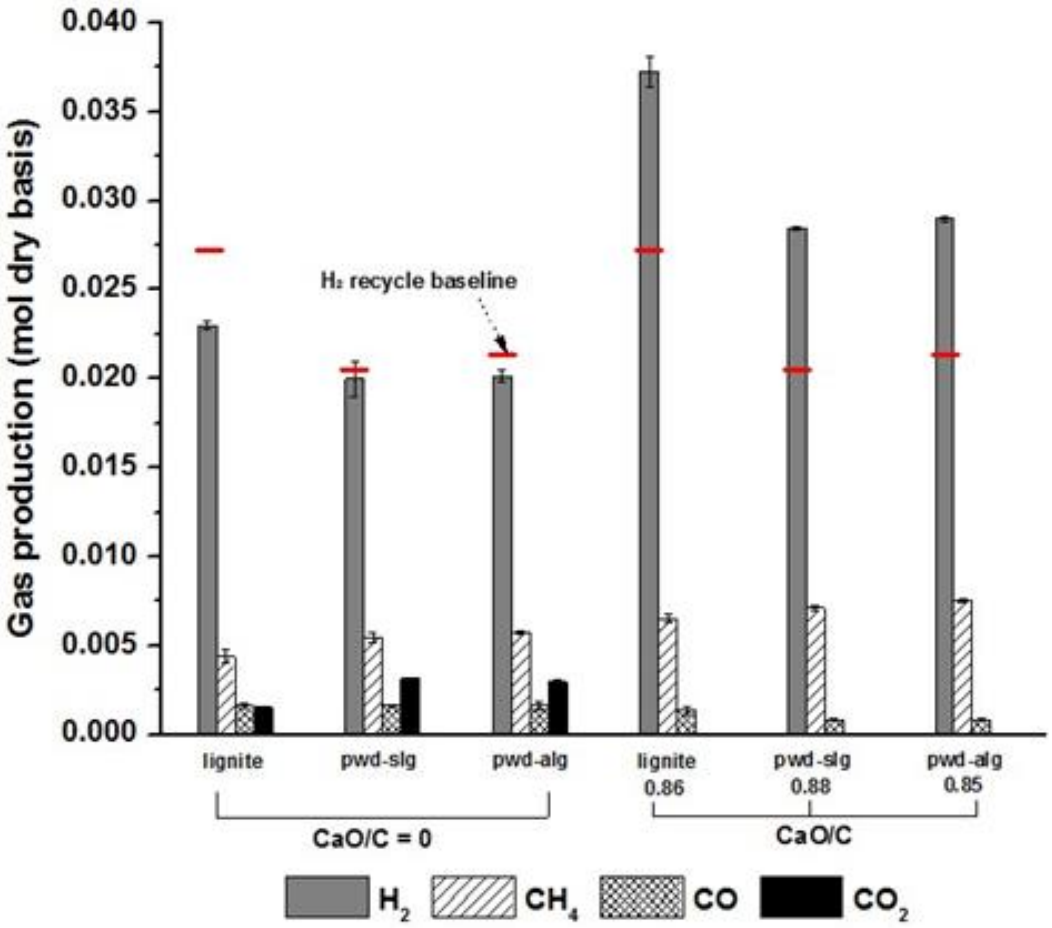

Fig.2.2 The effect of sorbent addition on different types of feedstock

The performance of SE-SHR with the gradual increase of CaO/C was further investigated. Lignite was used for the rest study in this thesis as a typical carbonaceous feedstock. The effect of CaO/C on carbon conversion distribution (CH_4, CO, CO_2, CO_2 captured, C_{2+}) is shown in Fig.2.3. The data presented shows the results with the baseline being no sorbent to the ratio of 1.14. The increase of CaO/C had a positive effect on the overall conversion of char and CO_2 removal. The char percentage decreased from 52% to 4% when the ratio was raised to 1.14. Due to the increase of CaO added, more CO_2 was removed and fixed in the sorbent, so less CO_2 was present in the gas phase. CO_2 was

reduced to essentially zero (about 0.05%). Meanwhile, the methane percentage increased gradually as more sorbent was added. C_{2+} percentage in particular was reduced most likely due to the catalytic effect of sorbent on components with higher molecular weight like tar[94-98]. The percentage decreased from 20% with no sorbent to 4% at the CaO/C of 0.86 and then leveled off. Only a marginal change in the carbon conversion was noted after the ratio of 1.14 and is not shown here.

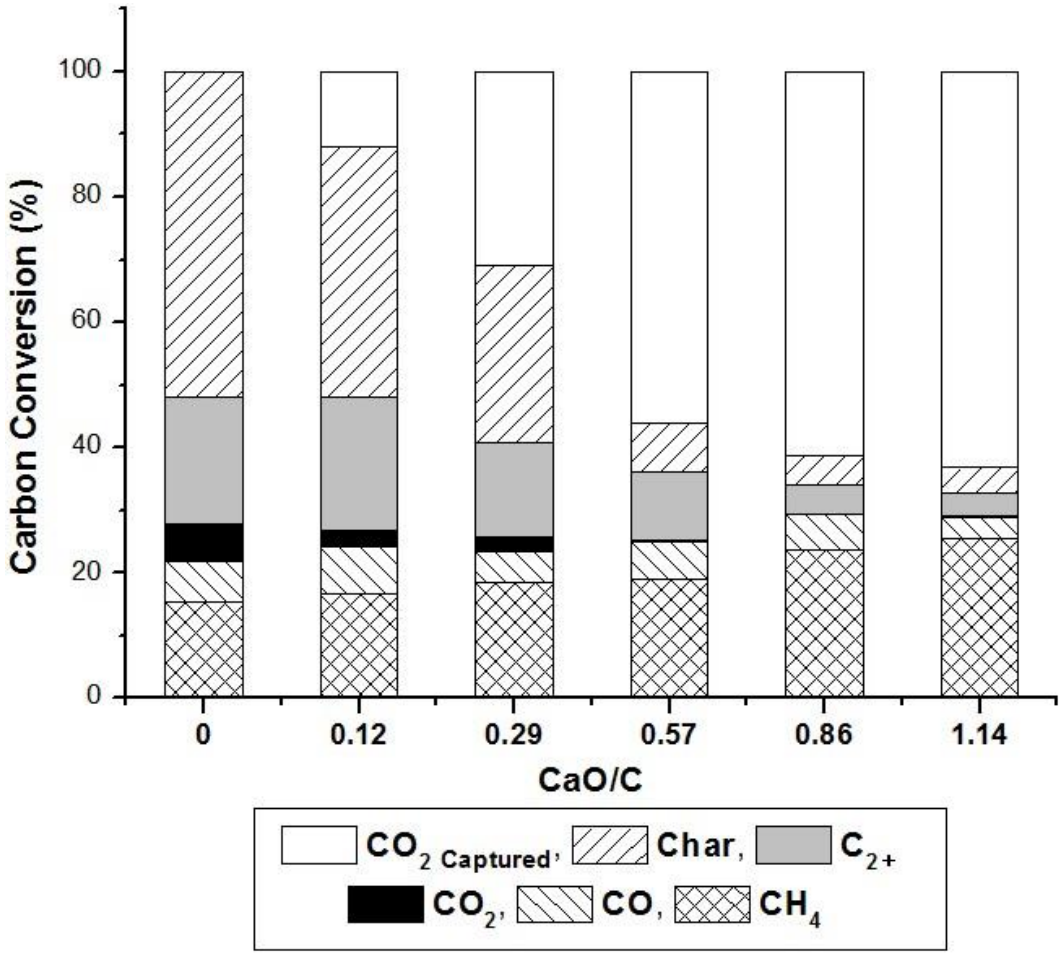

Fig.2.3 The effect of CaO/C ratio on carbon conversion

The gas production on a dry mole basis with CaO/C molar ratio is shown in Fig.2.4. Also shown in Fig.2.4 is the hydrogen recycle baseline required to maintain the sustained performance of SHR. Two trends were observed. First, the yield of H_2 and CH_4 increased with sorbent and second the output of CO and CO_2 decreased. Especially for H_2, the production was enhanced by about 61% at the ratio of 1.14 compared to the case without sorbent. Actually the increase in H_2 yield was related to the increase of CO_2 captured shown in Fig.2.3, which will be discussed later. Besides, the required H_2 amount was 0.027mol which is represented by the "H_2 recycle baseline" in Fig.2.4. Assuming the majority of H_2 could be separated, the H_2 production was acceptable for recycle use when the CaO/C was 0.29 or greater. Thus, to guarantee that sufficient H_2 was generated to sustain the steam hydrogasification reaction, the CaO/C should be at least 0.29. Besides, hydrogen sulfide was the main sulfur species existing in the SHR process[62]. As can be seen in Fig.2.4, the sorbent contributed to the capture of sulfur. The sulfur retained percentage was increased from 20% to over 90% with the CaO/C increased from 0.12 to 1.14.

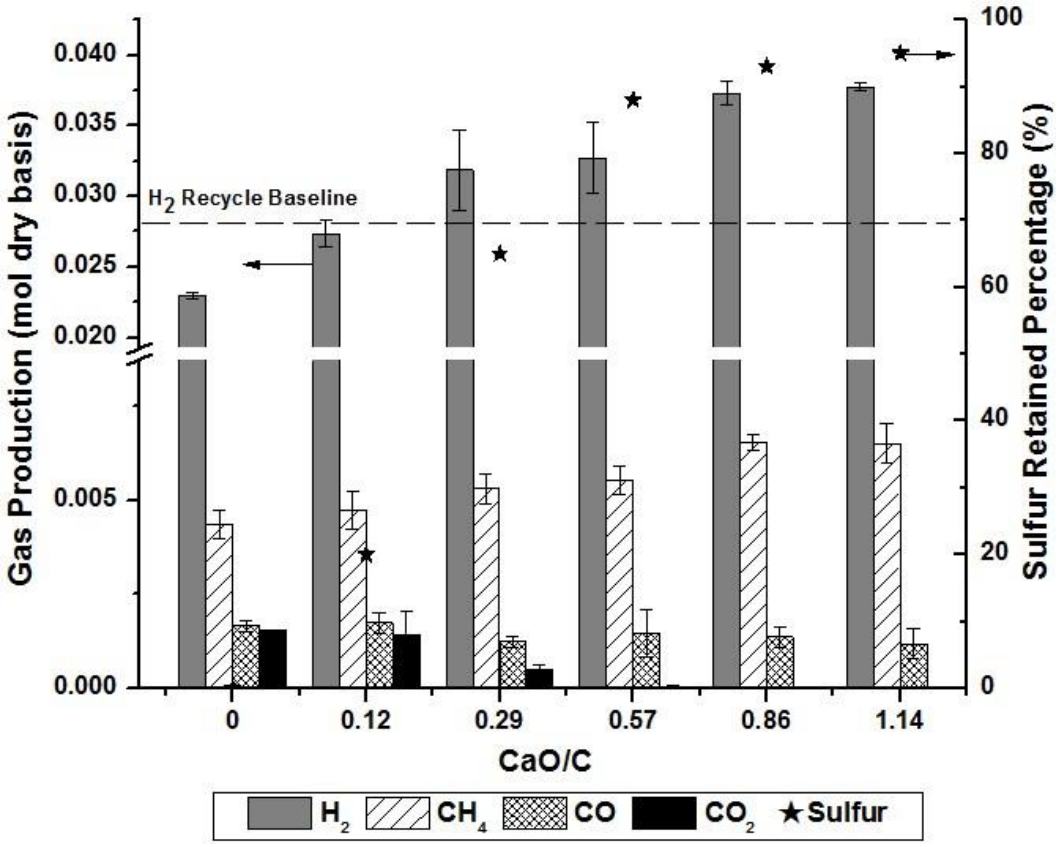

Fig.2.4 The effect of CaO/C ratio on gas production and sulfur retained percentage

These results clearly demonstrated the potential merits of the process coupling steam hydrogasification and sorption enhanced technology. The enhanced performance was primarily the consequence of the instant removal of CO_2. When the product CO_2 was removed from the system by the sorbent, reactions were moved forward to get higher yields of the other product gases like H_2. With more sorbent introduced, more CO_2 was captured and more energetic gases were produced.

In order to have a detailed explanation, Fig.2.5 lists the most important possible reactions involved in the SE-SHR.

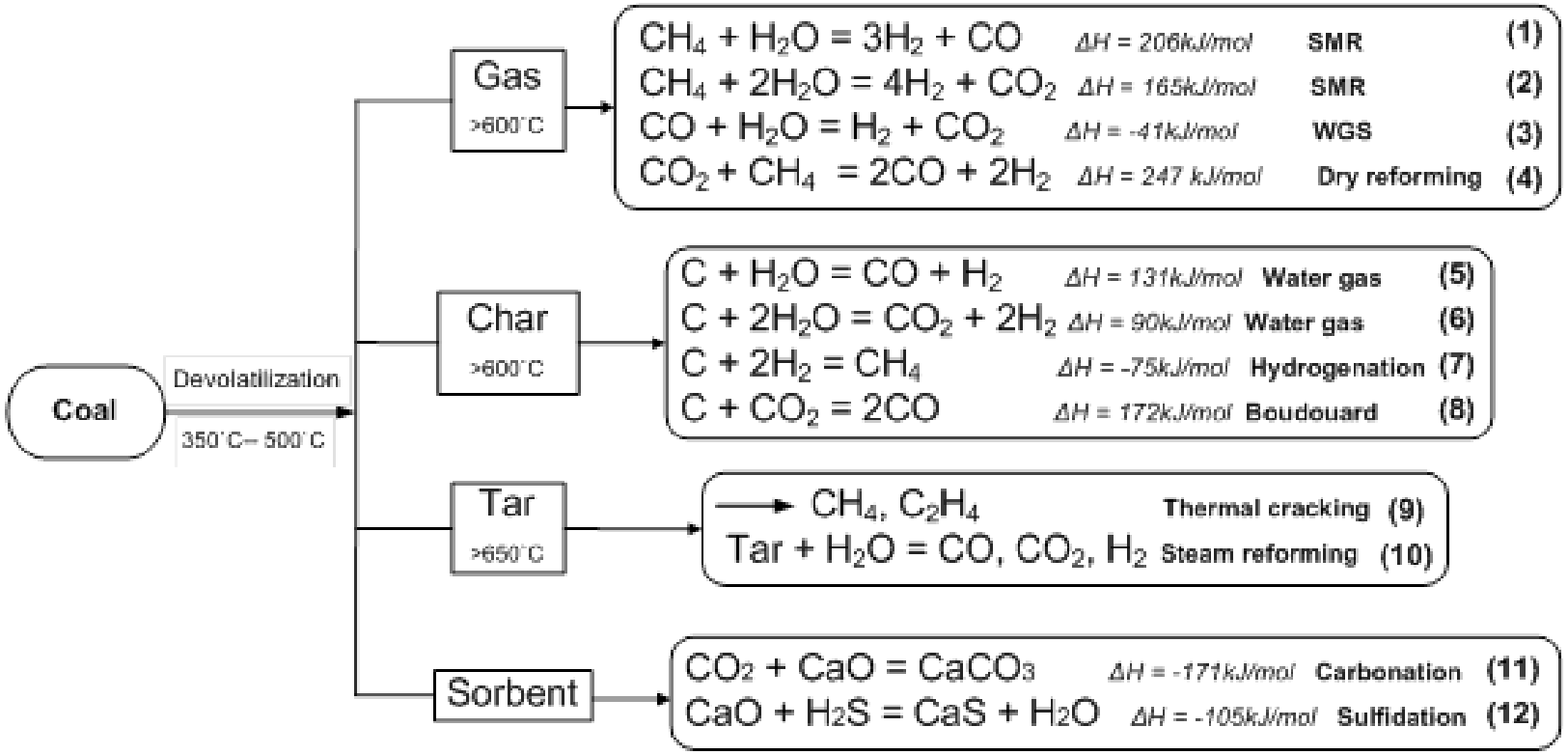

Fig.2.5 Schematic of thermochemical reactions involved
(All ΔH obtained from NIST Chemistry Webbook using heats of formation at 298K)

As shown in Fig.2.5, the devolatilization reactions occurred from 350°C to 500°C and coal was decomposed into gas, tar and char. Gas phase reactions and solid-gas reactions occurred at the same time. Cracking and reforming of volatile matter and tar occurred in the range of 600°C and 650°C and were most important for the final product gas composition. Char gasification became active from 600°C. Finally, as a consequence of the high pressure (i.e. the ultimate pressure of all experiments was around 2.2MPa) and comparatively lower reaction temperature (<800°C) inside the reactor, carbonation and sulfidation were co-existing.

With the instant and continuous removal of CO_2 from the product gas, most CO_2 related reactions were driven forward, including WGS reaction (eq.3), water gas reaction (eq.6) and SMR (eq.2). As seen from these equations, due to the enhanced shift, more CO, char and CH_4 were consumed. Meanwhile, more H_2 was produced. In particular, because of higher H_2 concentration, hydrogenation (eq.7) was enhanced, which offset the consumption of CH_4 and made its yield increase a little bit.

In addition, the Boudouard reaction (eq.8) was hindered due to the lack of CO_2. With much higher H_2 concentration, the other SMR (eq.1) and water gas (eq.5) reactions were possibly not favored to the right side. This led to less CO produced. Besides, the carbonation reaction (eq.11) was exothermic and at the point where it captured CO_2 it released heat with the temperature increase in its surrounding. Hence, it was most likely conducive to the decomposition of tar[76]. From eq.9 and eq.10, it indicated that the enhancement of tar thermal cracking and tar steam reforming resulted in the increase of

H_2 and CH_4. Previous study already showed only H_2S existing in the SHR system[59-62]. Therefore, it was believed that most sulfur was in the form of CaS by sulfidation (eq.12). Sun also reported good performance of co-capture of H_2S and CO_2 in a pressurized-gasifier-based process. In particular, H_2S was proved to be much less of a problem than SO_2 in impeding CO_2 capture[101]. Consequently, for SHR system with a reducing atmosphere, co-capture of both target gases is always favored. Summarily, the result was that the SE-SHR improved the production of H_2 and CH_4 with the abatement of CO, H_2S and CO_2 and more sorbent led to more H_2.

X-ray diffraction was used to characterize the samples with different CaO/C ratio before and after gasification. Lignite, lignite-CaO mixture with CaO/C of 0.29 and 0.86, and their corresponding gasfication residues were selected as the sample. The X-ray diffraction patterns are shown in Fig.2.6.

There was no crystalline structure detected in lignite and lignite residue due to its amorphous species. When CaO was mixed with the feedstock, it was identified in the form of $Ca(OH)_2$. It was because CaO is very easy to get hydrated on its surface during storage. In Fig.2.5, plot 4 and 5 show that $Ca(CO)_3$ was formed in SE-SHR. Especially for the case with more CaO addition (CaO/C=0.86), there was some CaO left in the gasification residue in the form of $Ca(OH)_2$. It indicated that CaO loading was over the CO_2 amount generated in SE-SHR. Besides, the char was found in terms of carbon.

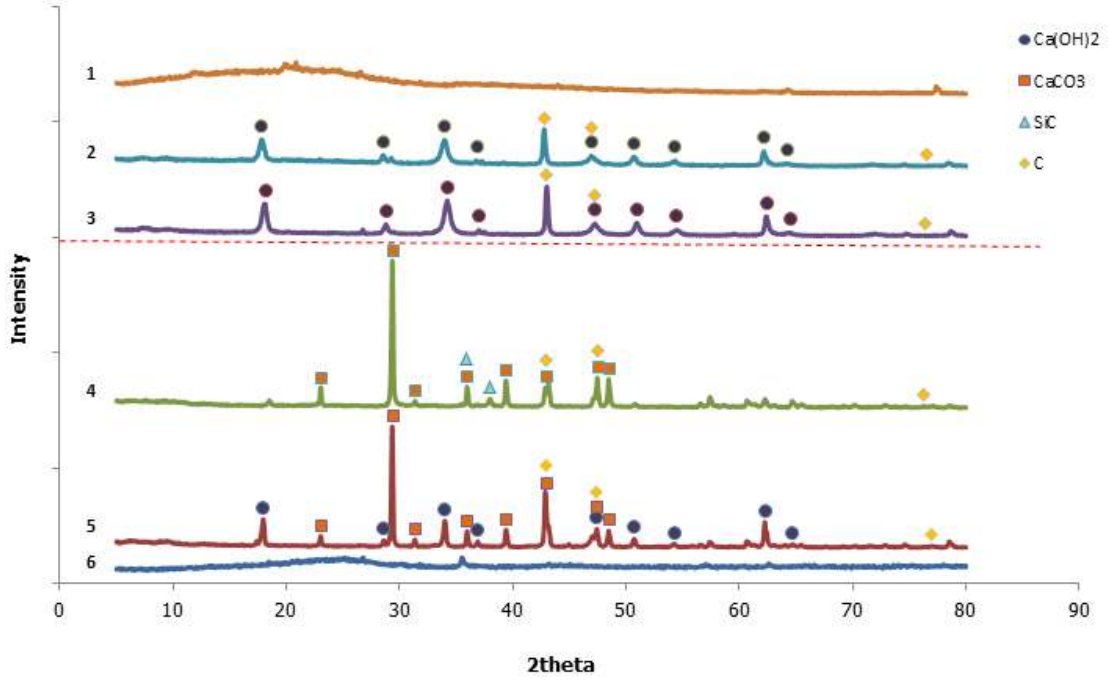

Fig.2.6 X-ray diffraction patterns of lignite, lignite-CaO mixture and corresponding gasification residue: (1. lignite 2. lignite-CaO mixture with CaO/C=0.29 3. lignite-CaO mixture with CaO/C=0.86 4. lignite-CaO gasification residue with CaO/C=0.29 5. lignite-CaO gasification residue with CaO/C=0.86 6. lignite gasification residue)

2.2.2 Relationship between energetic gas increment and captured CO_2 amount

The relationship between energetic gas increment (H_2 and CH_4) and captured CO_2 amount is depicted in Fig.2.7 and Fig.2.8. In Fig.2.7, it can be seen that the increase of H_2 was as a function of the amount of captured CO_2. Linear regression analysis was conducted on these data, the equation of which was shown as below. The correlation coefficient was 0.9922.

$$H_2 \text{ (Increment)} = 0.72CO_2 \text{ (Captured)} + 0.0004 \quad \text{(mol)}$$

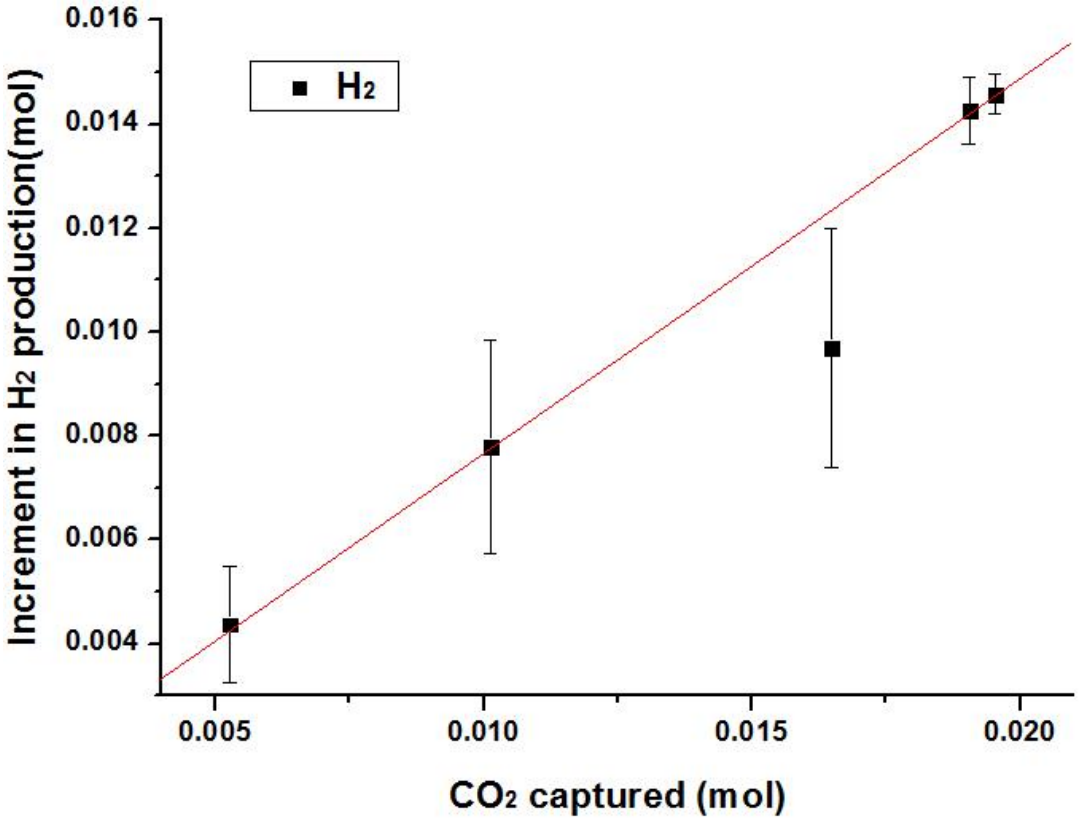

Fig.2.7 Relationship between H_2 increment and CO_2 captured amount

This intimate relationship indicated that some reactions having both H_2 and CO_2 as product, such as WGS and water gas, were actively involved in the SE-SHR.

As shown in Fig.2.8, CH_4 ascended gradually with the increase of captured CO_2 amount. The linear equation fitted for these points is listed below. The correlation coefficient was 0.9113.

CH_4 (Increment) = 0.14CO_2 (Captured) - 0.0007 (mol)

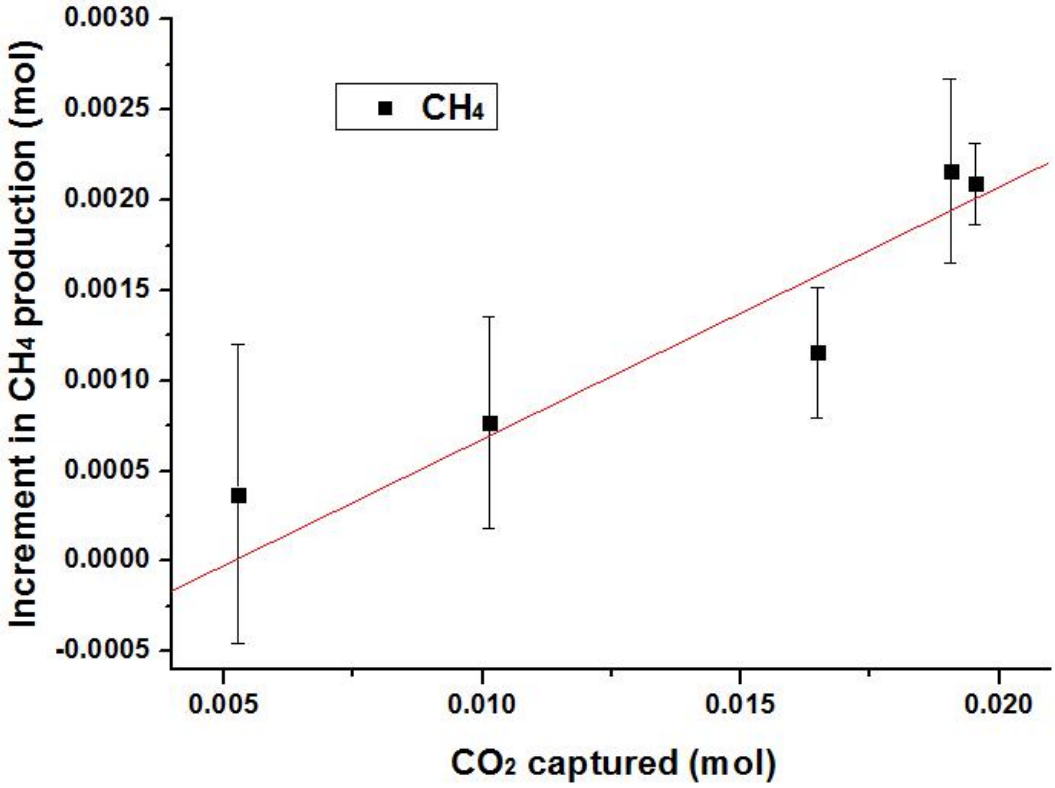

Fig.2.8 Relationship between CH_4 increment and CO_2 captured amount

The relationship between CH_4 and CO_2 was not as good as that between H_2 and CO_2. It was most likely because the increase of CH_4 was enhanced by hydrogenation reaction during SE-SHR. Hydrogenation is comparatively slower than the other reactions with regard to steam. Thus, the CH_4 increment was limited. Additionally, the final pressure in the reactor did not increase too much. The pressure could not favor the hydrogenation to produce more CH_4.

2.2.3 Effect of temperature

Temperature is an important variable in gasification. The temperature of the reactor was varied from 650°C to 800°C with and without the sorbent. The effect of temperature

on carbon conversion and gas production are shown in Fig.2.9 and Fig.2.10, respectively. From both figures, notice that an increase in temperature enhanced the conversion percentage and production of CH_4 with or without the sorbent. At each reaction temperature, adding the sorbent reduced the CO_2 significantly and also increased the H_2 when compared without sorbent. It can be seen that the conversion percentages of char and C_{2+} decreased after the introduction of sorbent. Additionally, when the temperature was raised, there was also a simultaneous increase in the percentage of CO_2 captured and H_2 yield which supported the positive influence on the shift conversions. However, due to the enhancement of water gas reaction, too high temperature like 800°C would produce more CO_2 which was over the capacity of the sorbent loading. So the optimum temperature should be around 750°C, with the consideration of improving CH_4 production and minimizing CO_2 emission. Furthermore, the H_2 production with sorbent addition was higher than the minimum recycle requirement at each temperature, showing that the reaction temperature could be reduced to as much as 700°C to get enough recycled H_2 disregarding to the other gas yields.

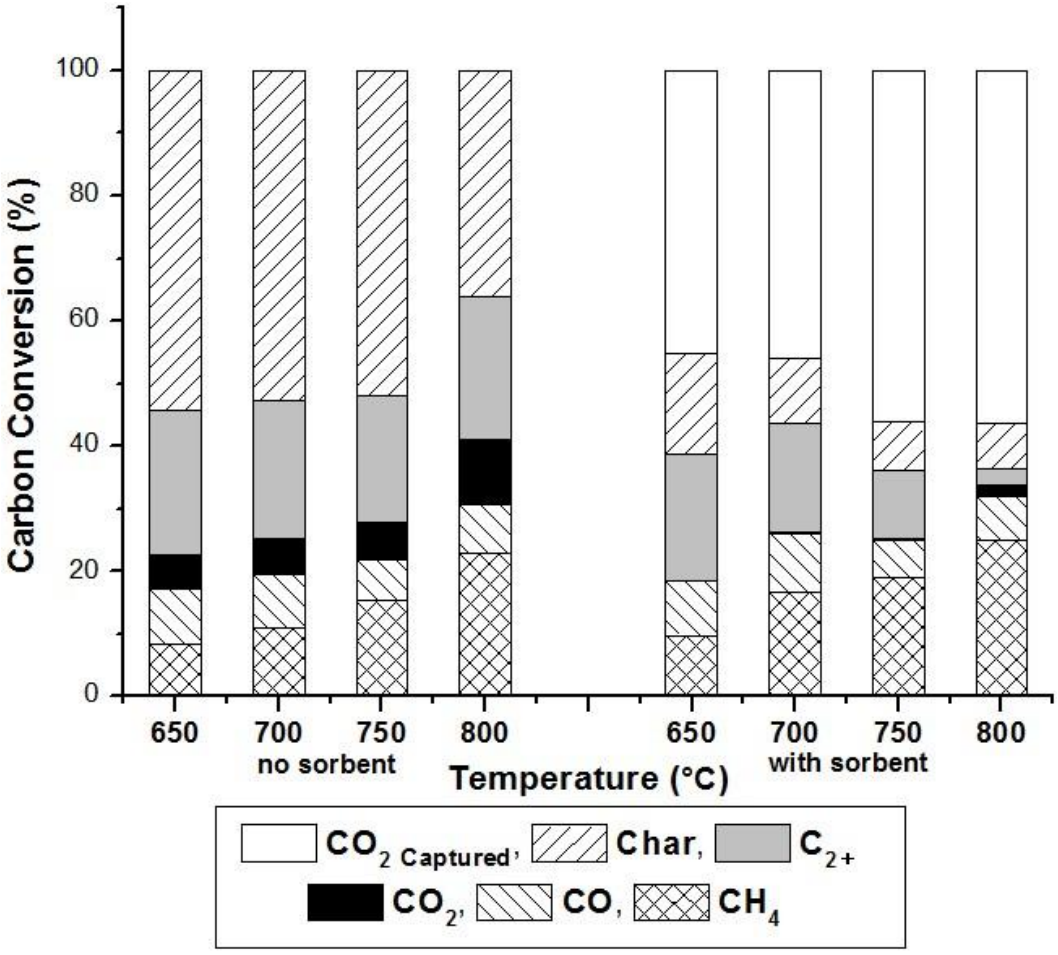

Fig.2.9 The effect of temperature on carbon conversion

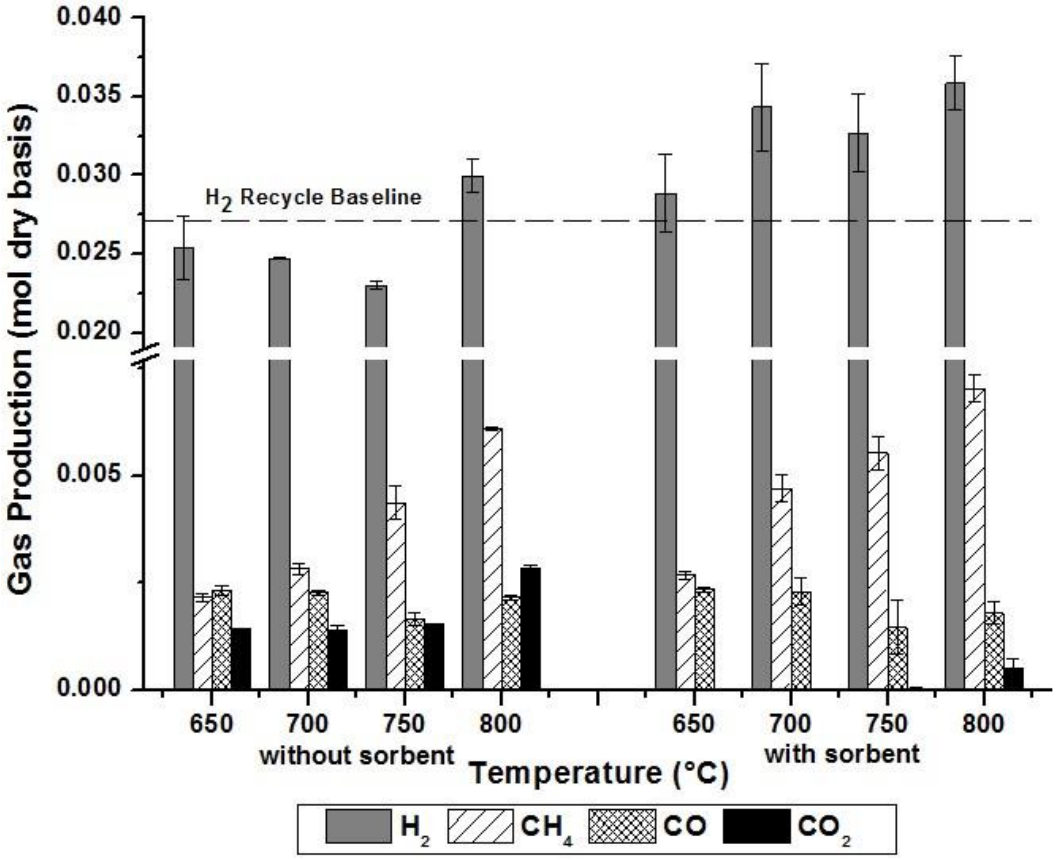

Fig.2.10 The effect of temperature on gas production

2.2.4 Effect of sorbent particle size

The particle size of sorbent is another important factor influencing the sorption enhanced performance. The change in gas production with the increase of the sorbent particle size is shown in Fig.2.11. It can be seen that CO_2 could be reduced to almost zero regardless of the particle size. Although the production of H_2 decreased slightly with the increase of particle size, H_2 could still meet the recycle requirement when particle size was increased to the range of 1.7-2mm. In the meantime, CH_4 and CO decreased slightly. Because large particle possessed less surface area, there were comparatively limited sites

for the gas solid reaction to proceed. This made less CaO react with CO_2, mitigating the increment of H_2 via shift reaction.

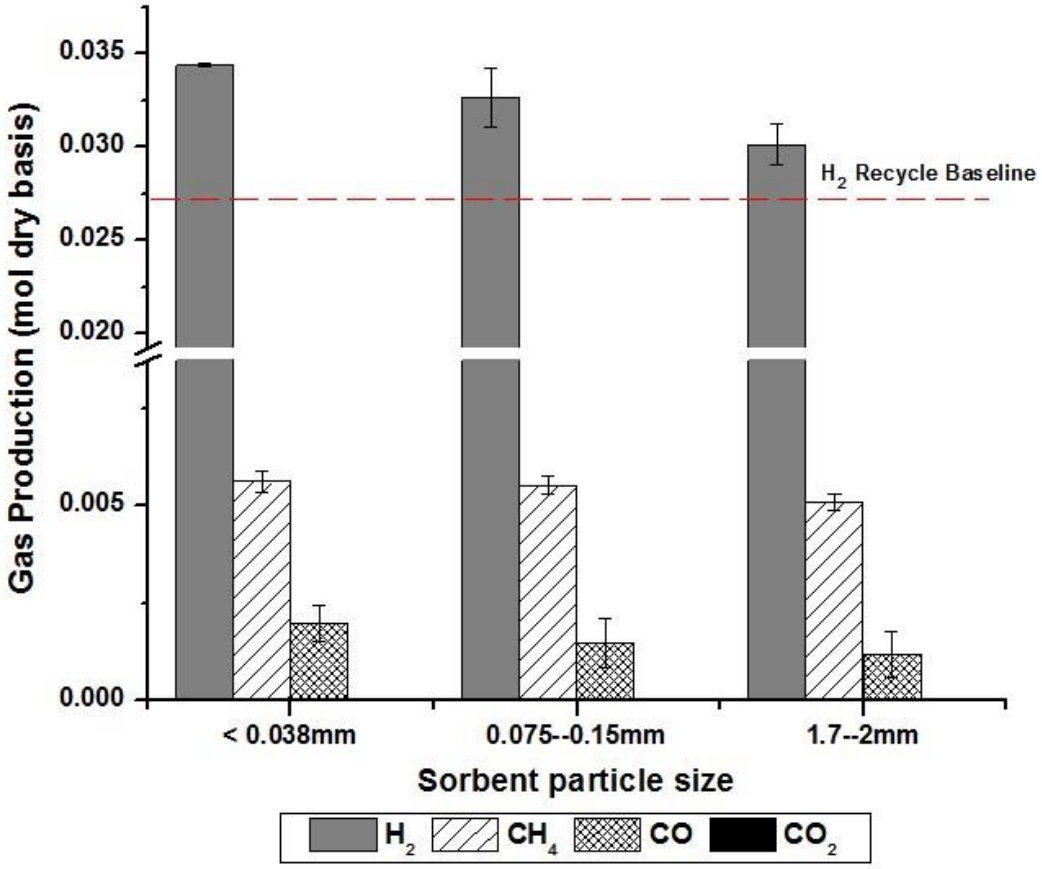

Fig.2.11 The effect of sorbent particle size on gas production

2.2.5 Comparison of SE-SHR and SE-HG

The sorption enhanced performance of HG and SHR is compared in Fig.2.12. Without sorbent addition, the H_2 yield of HG was less than that of SHR. SHR produced more CH_4 and CO_2 than HG did. It was mainly due to the enhancement by steam addition, improving the water gas reaction. When sorbent was added into the reactor (CaO/C=0.56), for both reaction types, CO_2 was hardly seen in the product gas and the yields of H_2 and

CH_4 were increased compared without sorbent. However, even with sorbent addition, SE-HG could not generate enough H_2 over the recycle baseline. Only SE-SHR could make it. This implied that steam played an important role in improving the H_2 yield in SE-SHR.

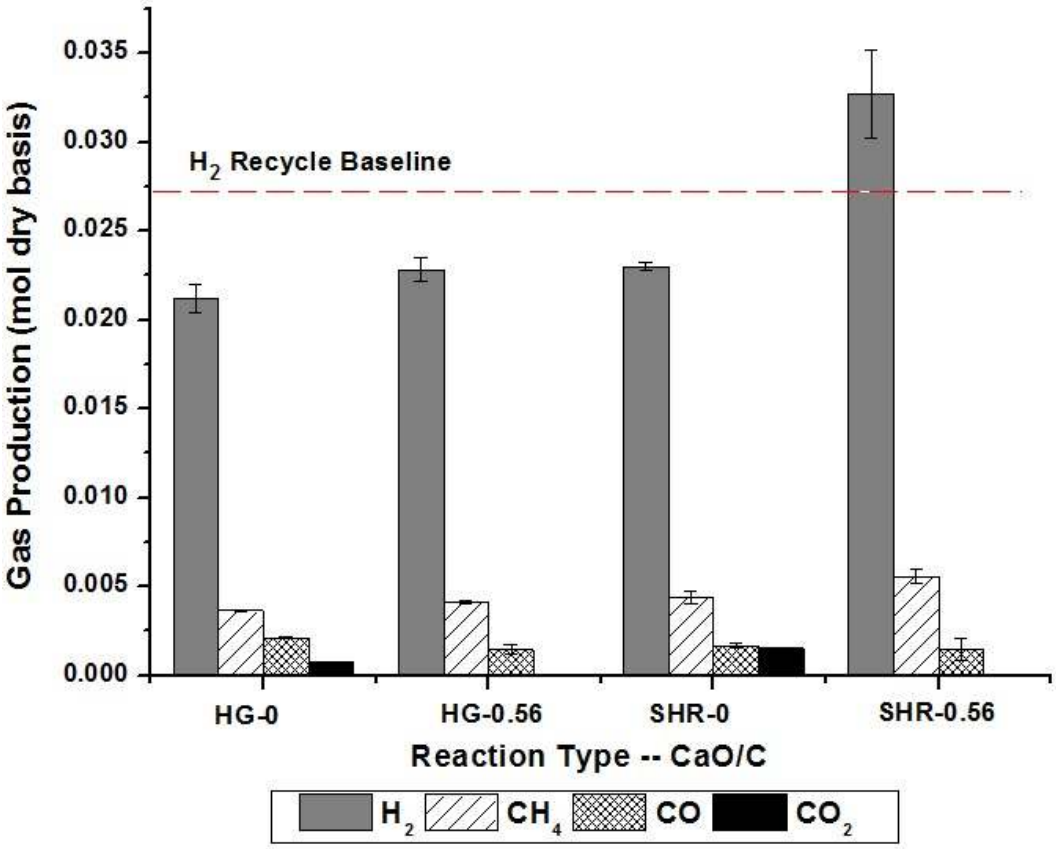

Fig.2.12 The comparison of gas production between SE-HG and SE-SHR

2.2.6 Effect of H_2/C ratio

Fig.2.13 shows the combined effect of Steam/C and H_2/C molar ratios on the H_2 yield. For both SE-SHR and SHR, at each Steam/C of 1.67, 2.22 and 2.78, the H_2 yield was enhanced with the increase of H_2/C. It was mainly due to more initial H_2 input. Excess amount of H_2 still remained in the reactor. The H_2 amount reached the maximum 0.042mol when H_2/C and Steam/C were set at 1.59 and 2.78, respectively. The H_2 recycle

baseline is plotted in terms of dotted line in Fig.2.13, which represents the initial H_2 input of 0.0158mol, 0.0271mol, and 0.0398mol, corresponding to each gasification condition. Except for the condition with H_2/C of 1.59 and Steam/C of 1.67, H_2 yields in SE-SHR all exceeded their corresponding baselines. It indicated that H_2 amount was already enough for recycle use in the gasifier and extra H_2 (the amount beyond the baseline) could be used for downstream processes like methanation. In particular, under the excluded condition aforementioned, lower steam input could not produce enough H_2 for cyclic use, implying that steam played a very important role in H_2 production. Thus, when Steam/C was increased to 2.22, the H_2 production was beyond the baseline. By contrast, H_2 yields in SHR did not exceed the recycle baseline.

By integrating the results of SE-SHR and SHR in Fig.2.13, the percentage increase in H_2 production was obtained and is shown in Fig.2.14. At each Steam/C, the percentage increase was descending with the ascent of H_2/C. It meant that more H_2 input lessened steam gasification during SE-SHR. This made less CO_2 generated, which mitigated the SE-SHR performance. Because less CO_2 was captured, less extra H_2 was generated.

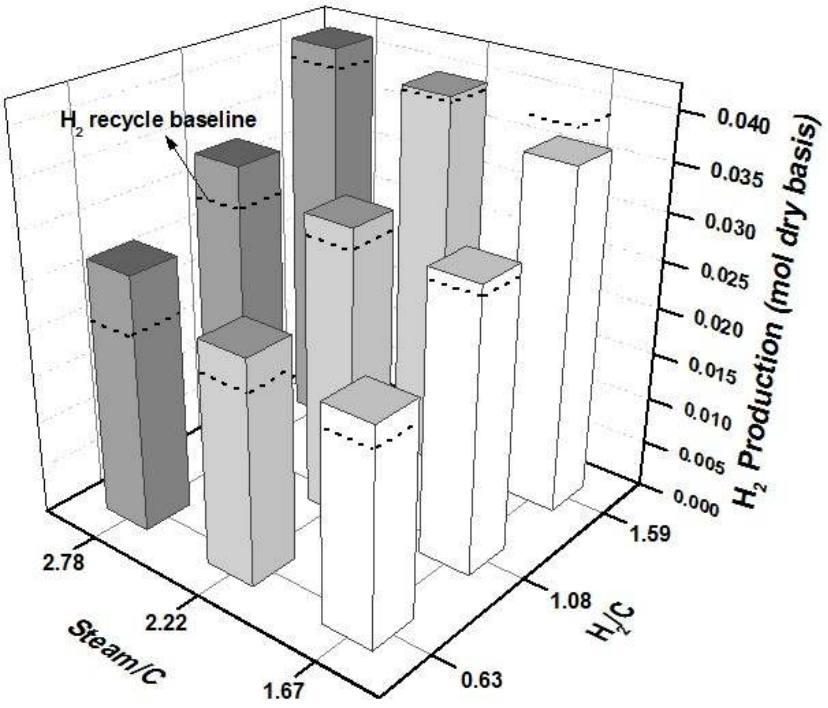

(a) SE-SHR

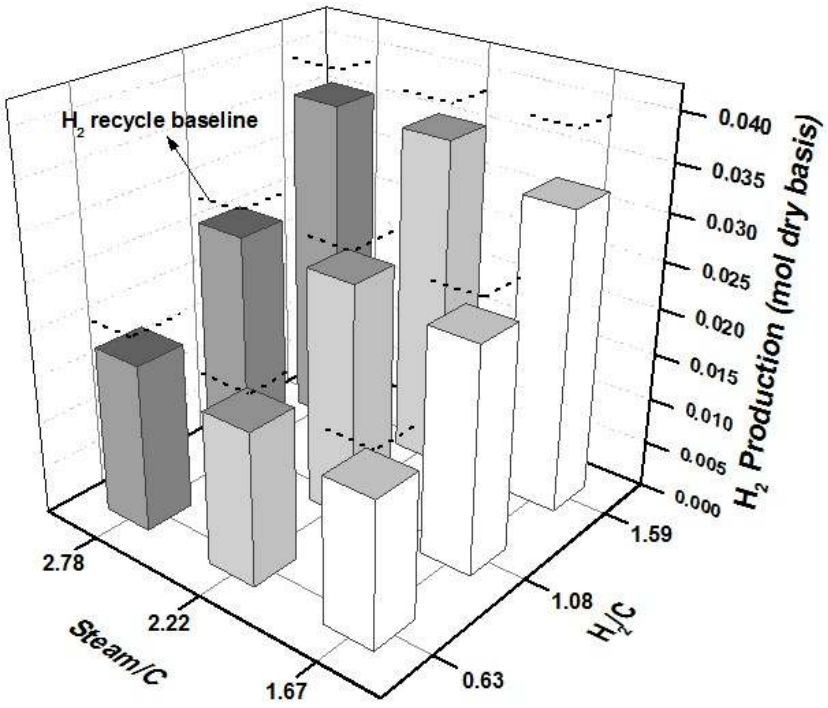

(b) SHR

Fig.2.13 The combined effect of Steam/C and H_2/C ratios on H_2 production

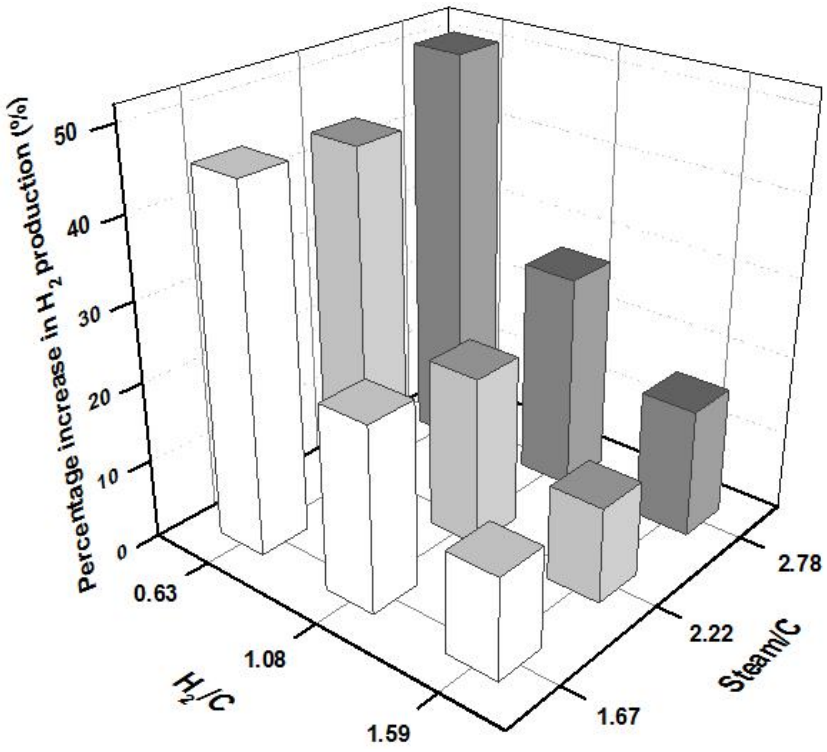

Fig.2.14 The percentage increase in H_2 production with sorbent addition

The data of CH_4 is shown in Fig.2.15. At each Steam/C, for both SE-SHR and SHR, the CH_4 yield was improved with the increase of H_2/C. It indicated that hydrogenation was enhanced with higher H_2 input and the hydrogasification was gradually predominant. Additionally, it can be seen that the CH_4 yield of SE-SHR was higher than that of SHR under the same gasification condition.

The results of CO and CO_2 are presented in Fig.2.16 and Fig.2.17, respectively. The increase of H_2/C in both SE-SHR and SHR reduced the yields of CO and CO_2 at each Steam/C. It implied that some CO and CO_2 related reactions (e.g. water gas reaction) were affected by more H_2 input. Besides, the CO and CO_2 yields of SE-SHR were lower than those of SHR.

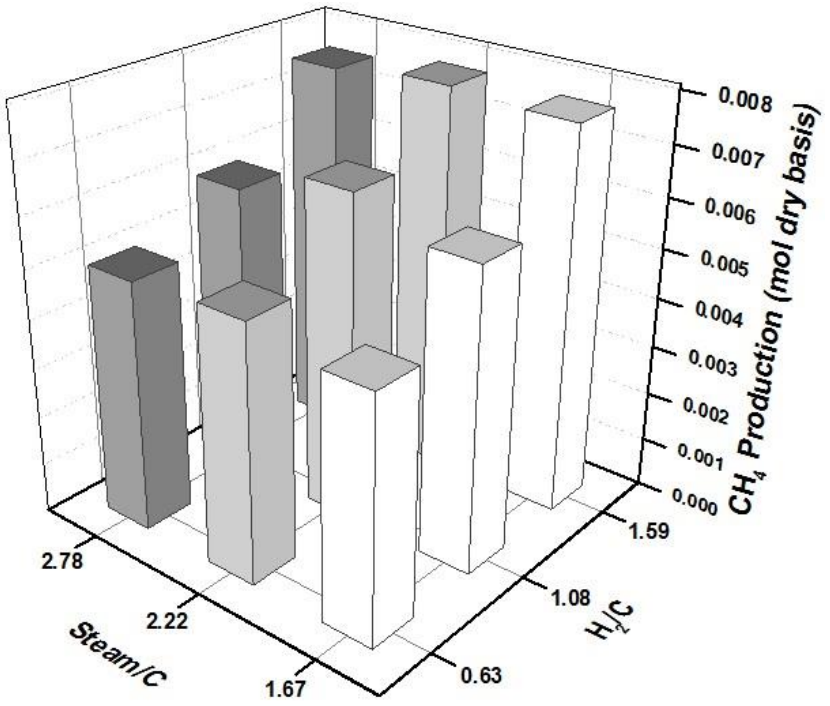

(a) SE-SHR

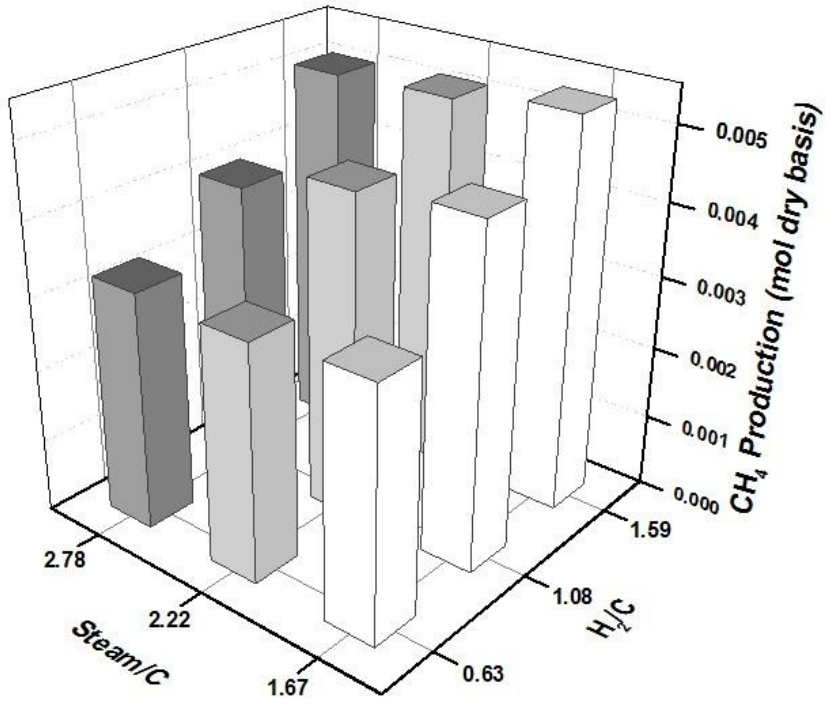

(b) SHR

Fig.2.15 The combined effect of Steam/C and H_2/C ratios on CH_4 production

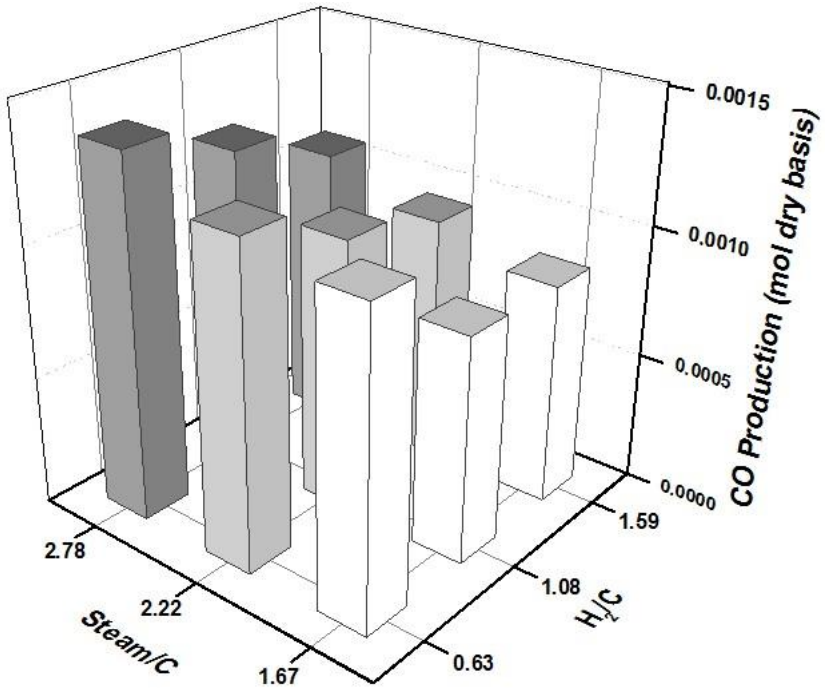

(a) SE-SHR

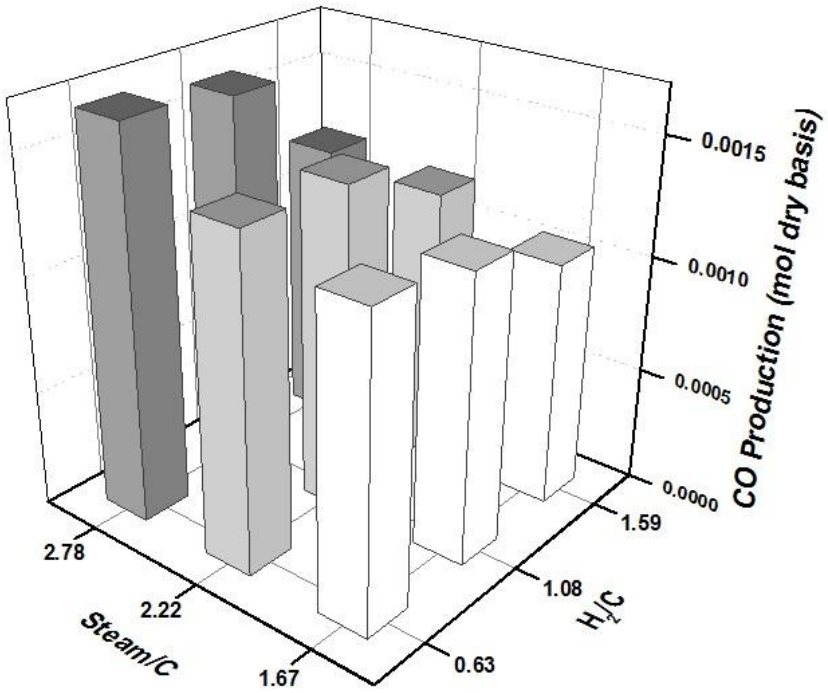

(b) SHR

Fig.2.16 The combined effect of Steam/C and H_2/C ratios on CO production

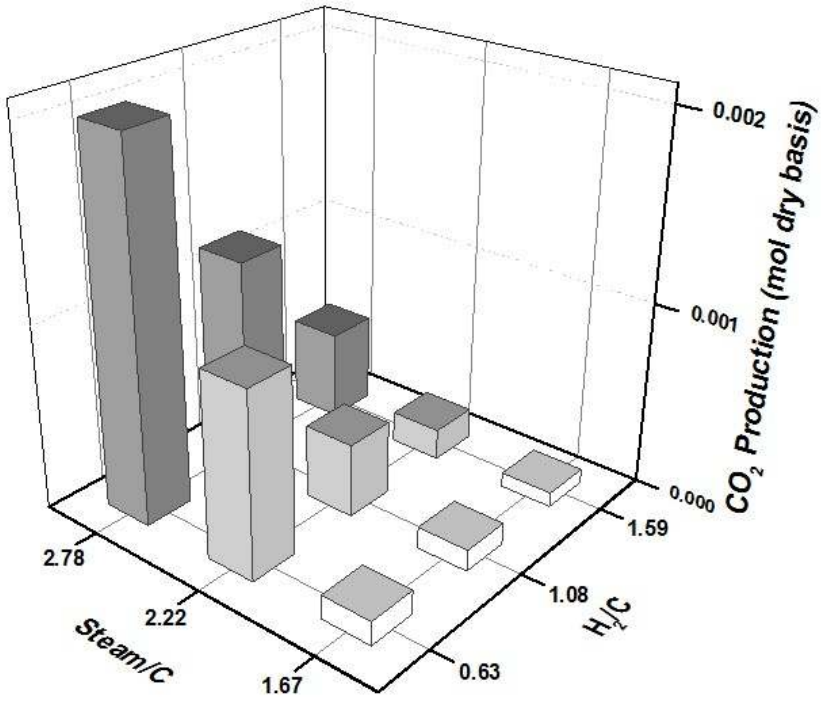

(a) SE-SHR

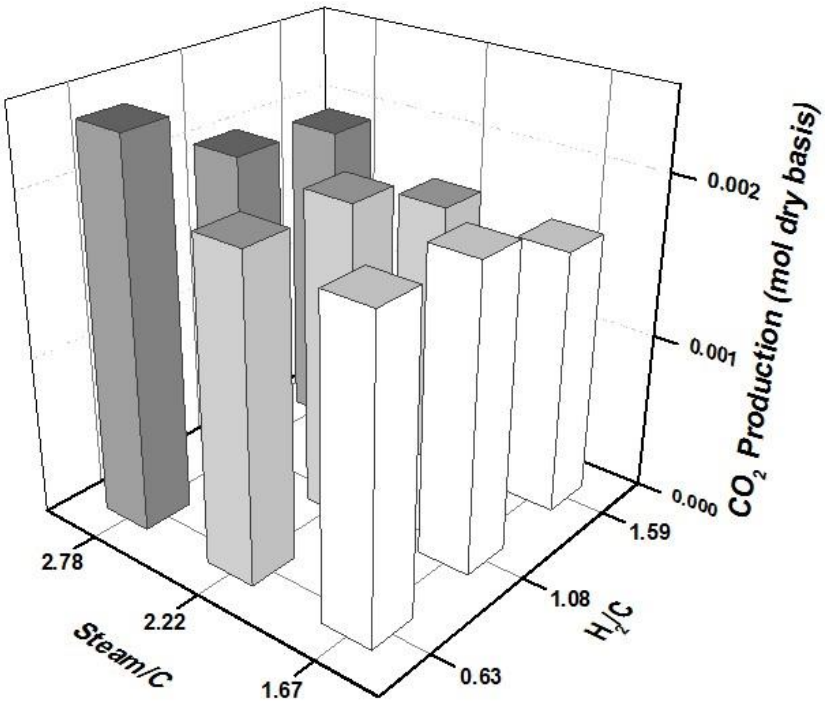

(b) SHR

Fig.2.17 The combined effect of Steam/C and H_2/C ratios on CO_2 production

By integrating the results of SE-SHR and SHR in Fig.2.17, the percentage decrease in CO_2 production is depicted in Fig.2.18. It can be seen that more CO_2 was captured with the increase of H_2/C at each Steam/C. Also, when Steam/C was set at 1.67, the decrease percentage could reach highest. All percentages were over 90% at three H_2/C ratios. It was mainly due to less CO_2 was produced in high H_2 containing environment. The fixed amount of sorbent (CaO/C=0.36) was sufficient for CO_2 capture with Steam/C of 1.67.

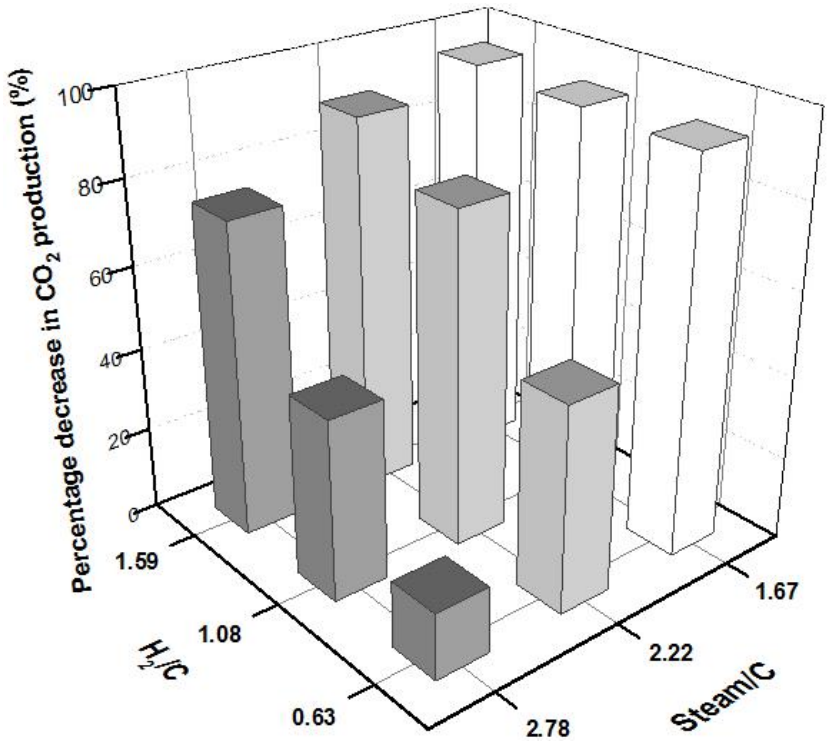

Fig.2.18 The percentage decrease in CO_2 production with sorbent addition

Summarily, with the increase of H_2/C at each Steam/C, the production of H_2 and CH_4 was enhanced while that of CO and CO_2 was decreased. The increase of H_2 was mainly because of more H_2 input. According to Fig.2.5, the enhancement of CH_4 production was mostly due to the improved hydrogenation (eq.7) with higher H_2/C. Also, SMRs (eq.1,

eq.2) were possibly affected by more H_2. Therefore, less CH_4 was consumed. In particular, the enhancement of CH_4 production in SE-SHR was partially contributed from more H_2 due to SE. The proposed pathway is shown in Fig.2.19(a). When char was exposed to more H_2 from two sources (input and SE), there were more chances for hydrogenation to happen between carbon and hydrogen than those for water gas reactions to happen between carbon and steam. In addition, more H_2 input could affect the production of CO and CO_2 during SMR (eq.1) and water gas reactions (eq.5, eq.6).

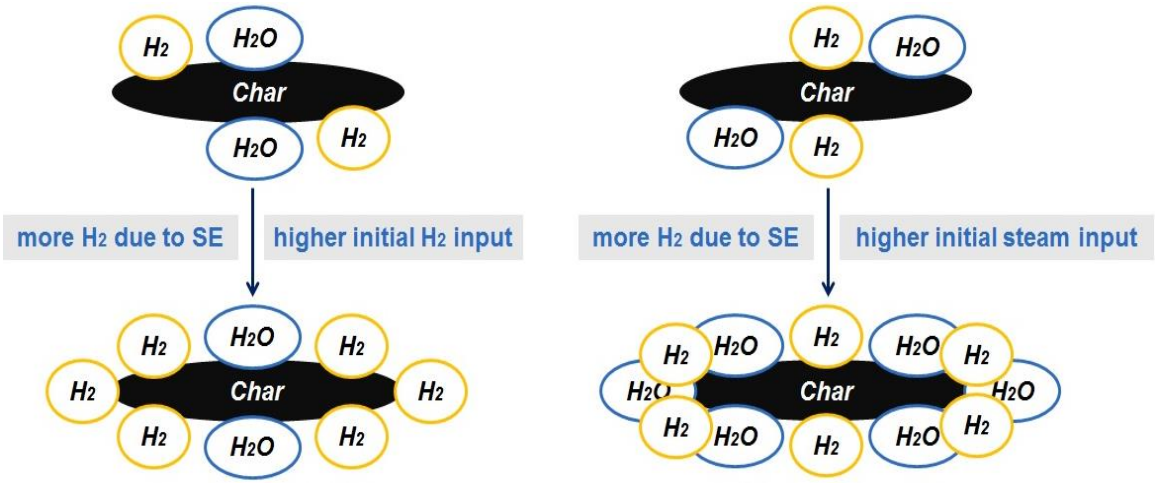

(a) (b)

Fig.2.19 Schematic representation of the proposed pathways describing the interaction of char with gasification agents during the SE-SHR:

(a) with higher H_2/C (b) with higher Steam/C

2.2.7 Effect of Steam/C ratio

In Fig.2.13, when H_2/C was fixed at 0.63, 1.08 and 1.59, the increase of Steam/C enhanced the H_2 production gradually. It implied that steam gasification resulted in more H_2 yield. When steam input was increased, sufficient H_2 amount could be guaranteed for

recycle use. Especially for the condition with H_2/C of 1.59, the extra H_2 production was enhanced from negative to positive by increasing Steam/C. The increase percentage in H_2 production is shown in Fig.2.14. The increase of Steam/C could produce more extra H_2 when Steam/C was increased to 2.78.

The production of CH_4 had different trend between SE-SHR and SHR. Fig.2.15(a) shows that the increase of Steam/C did not affect the CH_4 production during SE-SHR, while Fig.2.15(b) shows that the CH_4 production decreased slightly during SHR. For both SE-SHR and SHR, SMR could be improved with more steam input, leading to less CH_4. In particular, the consumption of CH_4 during SE-SHR was most likely offset by other reactions at the same time, resulting in the insensitive behavior to the Steam/C change. This will be discussed later.

Besides, the increase of steam enhanced the yields of CO and CO_2 remarkably at each H_2/C shown in Fig.2.16 and Fig.2.17. This was primarily due to the domination of steam gasification. In addition, it can be seen that more CO_2 could not be captured during SE-SHR with higher steam input because the CO_2 amount was already beyond the limited capacity of sorbent loaded. Correspondingly, in Fig.2.18, the decrease percentage in CO_2 production was reduced with the increase of Steam/C at each H_2/C. CO_2 yield reached highest when H_2/C was 0.63 and Steam/C was 2.78. Thus, more sorbent should be added under higher Steam/C.

Summarily, when Steam/C was raised at each H_2/C, the yield of H_2, CO and CO_2 was improved. When more steam was added, WGS (eq.3), water gas reaction (eq.6) and SMR

(eq.2) were enhanced. Hence, more CO_2 was generated. The increase of CO was because that SMR (eq.1) and water gas (eq.5) reaction were favored with more steam input. Furthermore, it was possibly due to the enhancement of Boudouard reaction (eq.8) and dry reforming (eq.4) when more CO_2 was generated. H_2 production was improved via several reactions with higher Steam/C, including SMRs (eq.1, eq.2), WGS (eq.3) and water gas reactions (eq.5, eq.6). With more CO_2 produced, enhanced dry reforming (eq.4) could also lead to more H_2. During the increase of CO_2, CO and H_2, CH_4 was always consumed as a reactant in couple reactions, such as SMRs (eq.1, eq.2) and dry reforming (eq.4). Therefore, CH_4 yield was decreased during SHR. On the other hand, because of simultaneous enhanced H_2 production during SE-SHR, hydrogenation (eq.7) was also enhanced. Hydrogenation most likely made up CH_4. Accordingly, CH_4 did not have too much change in its final yield. The schematic of this evolution was shown in Fig.2.19(b). It shows that more H_2 was generated due to SE and instantly involved in the competition with steam to react with char to produce CH_4.

2.3 Summary

The performance of SE-SHR was evaluated by varying different gasification parameters. The main findings are listed below.

1. It was found that the addition of sorbent could remove CO_2 within SHR and increase the energetic gas (H_2 and CH_4) production for different kinds of feedstock. In particular, the amount of H_2 was increased dramatically and enough for recycle use over the CaO/C molar ratio of 0.29.

2. Sorbent addition improved the H_2 production with CO_2 captured at different temperatures and the reaction temperature could be reduced to 700°C to get enough recycle hydrogen. Higher temperature favored higher energetic gas yield, but too high temperature (e.g. 800°C) would produce more CO_2.

3. Sorbent with different particle size had the same positive effect on CO_2 removal and H_2 enhancement. In particular, small particle size could produce more energetic gases than larger size did.

4. With sorbent addition, hydrogasification could minimize the CO_2 production but could not increase enough H_2 yield for recycle use. Only SHR with sorbent addition could meet the H_2 recycle requirement.

5. When H_2/C was increased, the production of H_2 and CH_4 was increased and that of CO and CO_2 was decreased. This could be explained as hydrogasification was favored over steam gasification.

6. When Steam/C was increased, the yield of H_2, CO and CO_2 was improved. It was because steam gasification was predominant. Particularly, since more H_2 was produced during SE-SHR, the consumption of CH_4 was compensated by hydrogenation and CH_4 production had little change.

3. Kinetics Study of Sorption Enhanced Steam Hydrogasification Reaction

In this chapter, the study is focused on the kinetics study of SE-SHR using coal. A new lab-scale mini reactor was designed and a new configuration was set up for kinetics study. The new configuration could minimize the gas loss during real time gas analysis. The formation rate of CO_2, CO and CH_4 in the first 150 seconds was studied at three temperatures (650°C, 700°C and 750°C). Moreover, the effect of sorbent loading and feedstock-sorbent contact type on the gas evolution was investigated. The activation energy of each gas was calculated accordingly. The kinetics data were compared between SE-SHR and SHR.

3.1 Introduction to the kinetics study of conventional gasification and SHR

The development of thermochemical technologies includes the design of different reactors. As a key part of CE-CERT process development, the design of steam hydrogasifier requires fundamental study such as kinetics. The kinetics study of gasification could reveal the reaction rates of target products, which would help determine the reactor specifications (e.g. residence time) and practical operational conditions (e.g. temperature).

The kinetics of conventional gasification of carbonaceous materials (e.g. biomass and coal) has been extensively investigated. Most studies such as steam gasification and hydrogasification were based on solid phase change and non-isothermal condition[102-106]. On the one hand, this kind of study required certain time to reach the desired reaction temperature by using thermogravimeter with comparatively lower heating rate,

which could not exactly reflect the practical operation. Some literatures already showed that heating rate could have a significant influence on the reaction rates and product yields[107,108]. Consequently, isothermal kinetics study with higher heating rate is preferred due to its similarity to the real reactor such as fluidized bed gasifier. Accordingly, some instant loading systems were used in recent studies to get better and reliable data. For example, piston-driven injection and free drop tube reactor were used to mimic the real feeding condition[109,110]. On the other hand, when solid phase (e.g. char) is used for developing kinetics models, it usually takes a long time (e.g. several minutes for hydrogasification) to reach the complete conversion of the solid. Thus, it is not suitable for SHR study because the residence time in the real gasifier is limited and the unreacted char will be delivered to the combustor for heat supply. Therefore, the kinetics study based on the formation rate of individual gas could be a better option.

Especially for sorption enhanced gasification, Fujimoto investigated the kinetics of in situ CO_2 removal steam gasification and calculated the kinetic constants of the primary and secondary degradations from the product distribution[111]. He mentioned that the comparatively lower activation energy might be due to the effect of CO_2 sorbent. However, this research used a gradual heating system and there was no comparison between with and without sorbent under the same experimental condition. Besides this paper, there was limited kinetics literatures published related to the sorption enhanced gasification. Thus, a comprehensive investigation of the sorbent effect on kinetic parameters under isothermal condition is necessary for a complex gasification environment with both hydrogen and steam.

The previous kinetics studies of SHR were conducted by using three different lab-scale reactors. The first one was a 12cc volume non-stirred batch reactor, referred to as the Micro batch reactor[48]. The schematic diagram of the Micro batch reactor system and the photograph are shown in Fig.3.1. The reactor temperature was controlled by immersion into a molten salt bath with preheated temperature. The configuration was consisted of a main reactor, a capillary transfer line, a residual gas analyzer (RGA) and a data acquisition system. These four essential components were always kept for all kinetics studies of SHR, even with the development of new reactor system.

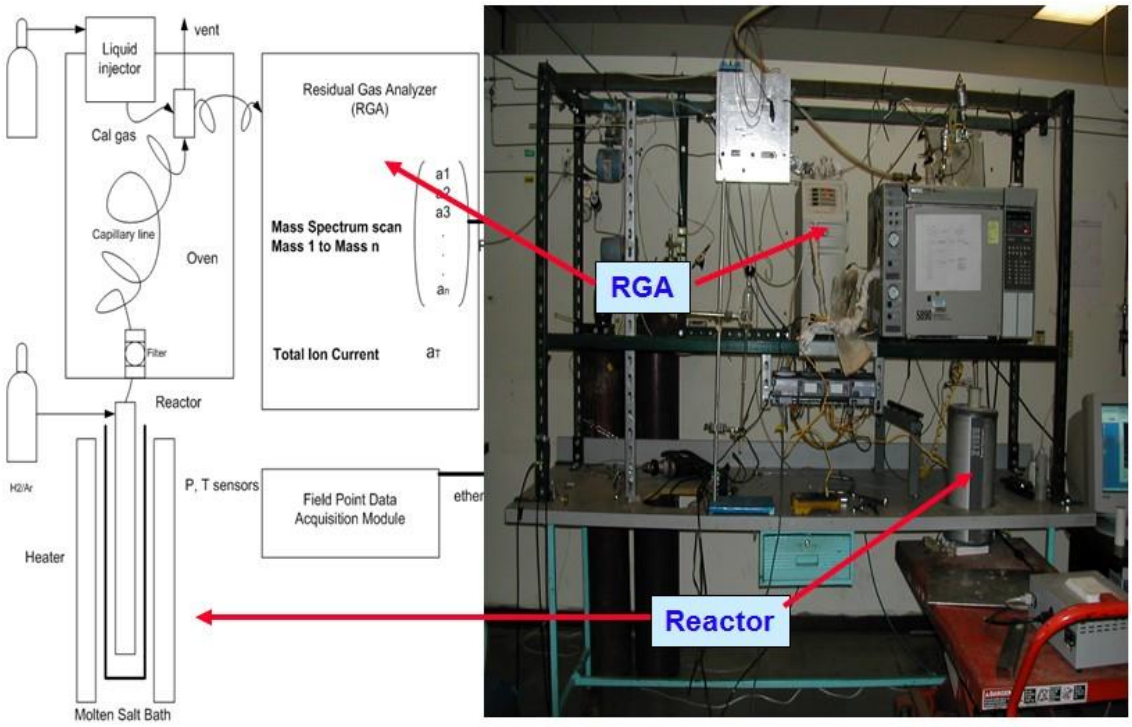

Fig.3.1 Micro batch reactor (Micro reactor) and configuration for kinetics study[48]

(a) Schematic diagram (b) Photograph

However, the Micro reactor could only take about 0.1g feedstock, which might not reflect the kinetics accurately. The reactor did not have inside mixing system. Hence, poor mass and heat transfer was expected. Besides, the partial evaporation of molten salt (i.e. Na_2CO_3) was a problem. Therefore, a continuous stirred batch reactor with 240cc was developed, referred to as the Mini batch reactor[112]. The schematic diagram and the photograph of the Mini reactor are shown in Fig.3.2. The mass and heat transfer was improved due to the addition of the continuous stirred impeller system. Moreover, the Mini reactor could withstand higher pressure up to 500psi than Micro reactor. The loading of Mini reactor was normally ranging from 0.5g to 1g.

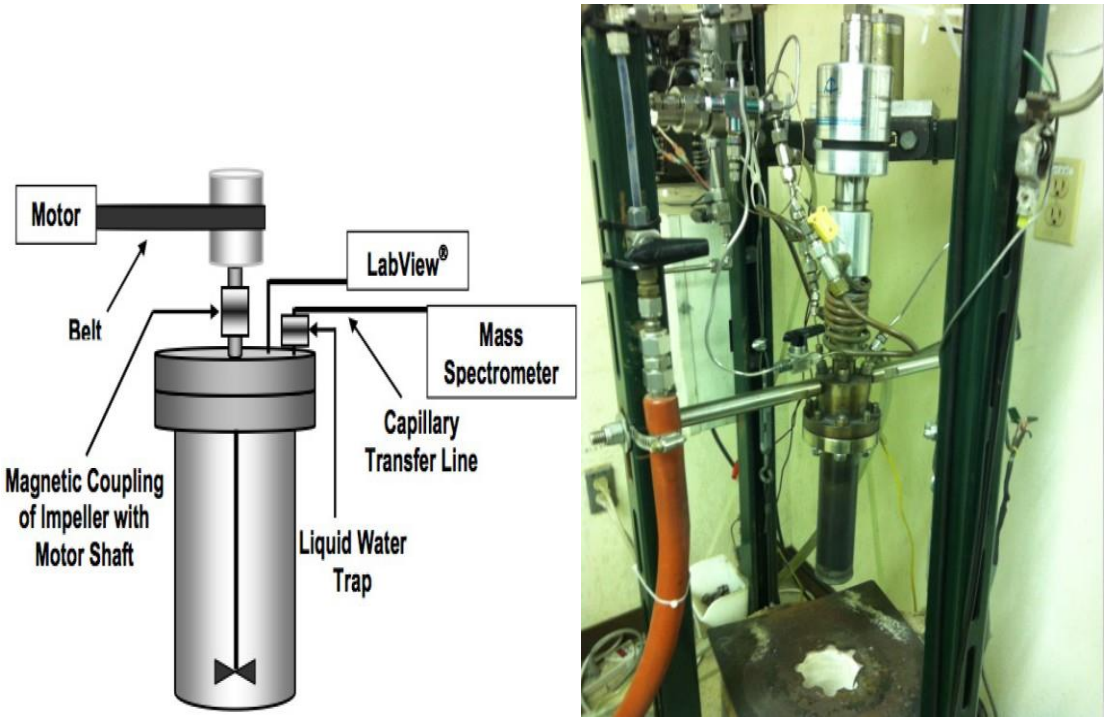

(a) (b)

Fig.3.2 Continuous stirred batch reactor (Mini reactor)

(a) Schematic diagram (b) Photograph

The heating rate in the Micro reactor was about 6K/sec; however, the Mini reactor was less than 1K/sec. The temperature profile is shown in Fig.3.3. Higher heating rate of Micro reactor was mainly because of the smallest volume. Though the heating rate was much faster than that of Mini reactor, it took over 2 minutes for Micro reactor to reach the gasification temperature of 750°C. The low heating rate of Mini reactor was due to larger reactor volume and greater wall thickness. Though Mini reactor improved the mass and heat transfer with higher feedstock loading and operation pressure, it was still pretty far from the superfast heating condition of practical gasification. This was the key factor influencing the accuracy of kinetics study. Consequently, the inverted stirred batch reactor (Inverted Mini rector) was developed for a better measurement of kinetic parameters. It is aimed to simultaneously address several problems (e.g. heating rate, mass and heat transfer, feedstock loading)

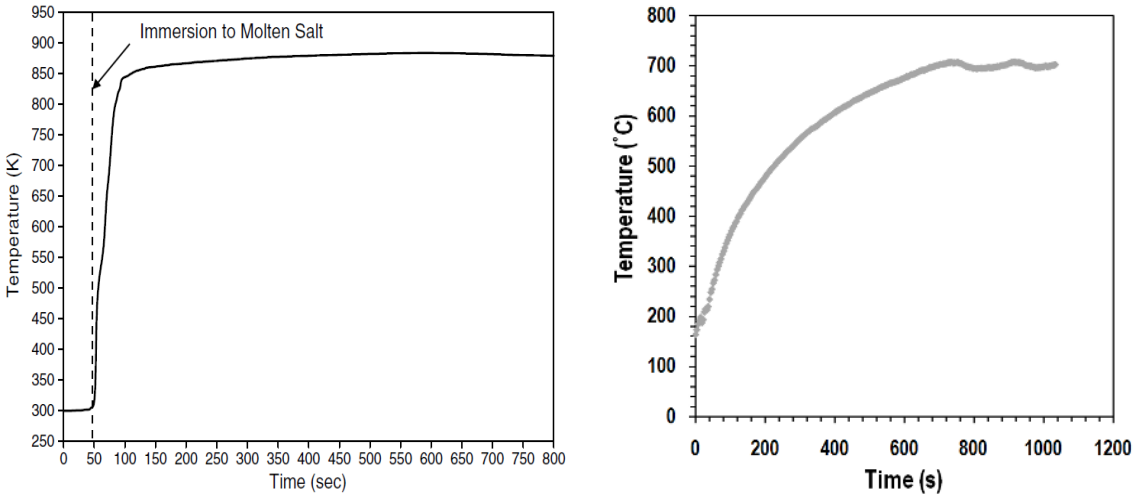

(a) (b)

Fig.3.3 The temperature profile during SHR kinetics study

(a) Micro reactor[48] (b) Mini reactor[113]

The schematic diagram and the photograph of the Inverted Mini reactor are shown in Fig.3.4. This configuration was consisted of a pressure-driven feeding system on the top, a reactor vessel with 280cc volume in the middle and an inverted-positioned impeller system at the bottom. The reactor contained a quartz tube with porous bottom plate in order to hold the dropped sample and to prevent the potential catalysis from the reactor material of Inconel. The feedstock was initially held on the injection ball valve and was then instantly introduced into the reactor by high pressure H_2 when the reactor temperature reached the desired point. The heating rate was estimated over 100K/sec.

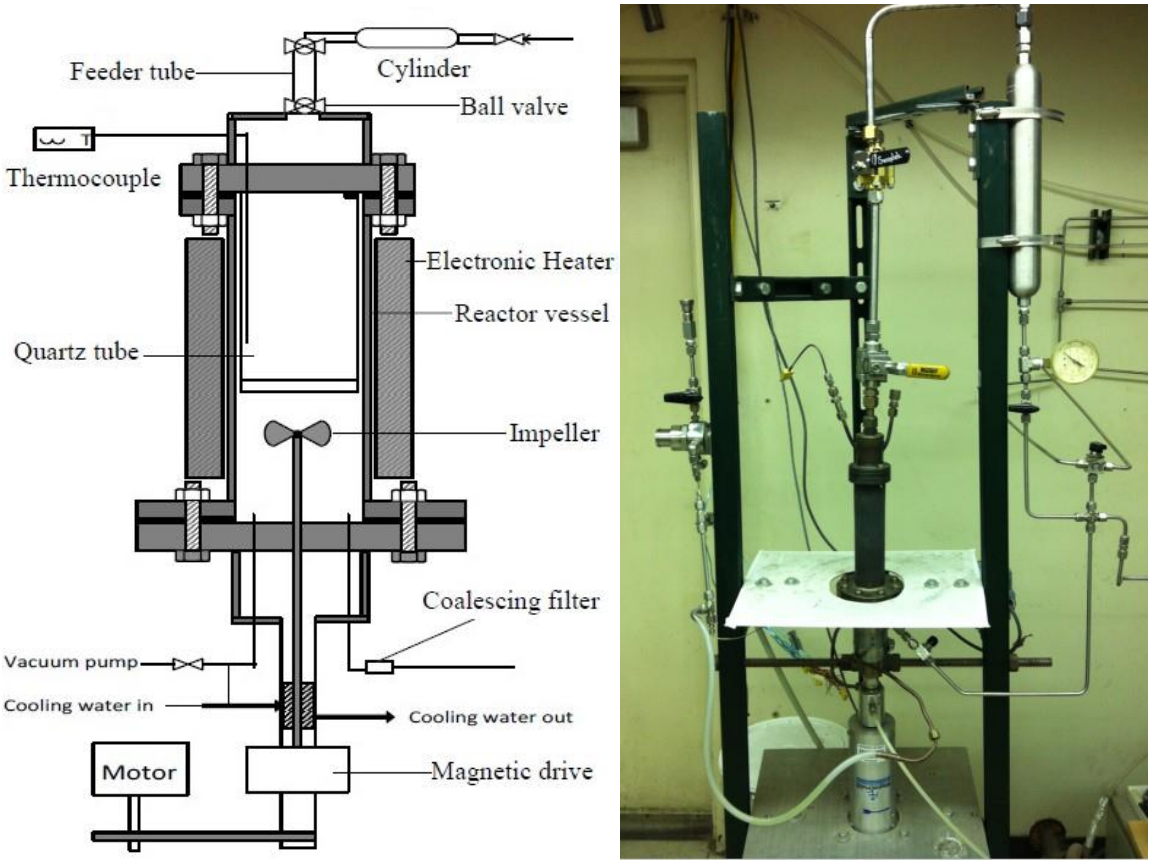

(a) (b)

Fig.3.4 Inverted stirred batch reactor (Inverted Mini rector)

(a) Schematic diagram[113] (b) Photograph

Though the configuration was improved a lot and the sample could be heated up to over 700°C in about 6 seconds with rapid heating rate, the reactor still had some practical issues. Because the injected feedstock was isolated with the impeller by the quartz tube and bottom plate, the mass and heat transfer between gasification agents and sample could be affected. The set-up of the whole system took longer time than the previous two due to two-flange design. Additionally, tar, the high molecular weight hydrocarbon, was condensed in the area of the impeller shaft, which caused clogging and damage to the bearings. Therefore, the system needed further improvements.

3.2 Development of a new configuration for the kinetics study of SE-SHR

As mentioned above, the configuration for SHR kinetics study always includes four essential components, including a reactor, a capillary line, a RGA and a data acquisition system.

3.2.1 Design of a new mini reactor

An original stirred batch reactor (New Mini reactor) with 650cc was designed and constructed, which is shown in Fig.3.5. The whole reactor system is comprised of a batch vessel made of stainless steel 316, a ceramic radiative heater, magnetic driven impeller, gas purge/release system, product gas collection system and instant loading unit. For instant loading unit, it contains high pressure gas storage cylinder and two injection control valves. Pressure and temperature in the vessel were detected by an Omega px750 pressure sensor and a K-type thermocouple, respectively. The data was recorded by LabView® 7.1.

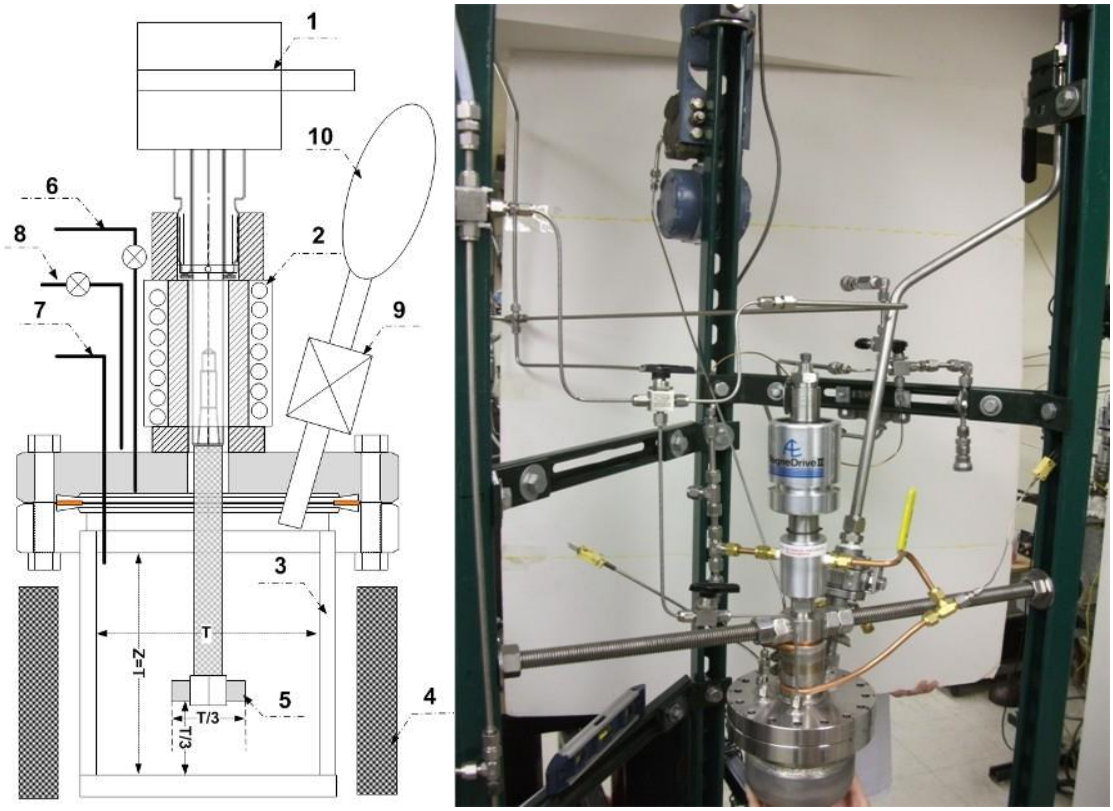

(a) (b)

Fig.3.5 New stirred batch reactor (New Mini reactor)

(a) Schematic diagram: 1.Magnetic agitator driven by belt 2.Cooling coils 3.Inconel reactor 4.Radiative heater 5.Impeller coupled with agitator 6.Gas purge and release system 7.Thermocouple and pressure gauge linked with LabView® 8.Gas collection system 9.Injection loading valve 10.High pressure gas cylinder (b) Photograph

The design of the New Mini reactor was according to the criteria of a basic stirred tank. The ‘‘typical’’ geometry for the agitated reactor vessel is also annotated in Fig.3.5. The diameter (T) was about 3.7 inch, which was the same as the height (Z). The impeller type selected for this study was a straight-blade impeller due to low cost and good turbulent regime. It was also used for the Inverted Mini and Mini reactors. The diameter of the impeller was 1/3 the reactor diameter. The distance between the impeller tip and the vessel bottom was also 1/3 the reactor diameter.

3.2.2 Residual gas analyzer and data acquisition system for real-time gas analysis

The RGA used in this study was QMS300 high pressure gas analyzer (Stanford Research Systems, Inc.). It was a quadrupole mass spectrometer (QMS) in a convenient bench-top configuration. The QMS system has a fast response time of less than 0.5 seconds[114]. The QMS system continuously sampled product gas at very low flow rates of 1~2 milliliters per minute at 1atm controlled by a standard short capillary line coupled with the RGA inlet. Complete spectra with peak intensity of each atomic mass unit (1 to 50) could be recorded in seconds (normally 3 seconds). The components (H_2, CH_4, CO and CO_2) in the producer gas were identified by specific mass-to-charge ratio. The corresponding ratios of these four components were 2, 15, 28 and 44, respectively. The real-time concentration of each species was determined based on the comparison with certified calibration gas.

The data of gas peak intensity from RGA was acquired second-by-second by LabView® software (National Labs, version 7.1) in a laptop. Also, the real time data of reactor pressure and temperature was integrated with RGA data according to their time stamps. Hence, the evolution of producer gas with pressure and temperature change could be logged.

3.2.3 Design criteria of the capillary line

A capillary transfer line was used to reduce the high pressure product gas from the reactor pressure (220psi) to 1atm (14.7psi). 1atm is the acceptable pressure for RGA. PEEK™ capillary tubing was chosen because it has excellent chemical resistance and abrasion resistance with long lifetime.

The test should be conducted in a quasi-close batch reactor with minimum gas loss. Thus, the capillary outlet flow rate was accurately controlled by adjusting the capillary length. Additionally, as mentioned above, the RGA only took 1~2 milliliters per minute at 1atm. Therefore, the capillary outlet flow rate should be just a little bit over 2 milliliters per minute. Both capillary outlet and RGA inlet were set at 1atm by using a T-fitting. Two sides of the fitting were connected with long capillary line and RGA inlet line. Another side was exposed to the atmosphere to release extra gas and pressure before the gas entered the RGA.

The modified Hagen-Poiseuille equation was used to estimate the outlet flow rate as shown below[115]. The modified equation was for compressible fluids with respect to the reactor pressure.

$$Q = \frac{\pi R^4}{16\eta L}\left(\frac{P_i^2 - P_o^2}{P_o}\right)$$

where, Q is the volumetric flow rate at the outlet, P_i is the inlet pressure, P_o is the outlet pressure, R is the internal radius of capillary line, L is the length of capillary line, η is the fluid viscosity.

Based on the previous study, the average viscosity of the product gas was around 0.0083mPa.s. This number was used for the calculation. The inlet pressure was the same as the reactor pressure around 200psi and the exact initial pressure was determined by the practical operation procedure. The outlet pressure was 14.7psi. The PEEK tubing (1560L) with 0.0025inch (internal diameter) purchased from Upchurch Scientific was used for the estimation and further experiments. Fig.3.6 shows the change of the capillary outlet flow

rate as a function of the reactor pressure with different capillary length. It can be seen that the flow rate was increased at the outlet with the increase of the reactor pressure for different capillary length. In particular, in the pressure range from 200psi to 220psi, the outlet flow rate of 1500cm capillary line could be maintained between 1.8cc/min and 2.2cc/min, which was good for minimizing the gas loss. The initial reactor pressure was set at 220psi after the injection by controlling the pressure difference between reactor and top cylinder. The capillary transfer line with 1500cm length was used for all kinetics experiments.

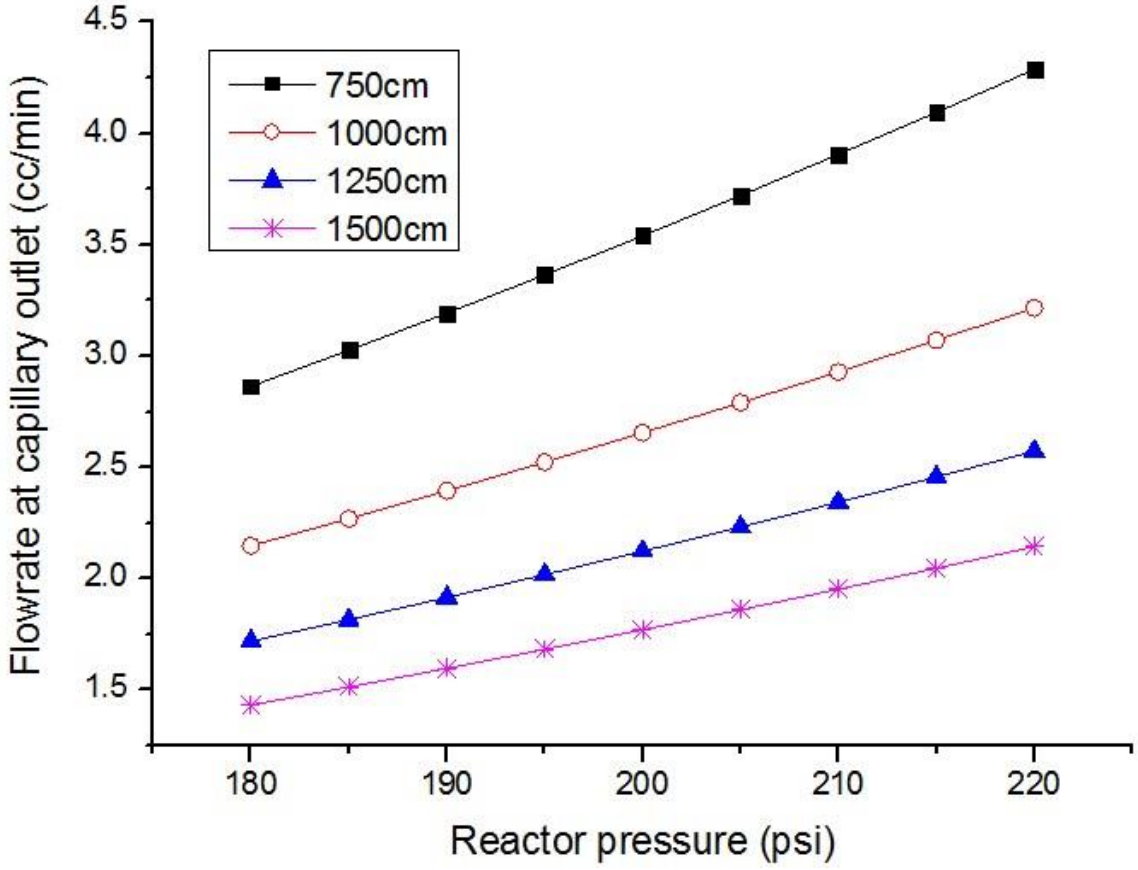

Fig.3.6 The flow rate at capillary outlet as a function of reactor pressure with different capillary length (0.0025inch internal diameter)

3.2.4 The new configuration for the kinetics study

The new configuration for kinetics study was developed by integrating aforementioned individual parts. The schematic diagram and photograph are depicted in Fig.3.7. One end of the long capillary line is linked with the reactor and the other end is connected with the T-fitting vent. There is a coalescing filter as the water trap located at the outlet of the reactor to absorb the residual moisture in the product gas after cooling. The other end of the T-fitting vent is connected with the short standard capillary line of the RGA. The perpendicular end is open to the air for surplus gas release. This vent guarantees operation pressure at 1atm to protect the RGA system during the test. The laptop shows all the real-time information.

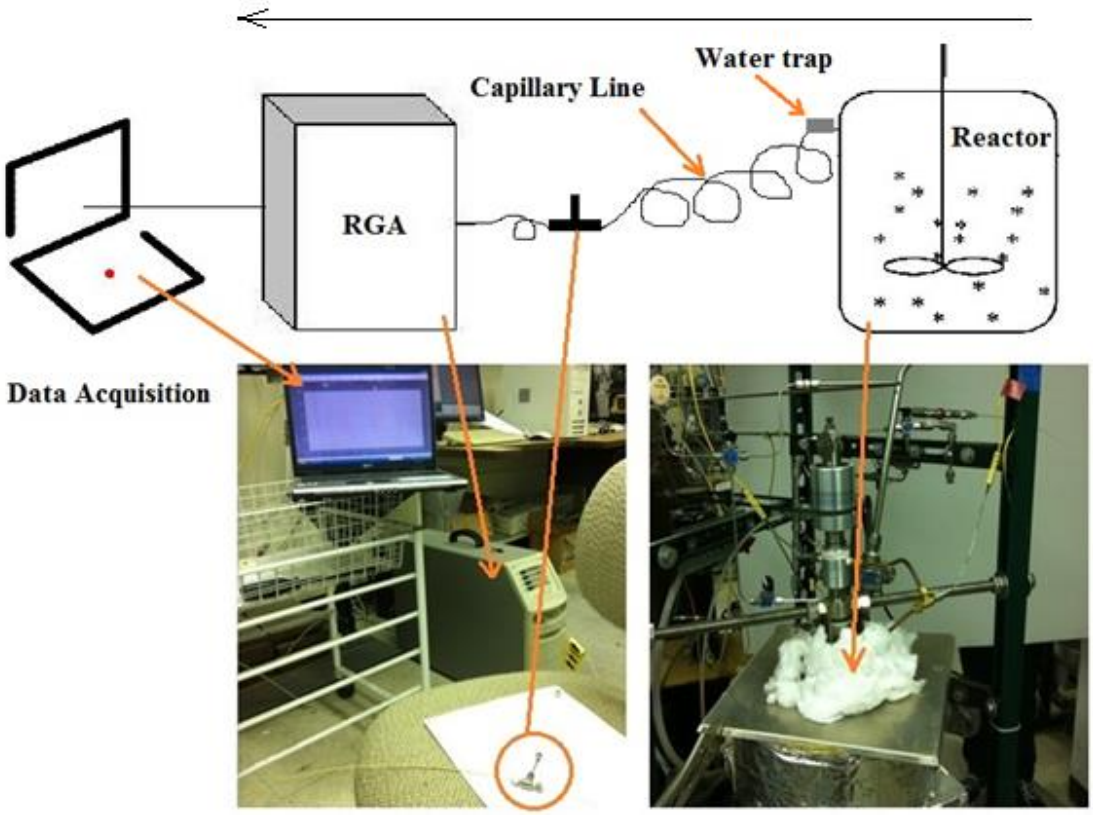

Fig.3.7 Schematic diagram and photograph of the new configuration for kinetics study

3.3 Materials and methods

Lignite from Nutratherm Australia was chosen as the feedstock and quicklime from Chem Lime Co. (Fort Worth, TX) was used as the sorbent. The composition analysis of lignite is shown in Table 2.1. The CaO composition in the quicklime was over 98% (wt% dry basis). The coal was dried, grounded and sieved to pass 150μm. The sorbent was also grounded and further sieved to the range from 75μm to 150μm. Three different temperature conditions were tested, which were 650°C, 700°C and 750°C. Certain amount of H_2 and water were loaded in the reactor at the beginning. The initial H_2/C ratio after the injection was regulated by adjusting the pressure of the top cylinder. Thus, the amount of the injected H_2 could be controlled. The detailed experimental parameters are listed below in Table 3.1.

Table 3.1 Design of experiment for SE-SHR kinetics study

Feedstock	Item	Parameter Value	Steam/C (molar ratio)	H_2/C (molar ratio)	CaO/C (molar ratio)	Temperature (°C)	Contact Type
Lignite	Effect of Temperature	650, 700, 750	1.2	3	0, 0.36	/	mixing
	Effect of CaO/C (molar ratio)	0, 0.36, 0.53	1.2	3	/	750	mixing
	Effect of feedstock-sorbent contact type	mixing, no mixing	1.2	3	0.36	750	/

It should be noted here that the mixing meant the lignite and quicklime were mixed first and located at the lower injection valve. No mixing meant the quicklime was put inside the rector at the beginning. Then the reactor was heated up to the reaction temperature. The inside impeller was always turned on to improve heat and mass transfer. It was aimed to have better gas-solid reaction and even temperature distribution. Juntgen already mentioned that hydrogenation was more favorable upon better and efficient contact between newly formed char and H_2[116]. After the desired temperature was reached, the upper valve and lower valve were opened and closed simultaneously in one second. The sample was fleetly pushed into the reactor by high pressure H_2 from the top cylinder. The initial pressure inside the reactor after the injection was set at 220psi by adjusting the H_2 pressure in the top cylinder according to the reactor pressure.

The gas collection valve was opened after the injection. Then the product gas was coming out due to the pressure difference between the reactor and the capillary outlet. The output gas was cooled down by the coolant first. Thus, some steam and tar were condensed back to the reactor. The remaining moisture and other particulates were removed by the filter before entering the capillary line. Then the permanent gas passed through capillary line to the RGA, by which the real-time concentrations of CH_4, CO and CO_2 were obtained. It should be mentioned here that H_2 was not considered as a product because it was existing as a gasification agent. It was always consumed during the gasification and thereby its formation rate could not be calculated.

In particular, heating up the feedstock to the desired temperature could be considered instantaneous like Inverted Mini. In the meantime, the inside pressure became stable after

the injection, which was controlled by the capillary line as mentioned above. In Fig.3.8, the temperature and pressure profiles are plotted for 750°C test. It can be seen that the temperature was very stable beyond the injection point. The pressure was suddenly increased and became level later. The pressure drop rate was only 0.08psi/sec. Consequently, the whole system could be assumed quasi-close batch reactor and isothermal condition for the first hundred seconds.

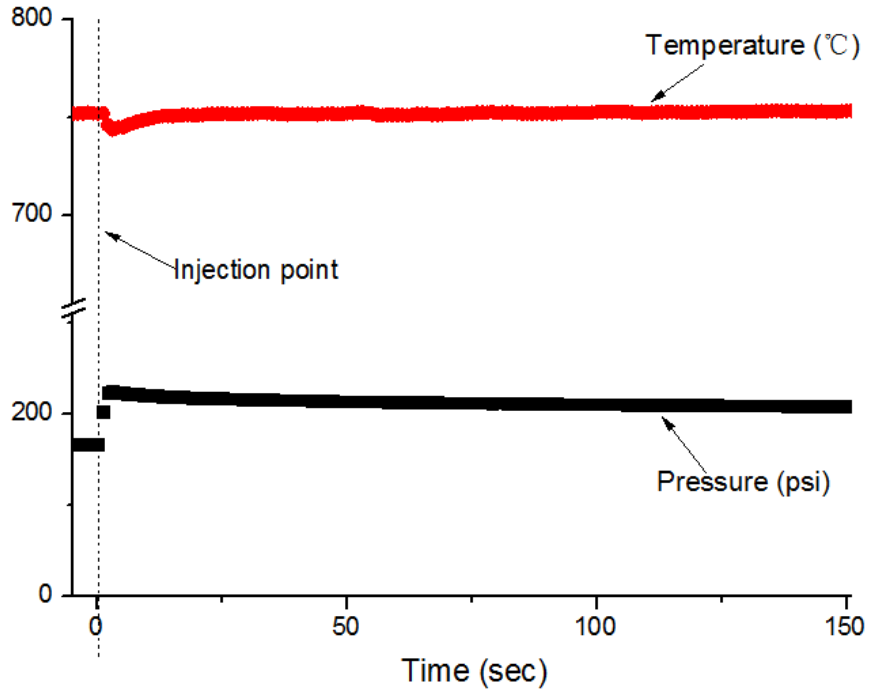

Fig.3.8 Profile of temperature and pressure after injection for 750°C test

As mentioned above, most kinetics model relied on char evolution using thermogravimetry with long residence time. According to the configuration of this study, the measurement of kinetic parameters was based on individual gas. It was assumed that each product gas species was generated from a single, independent molecular reaction

with different activation energy, though some parallel reactions occurred. Similar assumption was also published before[117].

The formation rate constant of CH_4, CO and CO_2 was calculated by least squares analysis of each evolution plot. The kinetics study was only focused on the first 150 seconds considering the residence time of practical gasification operation. After the rate constants were obtained in the temperature range from 650°C to 750°C, the activation energy of each gas could be calculated by Arrhenius equation as below.

$$k = A \exp(-E_a/RT)$$

where, A is the pre-exponential factor (M/sec, M is the gas concentration in the reactor), E_a is the activation energy, R is the gas constant which equals 8.314J/mol K, T is the gasification temperature (K).

The alternate expression of Arrhenius equation is as below. The relationship between Lnk and 1/T was plotted to get the slope. The slope was $-E_a/R$.

$$Lnk = -E_a/RT + LnA$$

3.4 Results and discussion

3.4.1 Effect of temperature

The evolution of each product gas (CO_2, CO and CH_4) during SHR and SE-SHR at three different temperatures (650°C, 700°C and 750°C) is depicted from Fig.3.9 to Fig.3.14. The Y-axis shows the percentage of each gas component, which was

proportional to the gas yield in the quasi-close batch reactor. The X-axis represents the time after the injection.

It can be observed from Fig.3.9 to Fig.3.14 that the gas evolution was enhanced when the temperature was raised from 650°C to 750°C during both SE-SHR and SHR. It meant that higher temperature favored faster formation rate regardless if the sorbent was introduced or not.

The CO_2 percentage during SE-SHR was lower compared to SHR at the same gasification temperature. For example, as depicted in Fig.3.9 and Fig.3.10, in 75 seconds at 750°C, the CO_2 percentage of SE-SHR was only 0.3% while that of SHR was close to 1.2%. The CO_2 yield of SE-SHR was almost 4 times lower. It indicated that sorbent instantly captured CO_2 as it formed in the reactor, which accordingly retarded the gas formation rate. CO had the same trend as CO_2. For example, as shown in Fig.3.11 and Fig.3.12, in 50 seconds at 650°C, the CO percentage of SE-SHR was 0.8% while that of SHR was about 1.6%. It was mainly because of the enhanced shift of WGS reaction. The shift made more CO converted to H_2 and CO_2 while CO_2 was being simultaneously captured by the sorbent. Hence, CO evolution was slower during SE-SHR.

CH_4 evolution was also affected by the addition of sorbent. As can be seen in Fig.3.13 and Fig.3.14, the CH_4 percentage of SE-SHR was a little bit lower than that of SHR at the same gasification temperature. It was possibly due to the enhanced consumption by SMR when CO_2 was being removed. Moreover, because of the low reactivity between char and H_2, the enhanced CH_4 production shown in Chapter 2 required longer residence time.

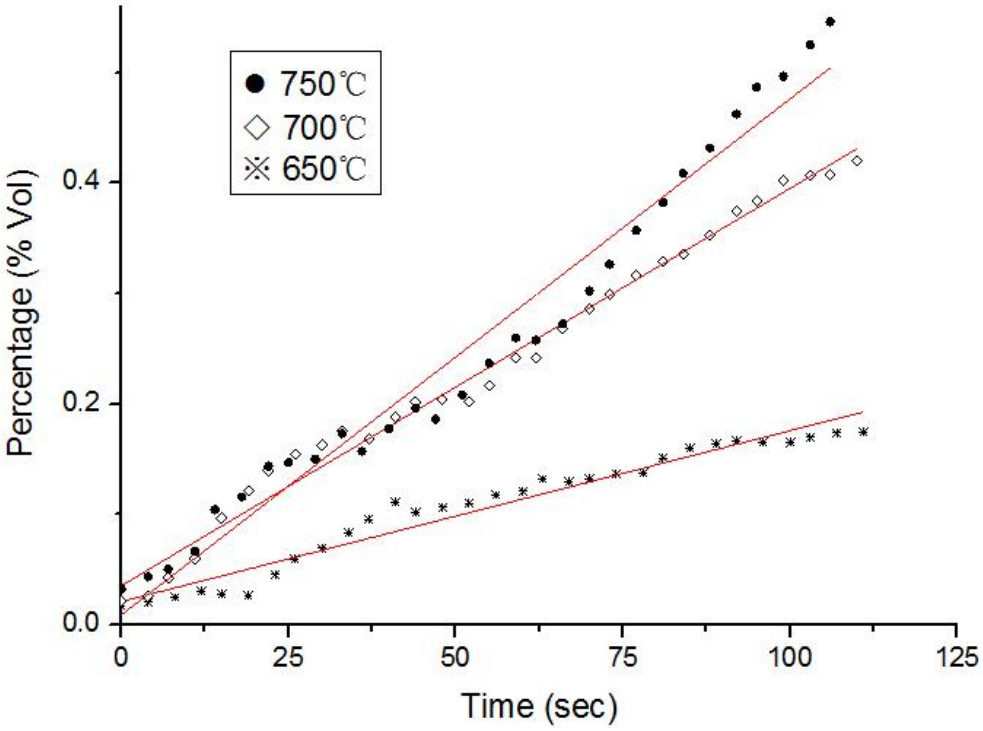

Fig.3.9 The evolution of CO_2 during SE-SHR at different temperatures

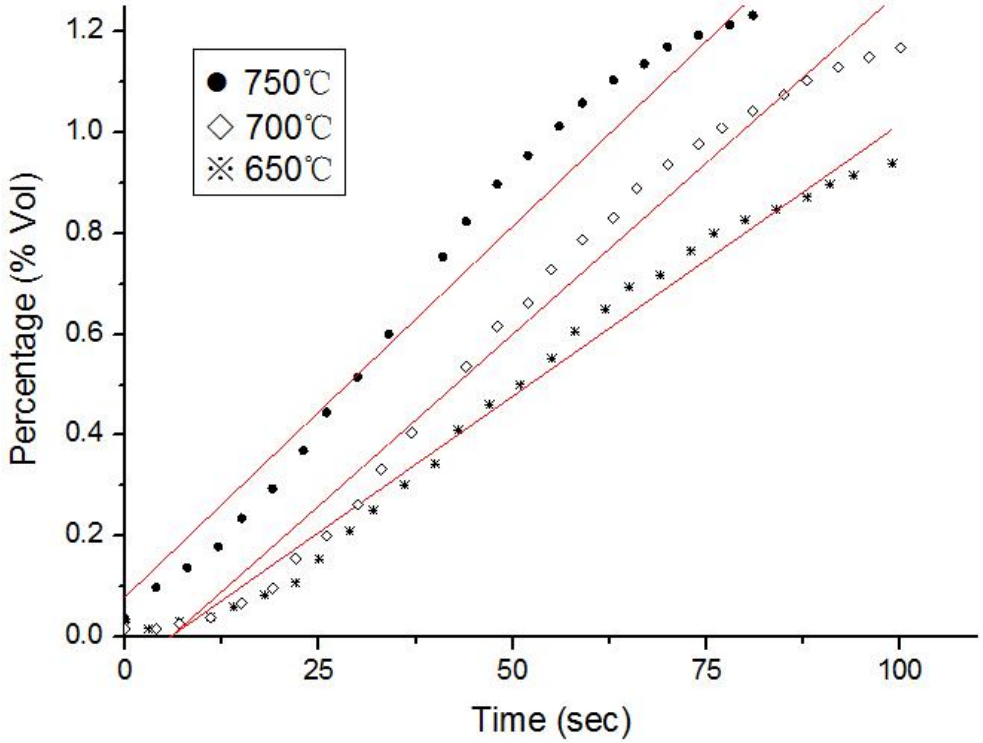

Fig.3.10 The evolution of CO_2 during SHR at different temperatures

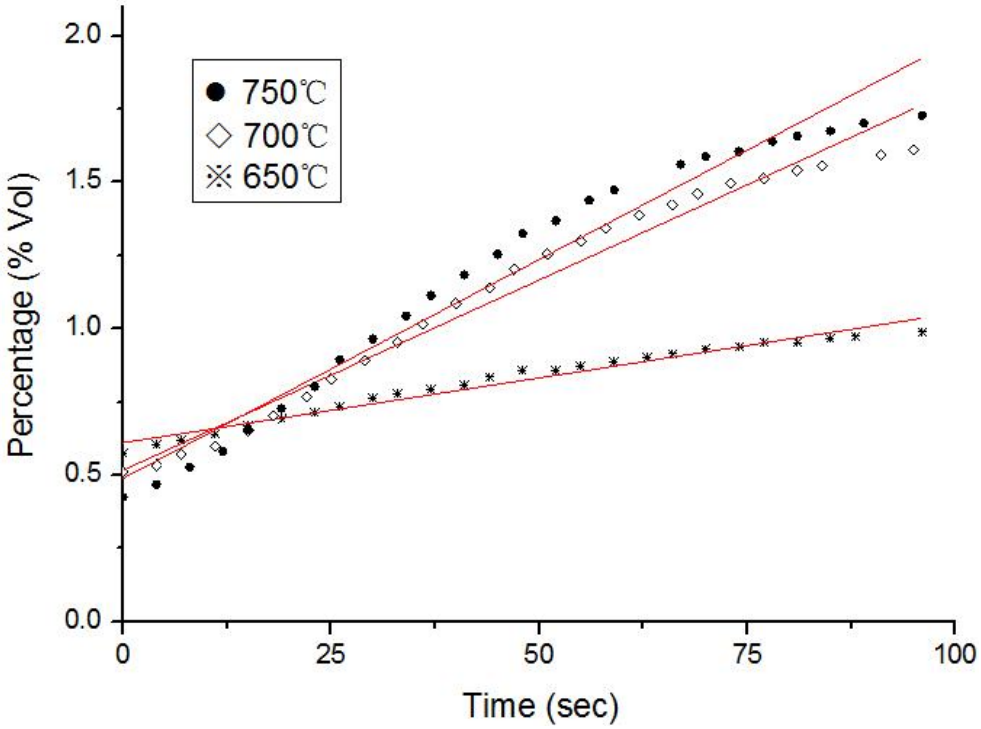

Fig.3.11 The evolution of CO during SE-SHR at different temperatures

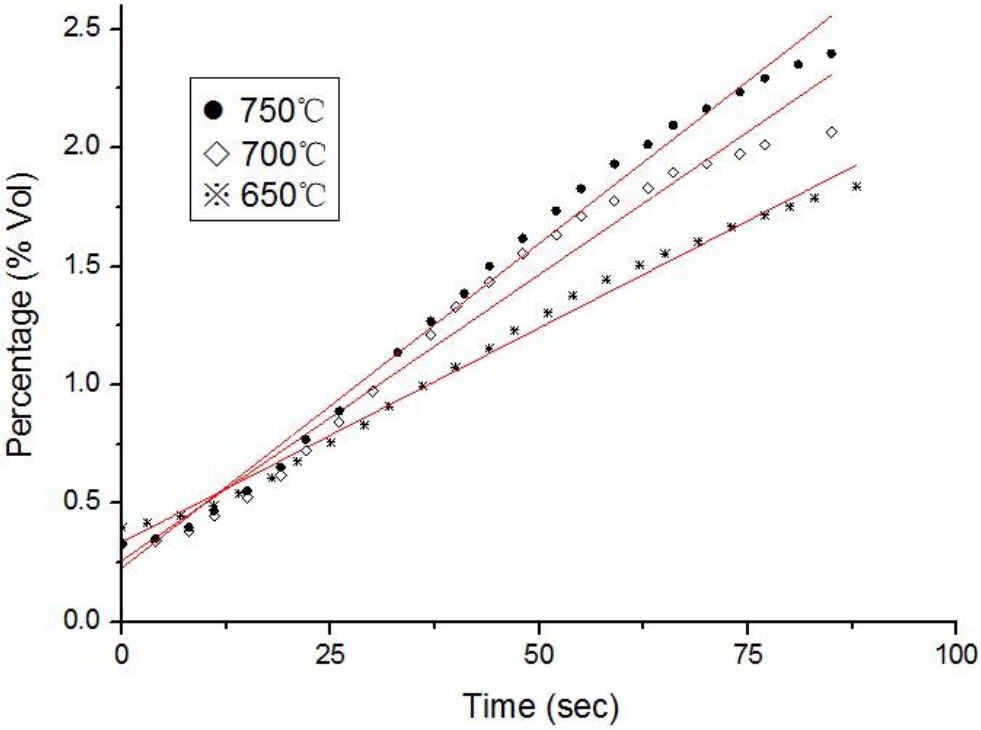

Fig.3.12 The evolution of CO during SHR at different temperatures

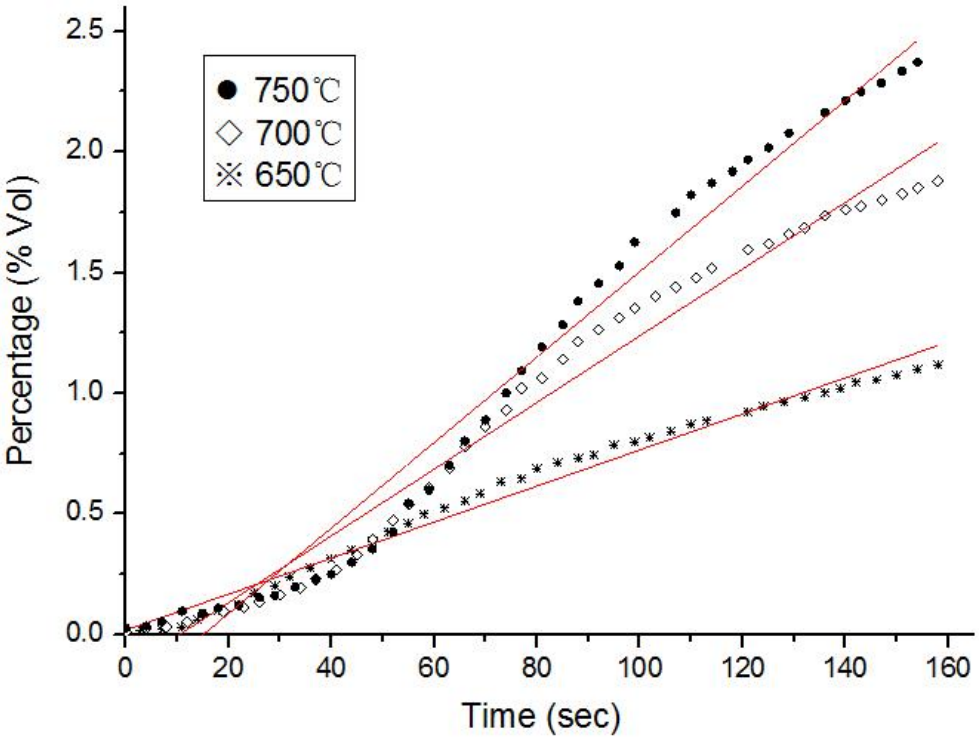

Fig.3.13 The evolution of CH_4 during SE-SHR at different temperatures

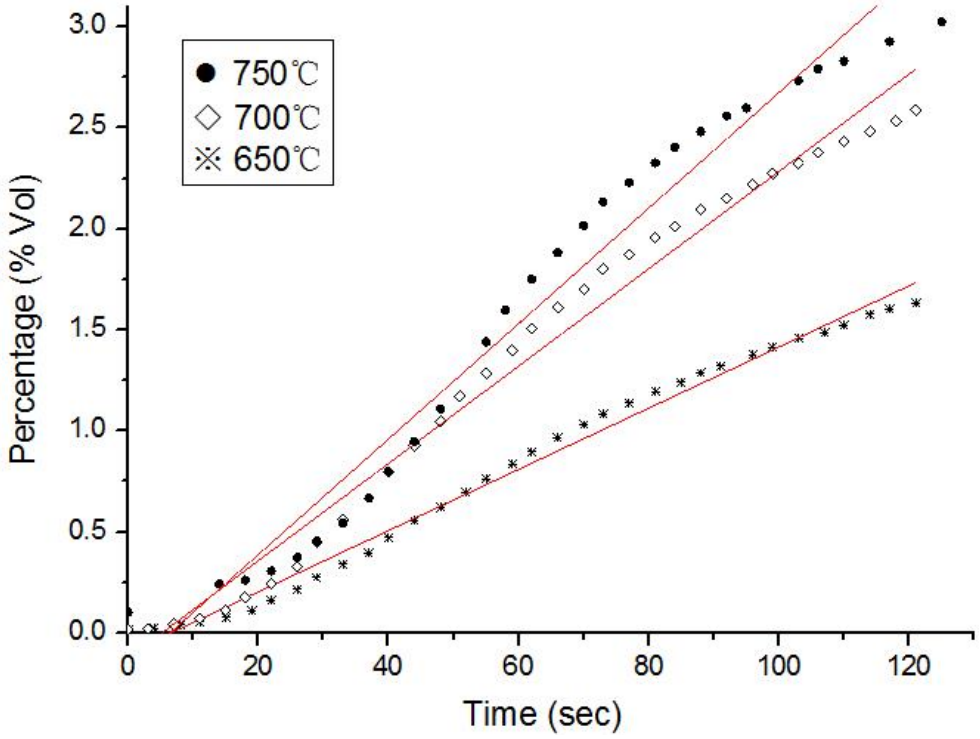

Fig.3.14 The evolution of CH_4 during SHR at different temperatures

The detailed formation rate constants and correlation coefficients of CO_2, CO and CH_4 during SE-SHR and SHR are listed in Table 3.2.

Table 3.2 Rate constant and correlation coefficient of product gas

	Temperature (°C)	Rate Constant (M/sec)			Correlation Coefficient		
		k_{CH4}	k_{CO}	k_{CO2}	R^2_{CH4}	R^2_{CO}	R^2_{CO2}
SE-SHR	650°C	0.0075	0.0044	0.0016	0.98	0.97	0.95
	700°C	0.0138	0.0129	0.0036	0.98	0.97	0.99
	750°C	0.0177	0.0149	0.0047	0.97	0.96	0.97
SHR	650°C	0.0152	0.0181	0.0108	0.99	0.99	0.98
	700°C	0.0241	0.0241	0.0136	0.98	0.97	0.98
	750°C	0.0286	0.0274	0.0147	0.97	0.99	0.96

The data in Table 3.2 shows that CH_4 mostly had higher rate constant at the same temperature compared to the other two gases. Also, it shows that the sorbent addition reduced CO_2 formation rate constant by one magnitude under the same gasification condition. The correlation coefficients were acceptable.

The percentage change of H_2 at 750°C is depicted in Fig.3.15. Though H_2 already existed in the reactor, the positive influence of sorbent on the H_2 production was found during SE-SHR. It can be seen that the H_2 yield during SHR decreased much faster than

it did during SE-SHR. The main reason was that sorption enhanced performance simultaneously made up the H_2 consumption during SE-SHR.

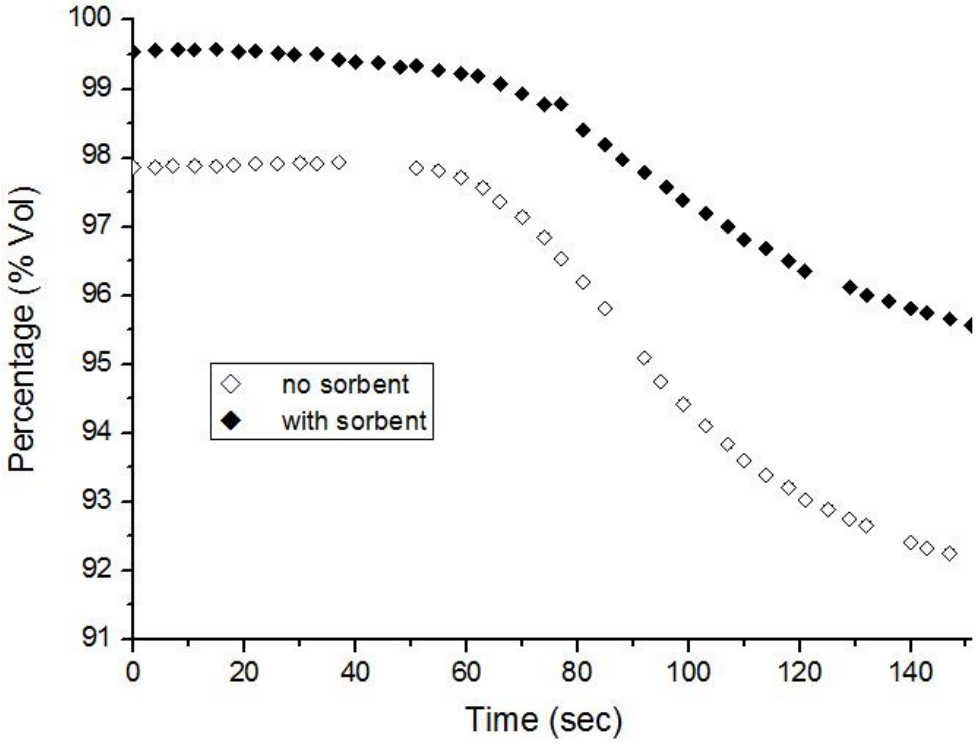

Fig.3.15 The percentage change of H_2 during SHR and SE-SHR at 750°C

3.4.2 Effect of sorbent loading

The evolution of CO_2 with different sorbent loading at 750°C is depicted in Fig.3.16. It can be observed that the increase of CaO/C slowed the evolution of CO_2. In other words, more CaO input could capture more CO_2 during gasification. In 100 seconds, the CO_2 percentage during conventional SHR was over 0.75%, while the percentage during SE-SHR was still around 0.25%. In particular, the CO_2 percentage with CaO/C of 0.53 was lower than that with CaO/C of 0.36. The CO_2 evolution in the syngas was further retarded by more sorbent addition.

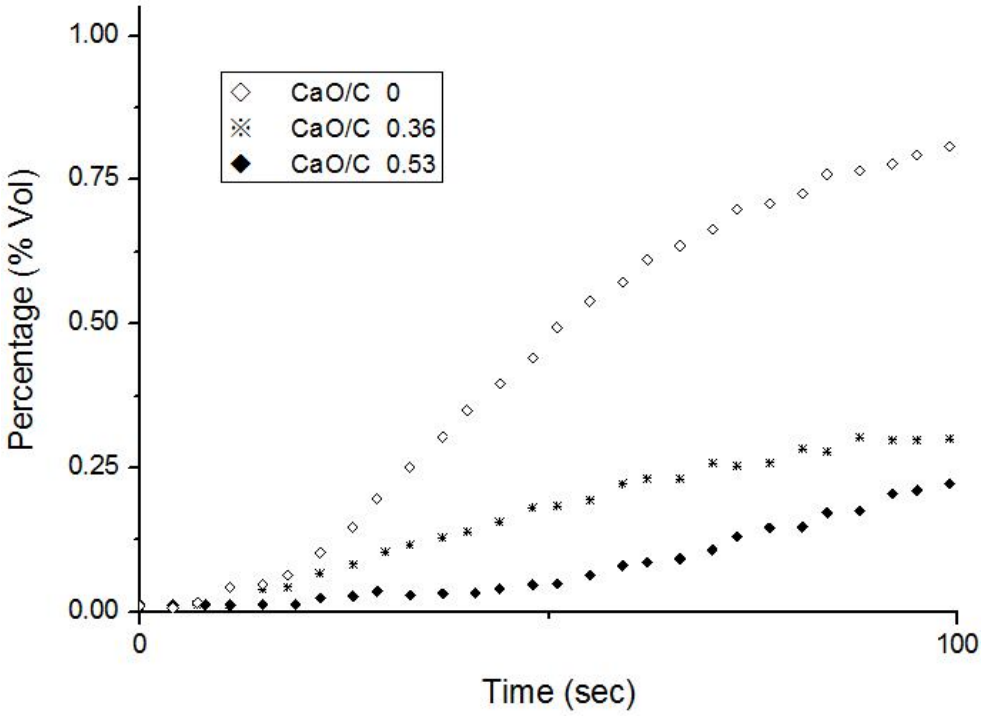

Fig.3.16 The evolution of CO_2 with different sorbent loading

3.4.3 Effect of feedstock-sorbent contact type

The CO_2 evolution with different feedstock-sorbent contact type at 750°C is shown in Fig.3.17. Three contact types included without sorbent (no contact with sorbent), with sorbent & no mixing (sorbent located inside the reactor), and with sorbent & mixing (sorbent mixed with feedstock at the injection valve). It can be seen that CO_2 evolved comparatively faster without sorbent compared to with sorbent. Additionally, the CO_2 formation rate of mixing type was lower than that of non-mixing type. It implied that efficient interaction between feedstock and sorbent played an important role in CO_2 capture. Accordingly, for future practical sorption enhanced technology application, fluidized bed or bubbling bed should be used for a better mass transfer performance.

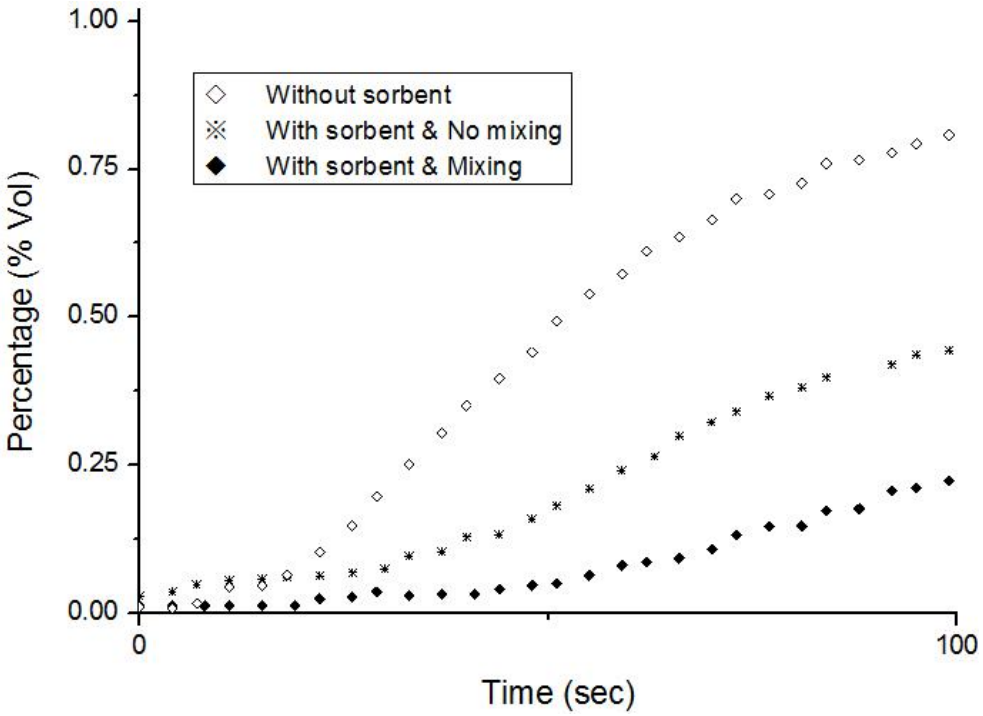

Fig.3.17 The evolution of CO_2 with different feedstock-sorbent contact type

3.4.4 Activation energy

The Arrhenius plots of CO_2, CO and CH_4 during SHR and SE-SHR are shown in Fig.3.18, Fig.3.19 and Fig.3.20, respectively. The slopes of CO_2 and CO during SE-SHR were much steeper than those during SHR. It indicated that activation energy changed. The slope of CH_4 during SE-SHR did not change too much.

Table 3.3 lists the calculated activation energies of CO_2, CO and CH_4 formation and corresponding Arrhenius pre-exponential factors during SE-SHR and SHR. It shows that the activation energies of CO and CO_2 were increased from 32.8kJ/mol and 24.5kJ/mol to 96.8kJ/mol and 86.3kJ/mol, respectively. It would be more difficult to generate CO and CO_2 in the syngas during SE-SHR. The activation energy of CH_4 was increased only by 18kJ/mol.

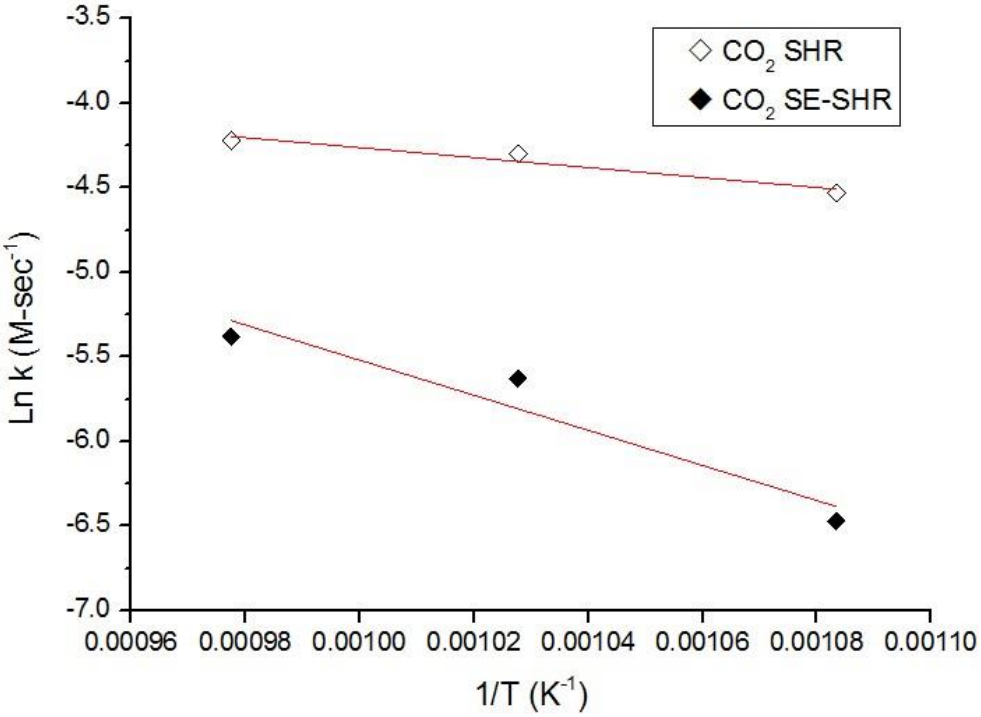

Fig.3.18 Arrhenius plots of CO_2 during SHR and SE-SHR

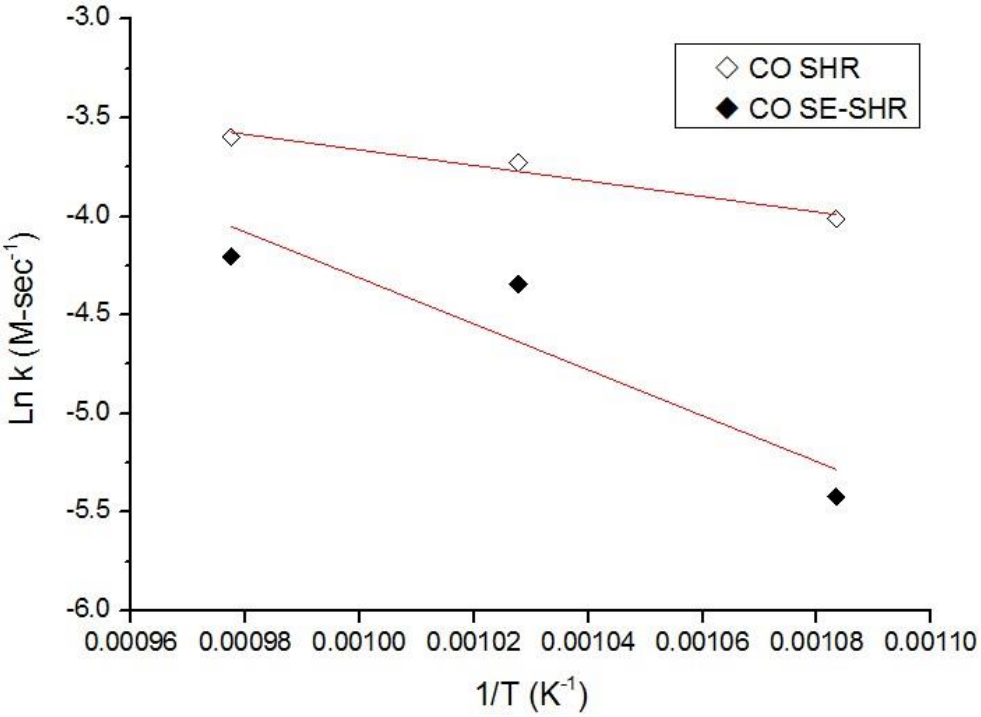

Fig.3.19 Arrhenius plots of CO during SHR and SE-SHR

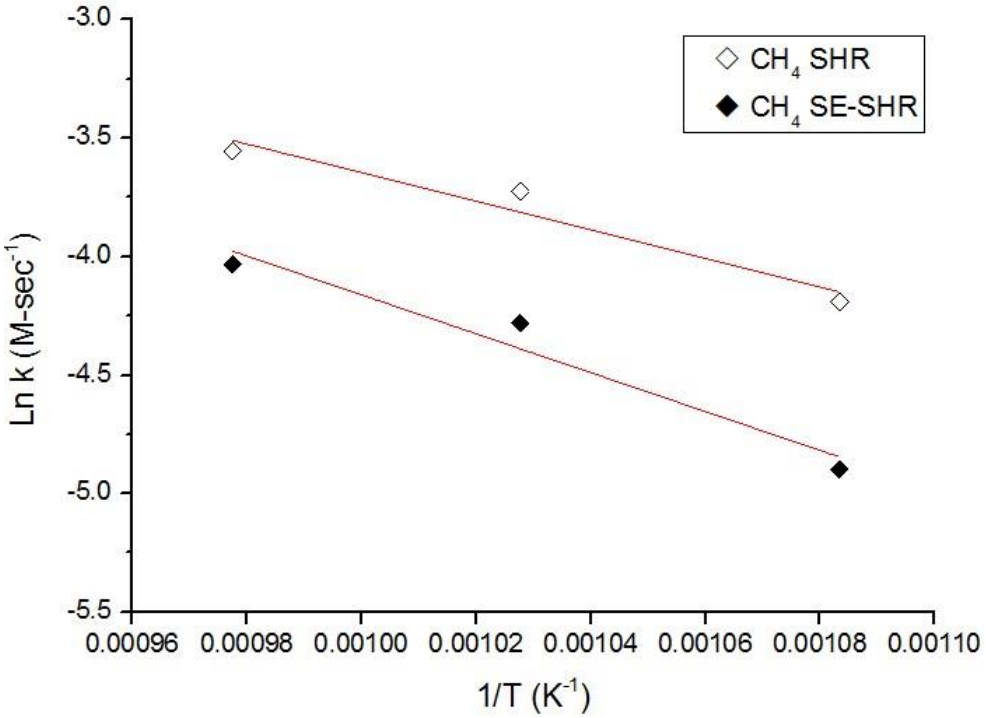

Fig.3.20 Arrhenius plots of CH_4 during SHR and SE-SHR

Table 3.3 Activation energy and Arrhenius pre-exponential factor of product gas

	Product Gas	Activation Energy	Pre-exponential factor
		E_a (kJ/mol)	A (M/sec)
SE-SHR	CH_4	68.3	57.29
	CO	96.8	1524.91
	CO_2	86.3	129.19
SHR	CH_4	50.2	10.92
	CO	32.8	1.32
	CO_2	24.5	0.27

3.5 Summary

A kinetics study of SE-SHR was conducted and compared to conventional SHR. A new lab-scale mini reactor and an improved configuration were designed and constructed. The reactor was considered as a quasi-close batch reactor when coupling with a specific capillary line. The main results were summarized as below.

1. Higher gasification temperature favored faster formation rates of CO_2, CO and CH_4 during both SE-SHR and SHR.

2. The formation rates of CO_2 and CO at 650°C, 700°C and 750°C during SE-SHR were much lower than those during SHR. It was mainly due to the enhanced shift of WGS with sorbent addition, making more CO converted with simultaneous CO_2 capture.

3. More sorbent loading could capture more CO_2, leading to slower CO_2 evolution.

4. Well-mixing of feedstock and sorbent had better performance on reducing CO_2 formation rate.

5. The activation energies of CO and CO_2 were increased remarkably during SE-SHR.

4. Technical Evaluation of Sorption Enhanced CE-CERT Processes

In this chapter, the sorption enhanced CE-CERT processes for FT fuel production and SNG production proposed in Chapter 1 are evaluated technically. The design and modeling of CTL and CTG plants are implemented using process simulation software. The overall heat and mass balance of each process is obtained. The optimum gasification condition of each process is determined based on the self-sustainability of hydrogen and the maximum production of synfuel. The SE-SHR based processes are compared to the corresponding conventional SHR based processes.

4.1 Process design methodology

Aspen Plus version 8.0 was used for the process simulation. Aspen Plus is the core product of Aspen Technology. This software provides a market-leading process modeling environment for conceptual design and optimization in both chemical and power industries. One outstanding feature of Aspen Plus is the excellent performance in handling non-conventional solid materials like coal.

The modeling included solid, liquid and gas phases, which required various packages to represent different chemical properties exactly. The feedstock used in the CE-CERT process, such as coal, biomass and biosolids, was defined as non-conventional component. HCOALGEN and DCOALIGT were set as the enthalpy model and density model of feedstock, respectively. For liquid and gas phases, all properties were retrieved from the default database.

The process modeling for FT fuel production was divided into seven main sections, which were feedstock pretreatment, gasification with combustion or regeneration, warm gas cleanup, SMR, H_2 separation, CO_2 removal, and FT synthesis.

The process modeling for SNG production was divided into six main sections, which were feedstock pretreatment, gasification with combustion or regeneration, warm gas cleanup, downstream gas processing (WGS or methanation), H_2 separation and CO_2 removal.

The major operation models used in the above two processes are listed in Table 4.1.

Table 4.1 Aspen Plus specification of operation unit

Operation Unit	Aspen Plus Model	Specification
Decomposition	RYield	Feedstock is decomposed to elemental C, H, O, N, S, Cl
Gasification	RGibbs	Possible products are specified including H_2, Cl_2, H_2O, HCl, C, CO, CO_2, CH_4, COS, H_2S, CS_2, CaO, $CaCO_3$, ash
Combustor	RGibbs	Char and air combustion
Regenerator	RGibbs	Char and air combustion with $CaCO_3$ decomposition
Burner	RGibbs	Optional for extra energetic gas combustion to supply heat
Solid separation	Sep	Product gas with sand or sorbent separation
Warm gas cleanup	Sep	H_2S and chloride removal
H_2 separation	Sep	H_2 split from the product gas
SMR	Equilibrium	Methane-rich product gas reforming
WGS	Equilibrium	Converting CO to H_2 and CO_2
Methanation	Equilibrium	Converting CO and CO_2 to CH_4
FT	Ryield	Empirical simulation of FT fuel distribution
CO_2 removal	Sep	CO_2 split from the product gas

In particular, feedstock was assumed to be first decomposed to elemental components before gasification by decomposition unit using RYield model. The decomposer temperature was 500°C. These elements were sent to the RGibbs reactor for gasification calculation. The detailed simulation parameters in gasifier are listed in Table 4.2.

Table 4.2 Simulation parameters in gasifier

Gasification Type	Parameter	Value								
SHR	*Input Condition (H_2/C-Steam/C)*	0.63-1.67	0.63-2.22	0.63-2.78	1.08-1.67	1.08-2.22	1.08-2.78	1.59-1.67	1.59-2.22	1.59-2.78
	Char leftover% (inert char)	64	62.4	61.2	60	58.8	58	58.8	56	54
SE-SHR	*Input Condition (H_2/C-Steam/C)*	0.63-1.67	0.63-2.22	0.63-2.78	1.08-1.67	1.08-2.22	1.08-2.78	1.59-1.67	1.59-2.22	1.59-2.78
	Char leftover% (inert char)	26.67	25	21.33	25	24.33	18.33	23.33	20.33	15.67
SHR & SE-SHR	*Gasifier temperature*	750°C								
	Gasifier pressure	2.2MPa								
SHR & SE-SHR	*Coal feed rate*	400 tonnes/day								
SHR & SE-SHR	*Sand or Sorbent feed rate*	400 tonnes/day								

The char leftover percentages are shown in Table 4.2, which are corresponding to different gasification conditions. The data was obtained experimentally from Chapter 2. These data was used to set the inert char percentage in the gasifier Gibbs model. The temperature and pressure in the gasifier was same for all simulations. Sand was used for conventional SHR and quicklime was used for SE-SHR. Both feed rates were the same as coal feed rate at 400 tonnes per day. It should be noted here that 400 tonnes of sand or sorbent per day was for simplifying the simulation on a daily basis. This sorbent loading made CaO/C molar ratio at 0.36 in the gasifier. However, it did not mean the practical inventory of bed materials circulating in the fluidized bed should be 400 tonnes.

The practical inventory depends on the hydrodynamics performance in the circulating system. Based on the preliminary hydrodynamics study, the optimum bed inventory to feedstock mass ratio in the circulating fluidized bed is about 250 for SHR system[118]. Assuming the residence time of feedstock in the gasifier is 30 seconds, the feedstock mass in the gasifier is 0.14 tonnes as for the feeding rate of 400 tonnes/day. Therefore, the total bed inventory is 35 tonnes.

If the system uses the mixture of sand (0.25mm average diameter) and CaO (0.15mm average diameter), the sorbent inventory should be 0.14 tonnes (CaO/C=0.36) and the sand inventory is 34.86 tonnes. However, due to attrition, elutriation and sintering issues, there is continuous loss in sorbent mass and CO_2 capture capacity. The particle size of used sorbent will become smaller. Then it cannot be captured by the cyclone and will leave the system. Thus, the sorbent should be refilled continuously to maintain 0.14 tonnes sorbent inventory and refresh the capture capacity.

In the warm gas cleanup unit, H_2S and chloride was captured at 350°C before entering the downstream processing unit. SMR in the FT fuel production was simulated using a built-in equilibrium block at the temperature of 850°C. The reactions considered in the SMR are given below[49].

$CH_4 + H_2O = 3H_2 + CO$ $\Delta H = 206kJ/mol$

$CH_4 + 2H_2O = 4H_2 + CO_2$ $\Delta H = 165kJ/mol$

$CH_4 + CO_2 = 2H_2 + 2CO$ $\Delta H = 247kJ/mol$

$CO + H_2O = H_2 + CO_2$ $\Delta H = -41kJ/mol$

In particular, FT reactor was simulated using an external model to predict the selectivity of the FT product. The empirical model was based on the ASF distribution[119]. The product distribution of hydrocarbons formed in the FT process can be generally expressed as follows. The main product included fuel gas (C1-C4), raw naphtha (C5-C11), middle distillate (raw diesel, C12-C20), and wax (C20+).

$Wn/n = (1-\alpha)^2 \alpha^{n-1}$

n = number of carbon atoms in the molecule

Wn = weight fraction of hydrocarbon molecules containing n carbon atoms

α = chain growth probability or the probability that a molecule will continue reacting to form a longer chain ($\alpha = r_p/(r_p + r_t)$), where r_p is rate of propagation and r_t is rate of termination of growing chains

The probability of chain growth in this study was assumed 0.9 in favor of diesel range production. CO conversion in the FT reactor was set at 0.78[55]. Unreformed CH_4, remained CO_2 and other hydrocarbons that enter the FT reactor were considered inert without growing to longer chains. Additionally, the fraction C4- according to the above model was redistributed to 74 mol% C1, 16 mol% C2, 6 mol% C3, and 4 mol% C4[35].

In the process for SNG production, the product gas after warm gas cleanup was used for WGS or methanation. WGS section was simulated by using two built-in equilibrium blocks in series adiabatically under the pressure of 2.2MPa. The product gas was sent to the first WGS reactor packed with high temperature catalyst. Before entering the second WGS reactor, the gas was cooled down to 190°C for further low temperature catalytic synthesis[120,121]. The reaction expected in the reactor is as below.

$CO + H_2O = H_2 + CO_2$ $\Delta H = -41kJ/mol$

In the case of SE-SHR with methanation, methanation section was simulated by using two built-in equilibrium blocks in series adiabatically. The pressure was set at 2.2MPa. The gas was cooled down to 300°C before entering the methanation unit[122,123]. The reactions in the methanation process are given below[124,125].

$3H_2 + CO = CH_4 + H_2O$ $\Delta H = -206kJ/mol$

$4H_2 + CO_2 = CH_4 + 2H_2O$ $\Delta H = -165kJ/mol$

$CO + H_2O = H_2 + CO_2$ $\Delta H = -41kJ/mol$

In addition, some reactor models and input parameters were controlled by calculator and design specification. These FORTRAN routines could automatically adjust related dependent variables when independent variables were changed, instead of manual adjustment of them every time. Calculator block was applied to the decomposition reactor and the FT reactor. Design specification was applied to steam input, H_2 input, H_2 recycle separation, H_2/CO syngas ratio, and air input for combustor/regenerator.

4.2 Process evaluation method

The primary standard for process evaluation is the self-sustainability of H_2. If the H_2 could not meet recycle requirement, the corresponding process was considered unfeasible. The mass balance of each process was conducted first to check the mass flow of each product. When the primary standard was satisfied, the maximum production of synfuel determines which process was the optimum. Lastly, the heat analysis was carried out to see if the optimum process could be self-sustainable on heat supply.

CH_4 conversion percentage of SMR was compared in the FT synfuel production. CO yield in the SMR product gas determined the production of final FT liquid fuels. Thus, the process with highest CO yield was chosen as the optimum. CO conversion percentage of WGS and methanation in the SNG production was calculated. CO_2 conversion percentage of methanation was also calculated. The process with highest CH_4 yield was considered optimum. The conversion percentage of CH_4, CO and CO_2 was the ratio of the output from the reactor over the input to the reactor.

In particular, the SNG quality was evaluated in terms of overall energy efficiency, methane conversion efficiency and Wobbe Index (WI). The overall energy efficiency was defined as followed:

Overall energy efficiency = Higher Heating Value $(HHV)_{SNG}/HHV_{Coal}$

Where, HHV_{SNG} was the sum of H_2, CH_4 and CO, of which HHV are 141.89, 55.62 and 10.09MJ/kg at 25°C respectively. The HHV_{Coal} value (dry basis) of Nutratherm lignite is 25.8MJ/kg.

Methane conversion efficiency can be defined as:

CH_4 Conversion% = CH_4 moles in the final SNG/Carbon moles in the coal

WI is the most efficient and robust single index and measure of gas interchangeability for practical operation, which is defined as the HHV of the fuel gas divided by the square root of its specific gravity with respect to air[126].

4.3 Results and discussion

4.3.1 Sorption enhanced CE-CERT process for FT synthetic fuel production with comparison to conventional CE-CERT process

The sorption enhanced CE-CERT process and the conventional CE-CERT process for FT fuel production were simulated using Aspen Plus software. The block flow diagram of two processes was similar and is shown in Fig.4.1. The only difference was using quicklime for sorption enhanced process instead of using sand for conventional process.

The feedstock was first pretreated and sent to the decomposer to get elemental component. The gasification section was assumed to have a decomposition unit first, which did not exist in the practical operation. This unit contributed to the further gasifier calculation based on Gibbs energy minimization. After the gasification section, the solid phase and gas phase were separated in the cyclone. Sand or $CaCO_3$ was conveyed with char to the combustor or the regenerator depending on SHR or SE-SHR. The hot sand or the regenerated quicklime was sent back to the gasifier for cyclic use.

The product gas went through warm gas cleanup unit before entering SMR section. Extra H_2 was separated from the output gas of SMR by controlling the downstream H_2/CO molar ratio at 2. The separated H_2 was delivered back to the gasifier. Then, the syngas underwent purification to remove CO_2. The final syngas entered FT reactor for FT liquid fuel synthesis. The product distribution was determined by an external empirical model. The product water was removed by condensation and the gas product (CH_4, CO and C1-C4 gas) was sent to the burner for extra heat generation. The remained product was mainly composed of FT liquid fuel and wax.

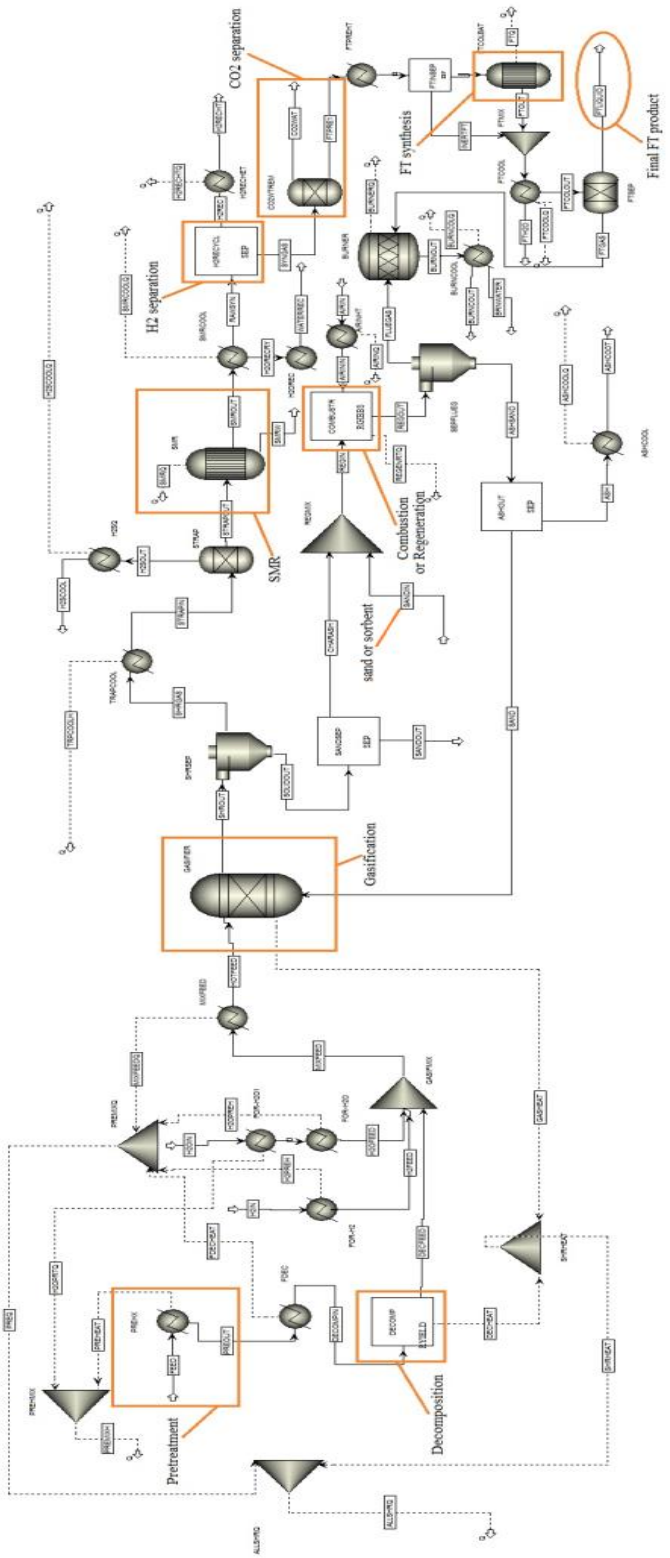

Fig.4.1 Block flow diagram of Aspen simulation for FT liquid fuel production based on SHR or SE-SHR

The production of H_2 and CO from SMR of SHR based process and SE-SHR based process is shown in Fig.4.2 and Fig.4.3, respectively. Before entering FT reactor, the amount of H_2 and CO should be evaluated to check if H_2 is enough for recycle use and how much carbon input for the FT synthesis.

The H_2 recycle baselines are plotted in these pictures. The H_2/C of 0.63, 1.08 and 1.59 was corresponding to the input value of 12557kmol/day, 21526kmol/day and 31691kmol/day, respectively. It can be seen that all H_2 yield was over its corresponding recycle baseline, indicating the process could be self-sustainable on H_2 supply. The H_2 production was much higher of SE-SHR based process than that of SHR based process under the same gasification condition. The extra H_2 could be used for further hydrotreating of some FT products like middle distillate (raw diesel).

The trend of CO was different. At each H_2/C of SHR based process, the CO yield was decreasing when Steam/C was raised. This was mainly due to less CH_4 produced from the gasifier with the increase of Steam/C. Thus, less CO was finally produced from the SMR reactor. On the other hand, the CO amount of SE-SHR based process was enhanced when Steam/C was increased. It was because that CH_4 yield did not change too much in the gasifier due to sorption enhanced performance. With higher steam input, more CO production was generated in SMR.

More CO output meant more carbon input for FT synthesis, leading to higher FT product yield. The highest CO production was obtained under the gasification condition (H_2/C-Steam/C) of 1.59-2.22 and 1.59-2.78 for SHR based process and SE-SHR based

process, respectively. These two conditions were considered optimum for further mass and heat balance analysis.

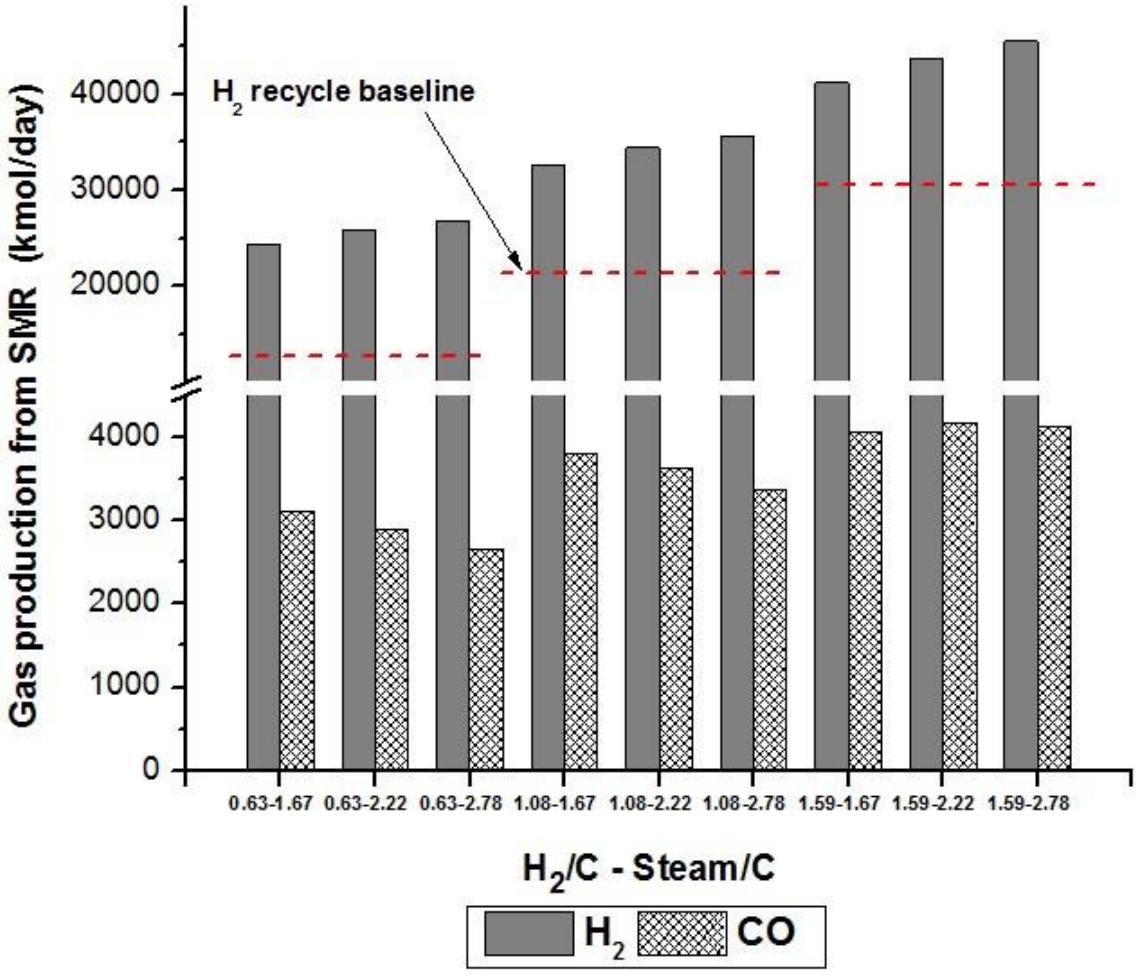

Fig.4.2 The production of H_2 and CO from SMR of SHR based process for FT liquid fuel production

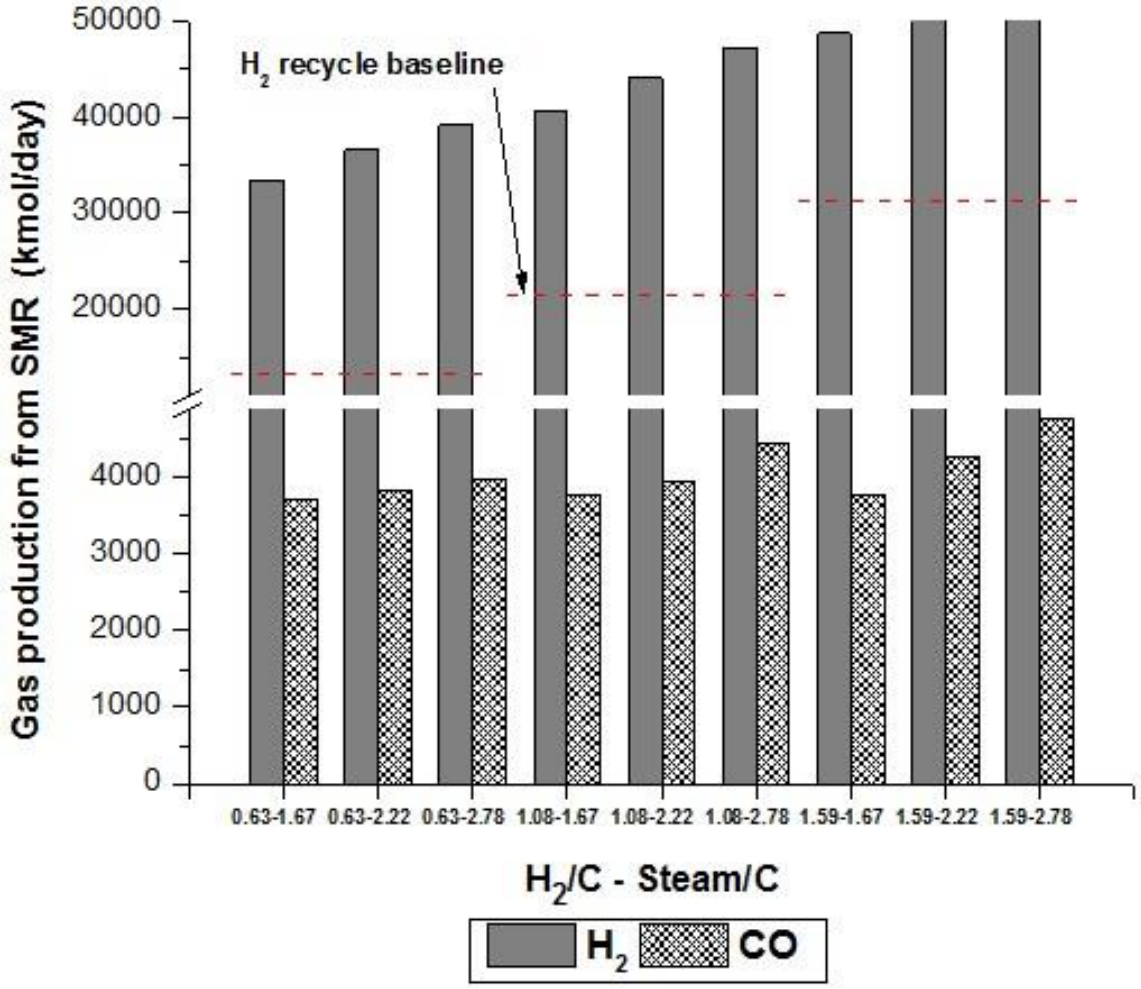

Fig.4.3 The production of H_2 and CO from SMR of SE-SHR based process for FT liquid fuel production

The production of CH_4 and CO_2 from SMR of SHR based process and SE-SHR based process is shown in Fig.4.4 and Fig.4.5, respectively. Also, CH_4 conversion percentage of SMR is depicted in these pictures. At each H_2/C, the CH_4 yield was reduced with the increase of steam during both processes. Accordingly, the CO_2 production was augmented and the CH_4 conversion percentage was increased. In particular, the CH_4

conversion percentage of SE-SHR based process was much lower than that of SHR based process under the same gasification condition. This was primarily due to more H_2 generated from SE-SHR gasifier, which affected the conversion of CH_4 from the equilibrium point of view.

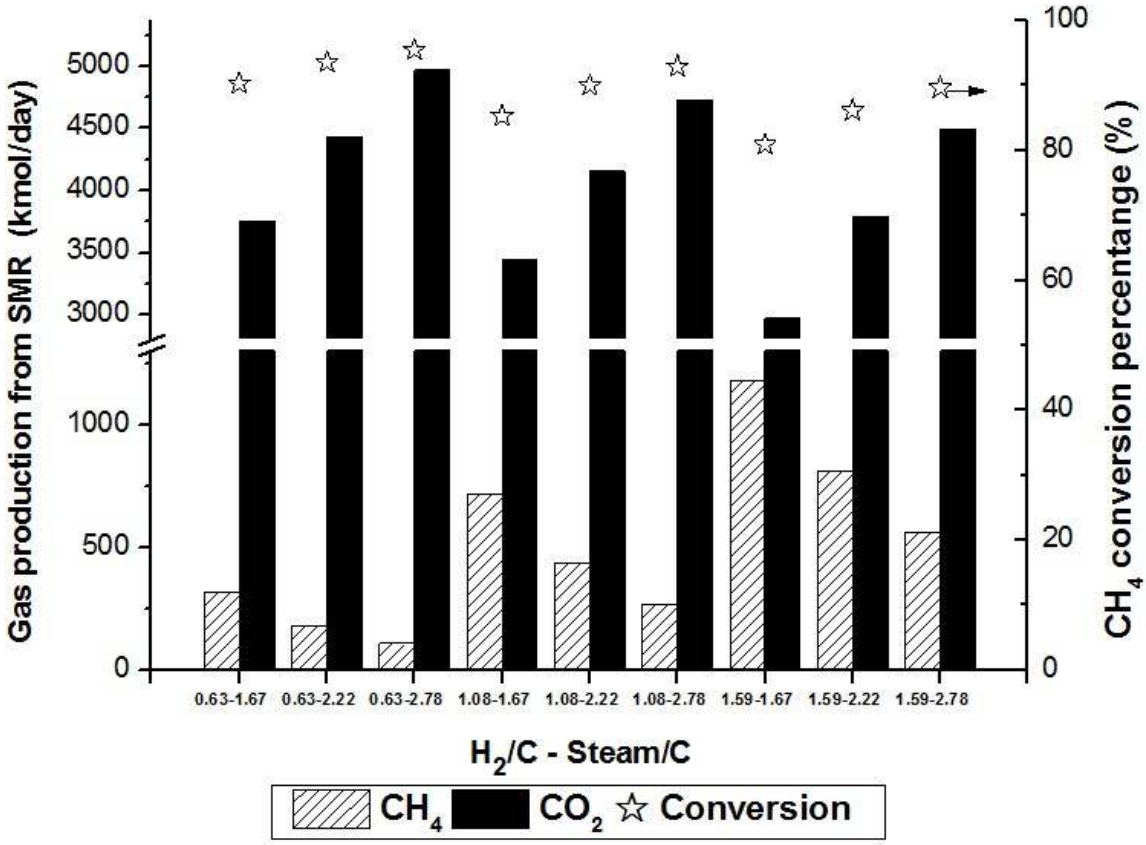

Fig.4.4 The production of CH_4 and CO_2 with CH_4 conversion percentage from SMR of SHR based process for FT liquid fuel production

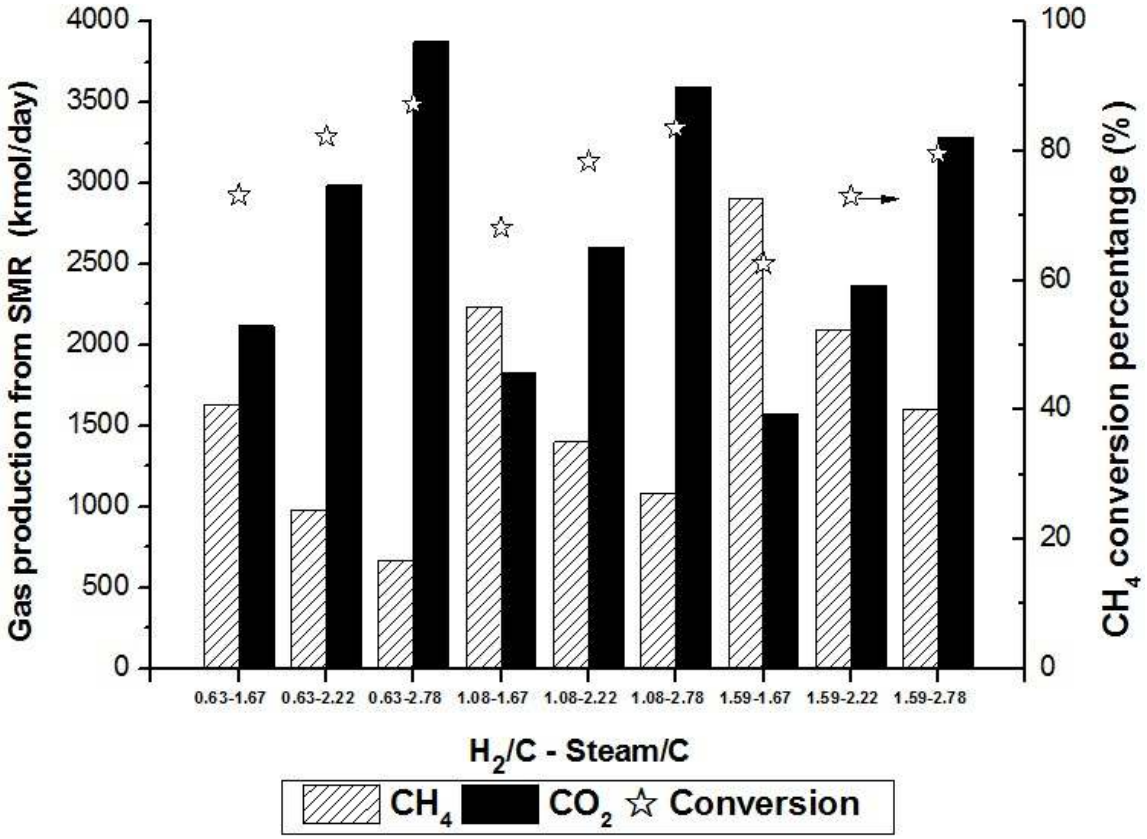

Fig.4.5 The production of CH_4 and CO_2 with CH_4 conversion percentage from SMR of SE-SHR based process for FT liquid fuel production

As mentioned above, the optimum gasification condition (H_2/C-Steam/C) for SHR based process and SE-SHR based process was 1.59-2.22 and 1.59-2.78, respectively. The final product distribution and yield from FT reactor under these two optimum gasification conditions was obtained and is shown in Fig.4.6. Due to higher carbon input for FT synthesis, the production of FT gas, raw naphtha, raw diesel and wax using the optimum SE-SHR based process was higher than those using the optimum SHR based process. Correspondingly, with further treating and upgrading of these raw stuffs, the ultimate production of gasoline and diesel fuel could be enhanced based on SE-SHR process.

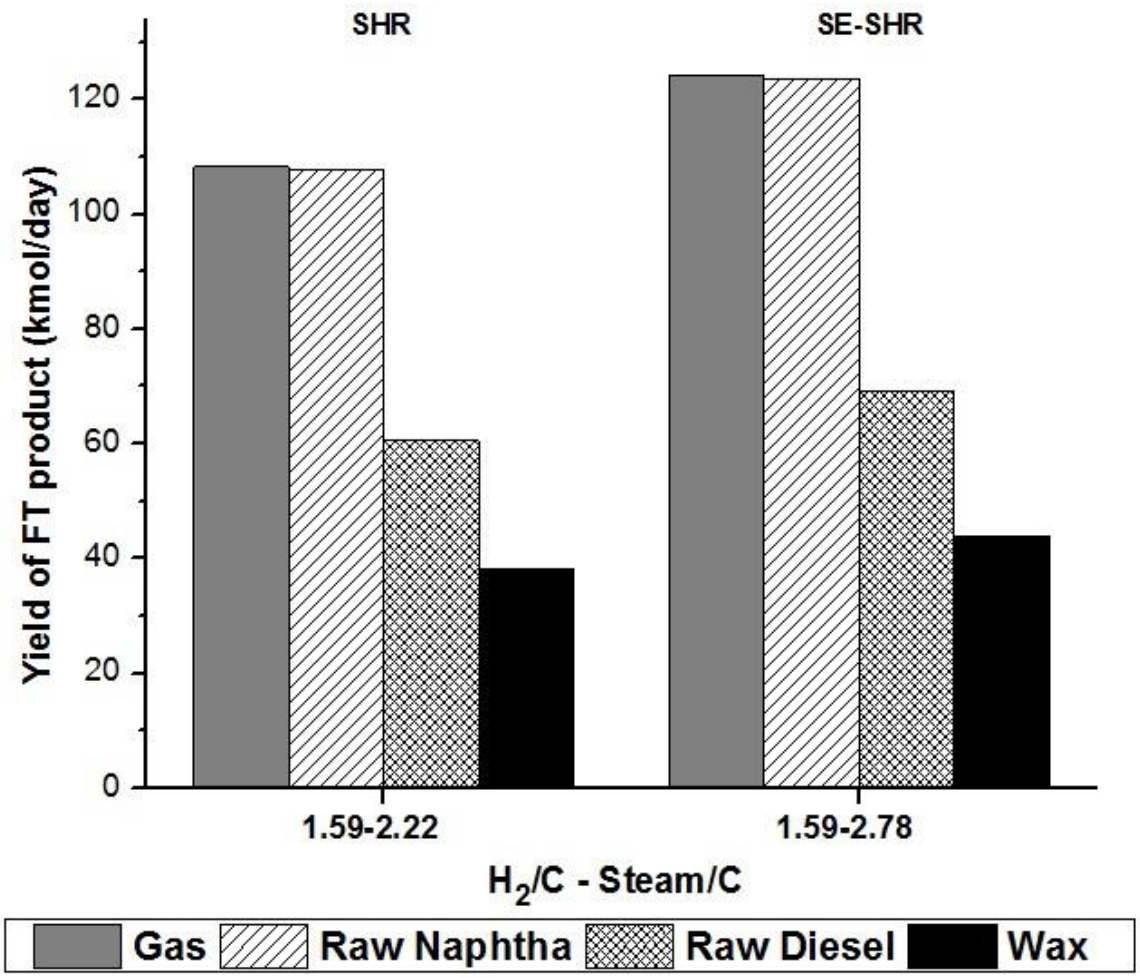

Fig.4.6 The comparison of two optimum cases in FT product yield

The detailed mass and heat analysis of two optimum processes are shown in Fig.4.7 and Fig.4.8. The mass balance of SHR based process is shown in Fig.4.7(a). It can be seen that 19932kmol carbon was conveyed to the gasifier and 11162kmol carbon in the form of char was finally burned in the combustor. 3787kmol CO_2 was captured before the syngas entered FT reactor. The carbon in the syngas was finally distributed to 3093kmol carbon in FT liquid and solid product, 903kmol CH_4 including the CH_4 newly produced

by FT synthesis, 72kmol other FT gas product excluding CH_4, and 915kmol unconverted CO.

The corresponding heat balance is shown in Fig.4.7(b). The energy recovered from the combustor and the burner was enough for the heat requirement of SHR. The energy recovered from the flue gas cooling could supply the heat required by the air pretreating. The heat from the gas cleanup cooling and the SMR syngas cooling could be used for the pretreatment and the SMR reactor. Additionally, there was more energy output from the FT section.

The mass balance of the optimum SE-SHR based process is shown in Fig.4.8(a). With the same carbon input, 13112kmol CO_2 finally exited from the regenerator and the burner. Compared to the optimum SHR based process, the CO_2 output in the flue gas was similar. Also, less CO_2 (3277kmol) was required to be captured before the FT reactor. Especially for recycle H_2, more extra H_2 (14695kmol after the reduction of input H_2 amount) could be obtained in the SE-SHR based process, compared to 3632kmol in the SHR based process.

According to the heat analysis of the optimum SE-SHR based process shown in Fig.4.8(b), the total heat from the burner and the cooling was enough for the regenerator, the air preheating and the SE-SHR gasifier. The energy needed by the SMR reactor and the pretreatment could be from the SMR syngas cooling, the gas cleanup cooling and the FT section. Though there was less net energy output in the SE-SHR scenario, the heat demand and the heat supply still could be paired.

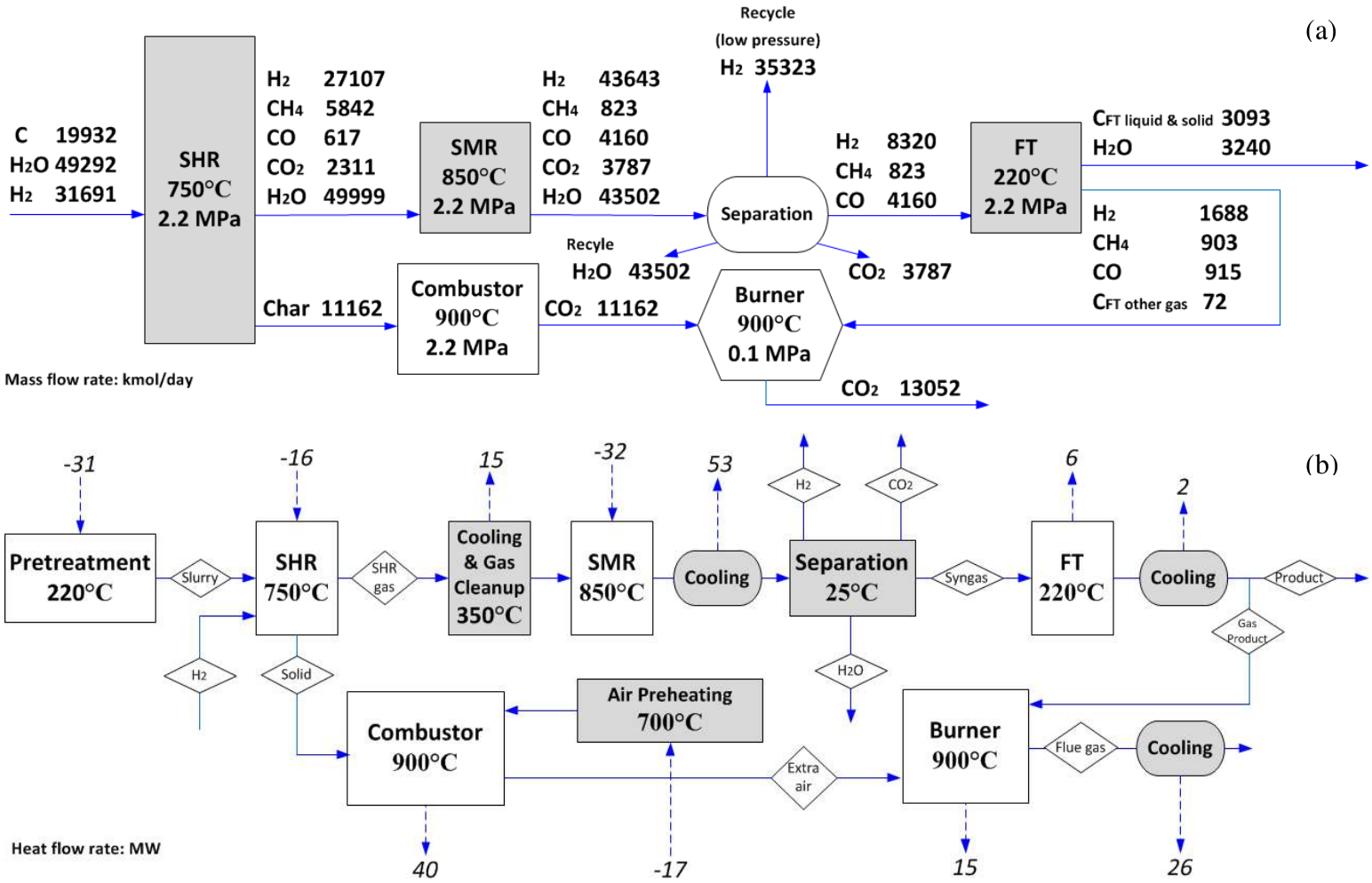

Fig.4.7 The mass and heat balance of main processing units of SHR based process for FT liquid fuel production

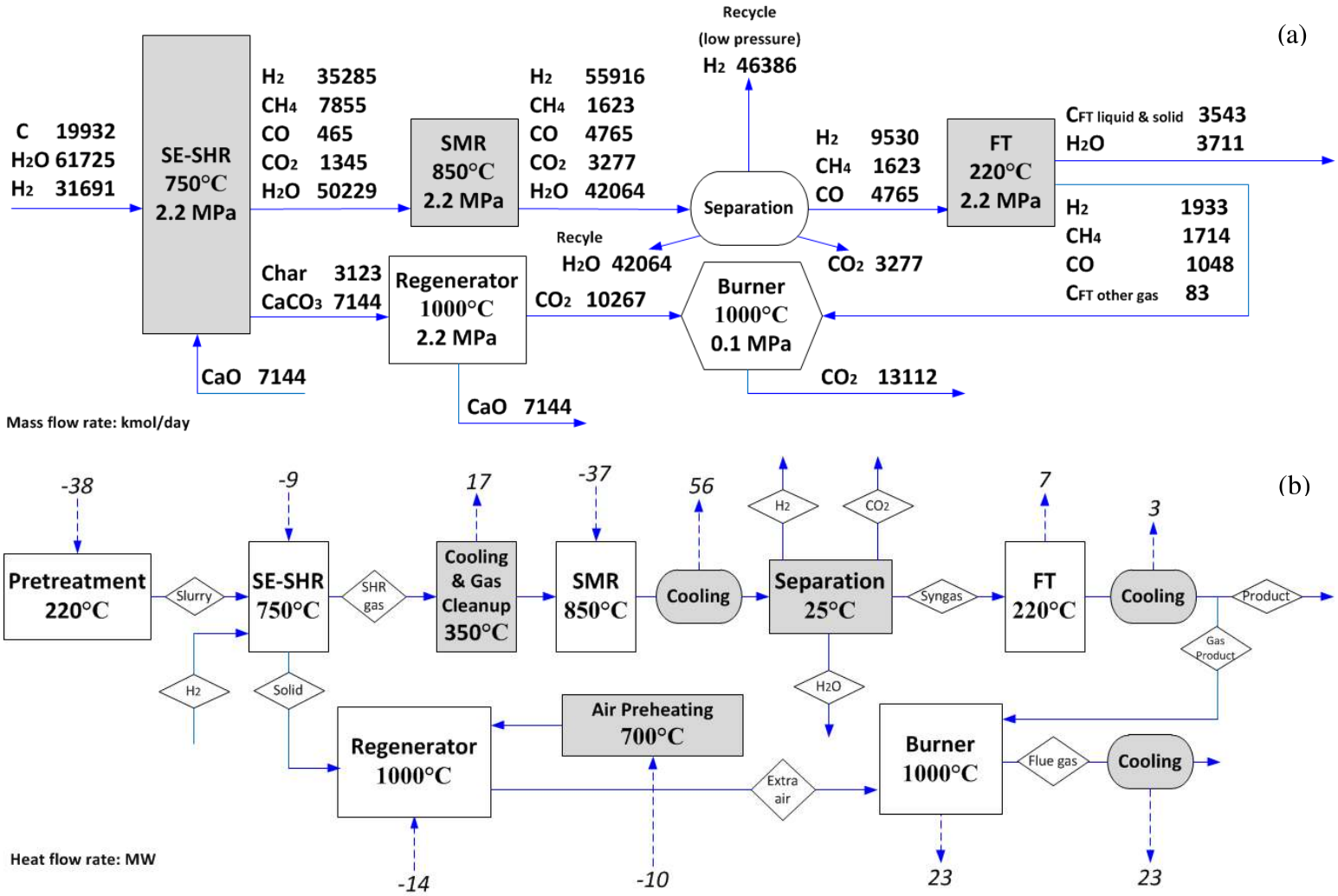

Fig.4.8 The mass and heat balance of main processing units of SE-SHR based process for FT liquid fuel production

The carbon balance is depicted in Fig.4.9. Compared to the optimum SHR based process, less carbon went to flue gas and separated CO_2 in the optimum SE-SHR based process. 14% of carbon was converted to FT gases. More CH_4 generated from the SE-SHR contributed to the FT gas primarily. Besides, 18% of FT liquid fuel and wax could be produced in the optimum SE-SHR based process.

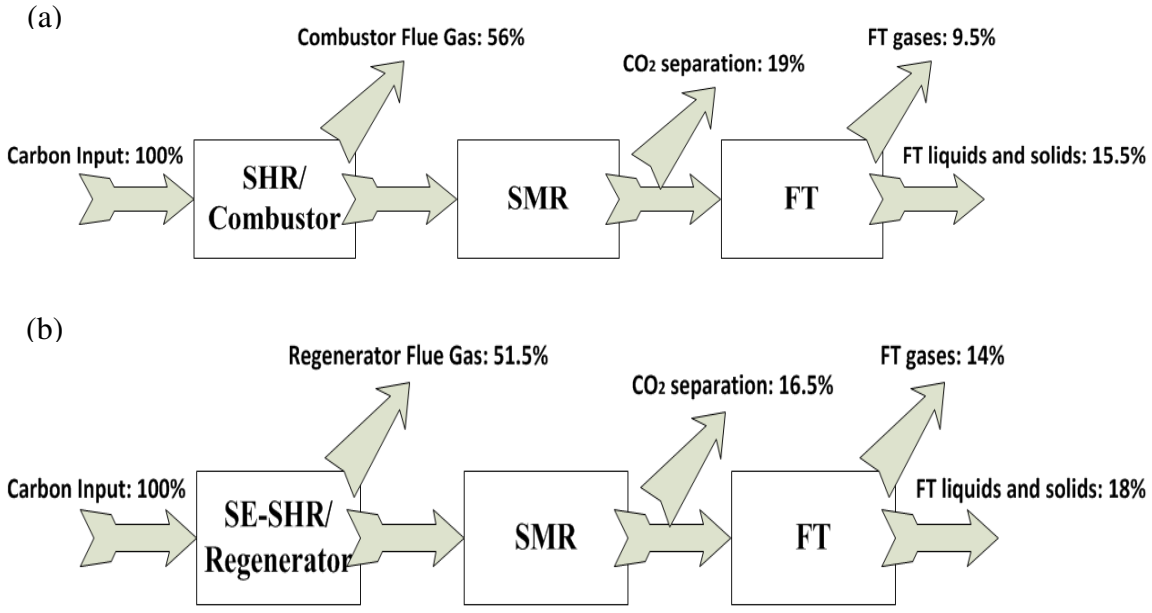

Fig.4.9 Carbon balance of SHR based and SE-SHR based processes for FT fuel production (a) SHR based (b) SE-SHR base

4.3.2 Sorption enhanced CE-CERT processes for SNG production with comparison to conventional CE-CERT process

The sorption enhanced CE-CERT process and the conventional CE-CERT process for SNG production were simulated using Aspen Plus software. The block flow diagram of SHR-WGS based and SE-SHR-WGS based processes was similar and is shown in Fig.4.10. The only difference was using quicklime for sorption enhanced process.

Similar to the process for FT fuel production, the process was simulated using pretreatment section, decomposition section, gasification section, and combustor or regenerator section. After the producer gas was cleaned up, it was sent to the WGS section to convert CO to H_2 and CO_2. Then 99% of H_2 and CO_2 were removed from the output gas. Water was separated from the product by condensation. The remained product gas was SNG.

The process based on SE-SHR-Methanation was a little bit different from the above two processes, which block flow diagram is shown in Fig.4.11. The difference was in the downstream processing unit. Methanator was used instead of WGS, in which CO and CO_2 reacted with extra H_2 to make more CH_4. Accordingly, only H_2 was required to be separated from the gas product.

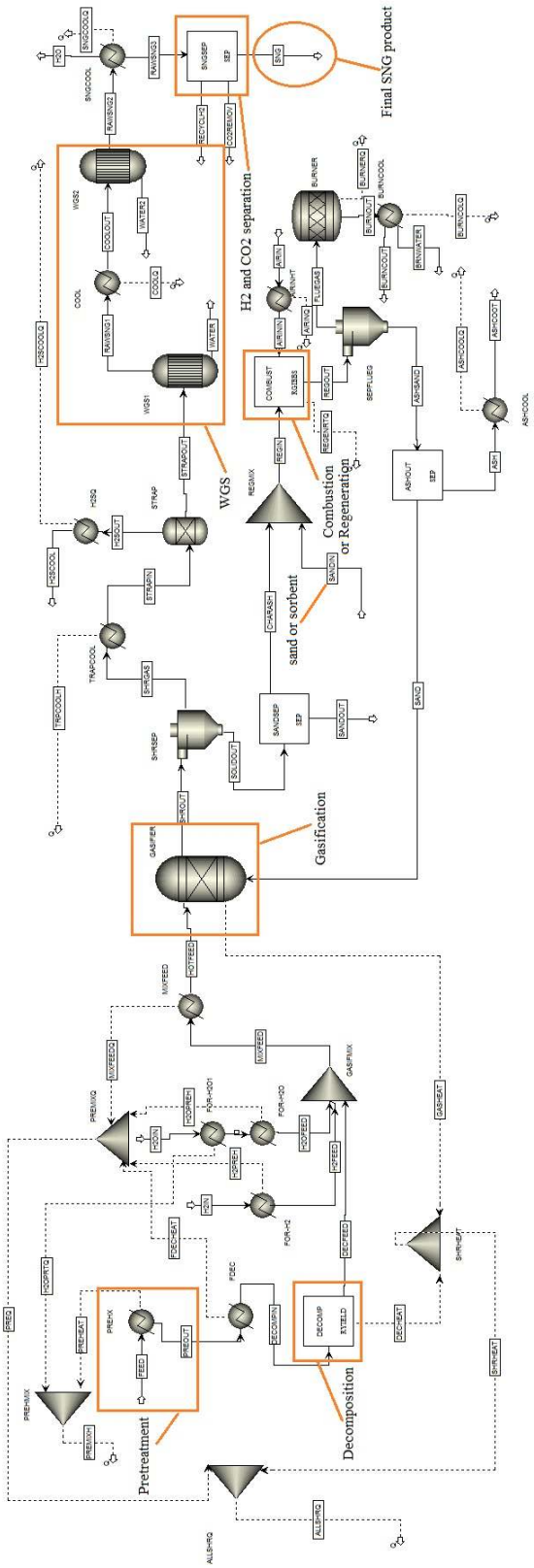

Fig.4.10 Block flow diagram of Aspen simulation for SNG production based on SHR-WGS or SE-SHR-WGS

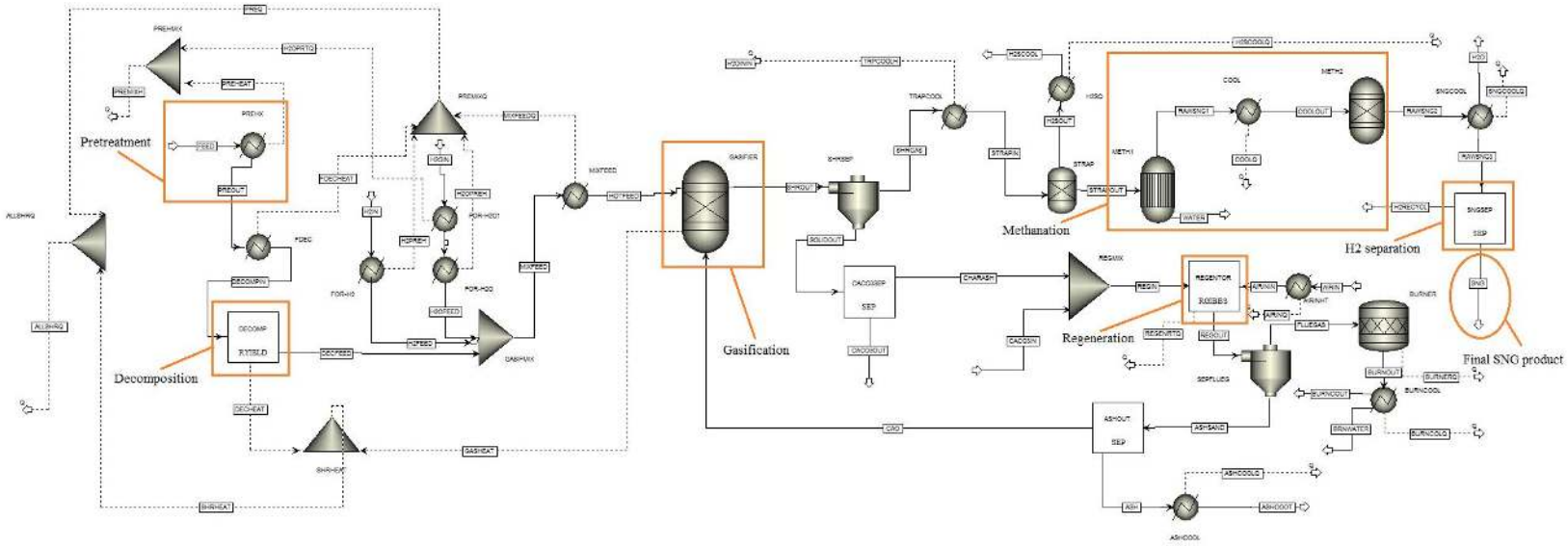

Fig.4.11 Block flow diagram of Aspen simulation for SNG production based on SE-SHR-Methanation

The production of H_2 and CH_4 from WGS of SHR based process is depicted in Fig.4.12. The H_2 recycle baselines are plotted in the figure, which represent the H_2/C of 0.63, 1.08 and 1.59. It can be seen that the H_2 yield from the WGS reactor under some gasification conditions could not meet the recycle requirement, such as H_2/C of 1.59. Due to the enhancement of steam gasification, CH_4 production was decreased with the increase of Steam/C. The maximum CH_4 yield was obtained with sufficient recycle H_2 under the gasification condition (H_2/C-Steam/C) of 1.08-2.22.

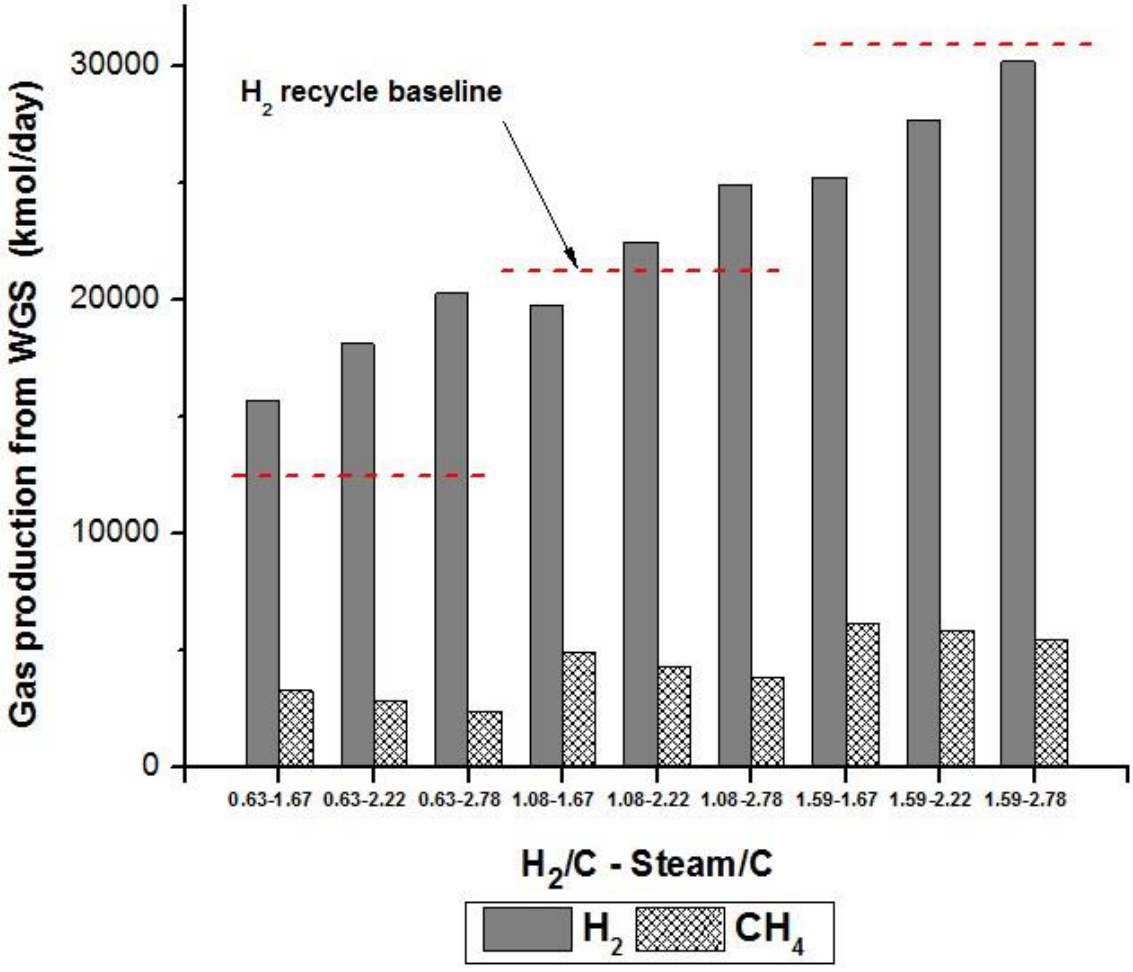

Fig.4.12 The production of H_2 and CH_4 from WGS of SHR based process for SNG production

The production of H_2 and CH_4 from WGS of SE-SHR based process is shown in Fig.4.13. It can be seen that all H_2 yields from the WGS reactor were beyond corresponding recycle baseline. It meant the process under these gasification conditions could be self-sustainable on H_2 supply. Due to the enhancement of steam gasification, CH_4 production decreased a little bit. The maximum CH_4 yield was produced under the gasification condition (H_2/C-Steam/C) of 1.59-1.67.

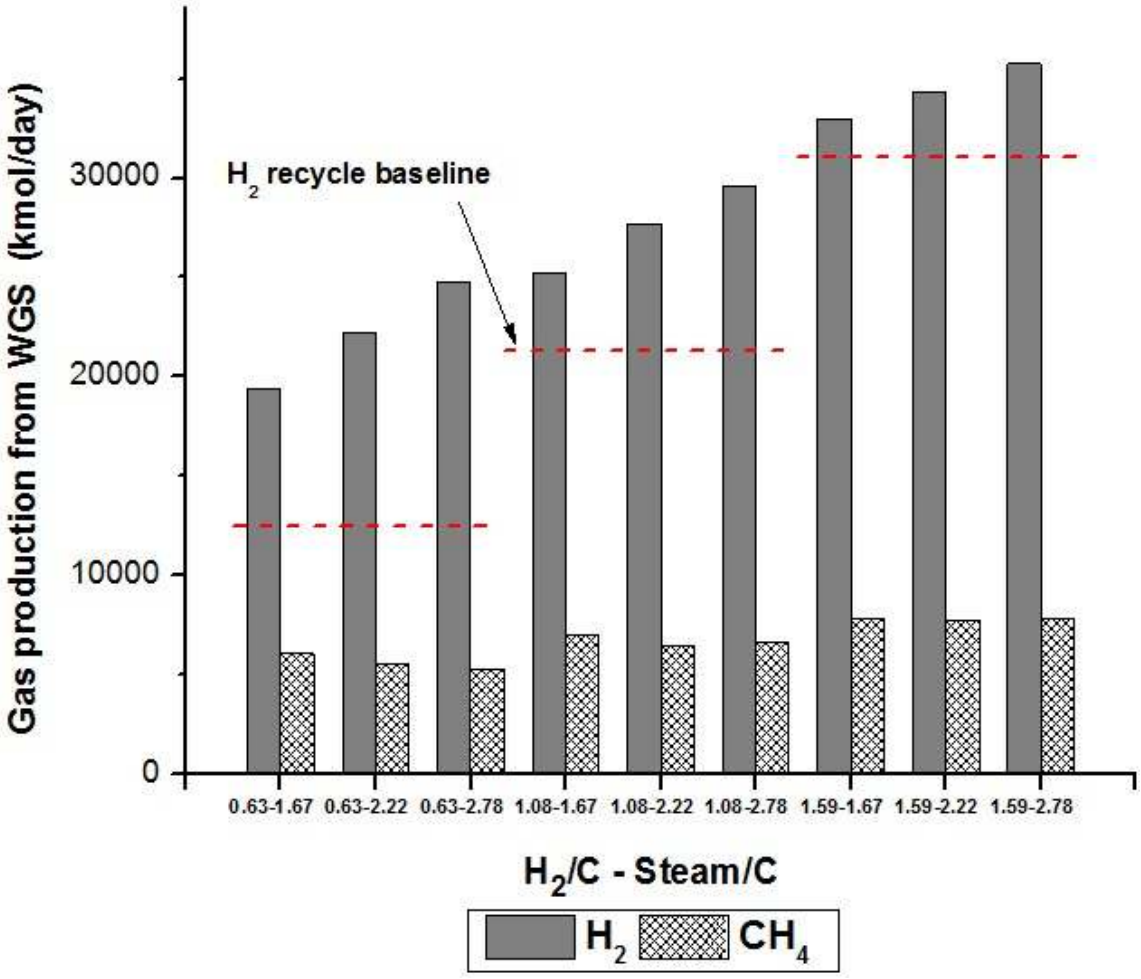

Fig.4.13 The production of H_2 and CH_4 from WGS of SE-SHR based process for SNG production

The production of H_2 and CH_4 from methanation of SE-SHR based process is shown in Fig.4.14. It can be seen that only the H_2 yield from the methanator under the gasification conditions of 0.63-1.67, 0.63-2.22, 1.08-1.67 and 1.08-2.22 could meet the recycle requirement. Due to the enhancement of steam gasification, more CO and CO2 were produced in the producer gas, which contributed to the further CH_4 synthesis. Consequently, CH_4 yield was ascending with the increase of Steam/C. The maximum CH_4 yield was produced under the gasification condition (H_2/C-Steam/C) of 1.08-2.22.

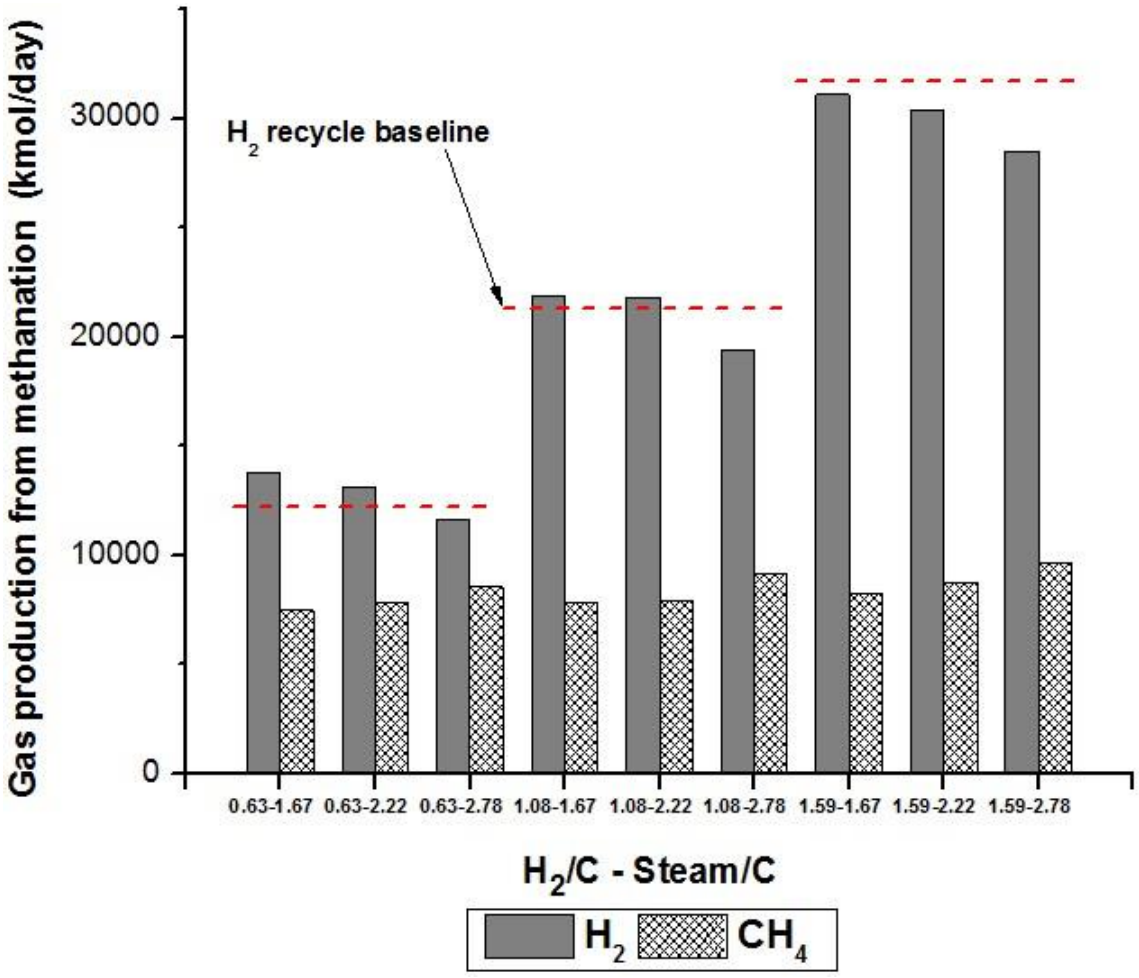

Fig.4.14 The production of H_2 and CH_4 from methanation of SE-SHR based process for SNG production

The production of CO and CO_2 from WGS of SHR based process and SE-SHR based process is shown in Fig.4.15 and Fig.4.16, respectively. Besides, CO conversion percentage of WGS is also depicted in these figures. At each H_2/C, the yield of CO and CO_2 was enhanced with the increase of Steam/C during both processes. This trend was in accordance with the trend in the gasifier. The CO_2 production from WGS of SE-SHR based process was much less than that of SHR based process. The CO_2 production was reduced at least by 50%. The CO conversion percentage was close to 100% for both processes. It was because of two WGS reactors set in series, high temperature shift and low temperature shift as aforementioned.

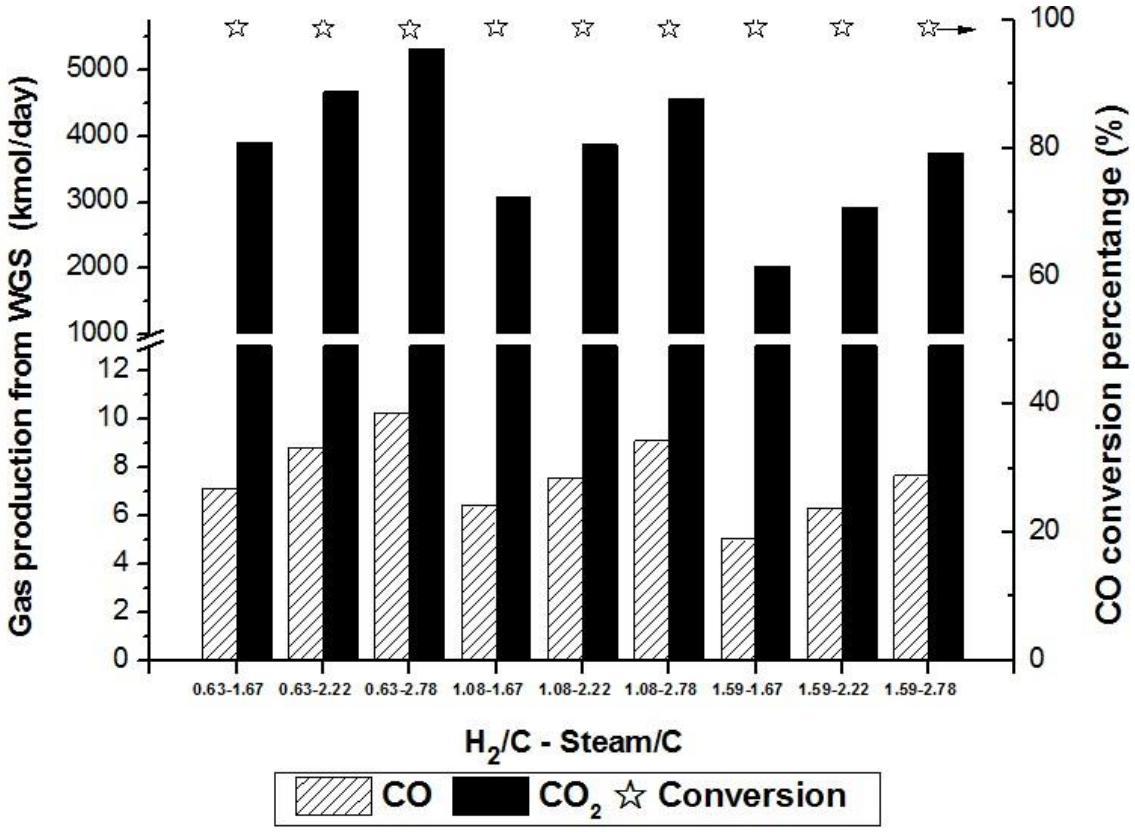

Fig.4.15 The production of CO and CO_2 with CO conversion percentage from WGS of SHR based process for SNG production

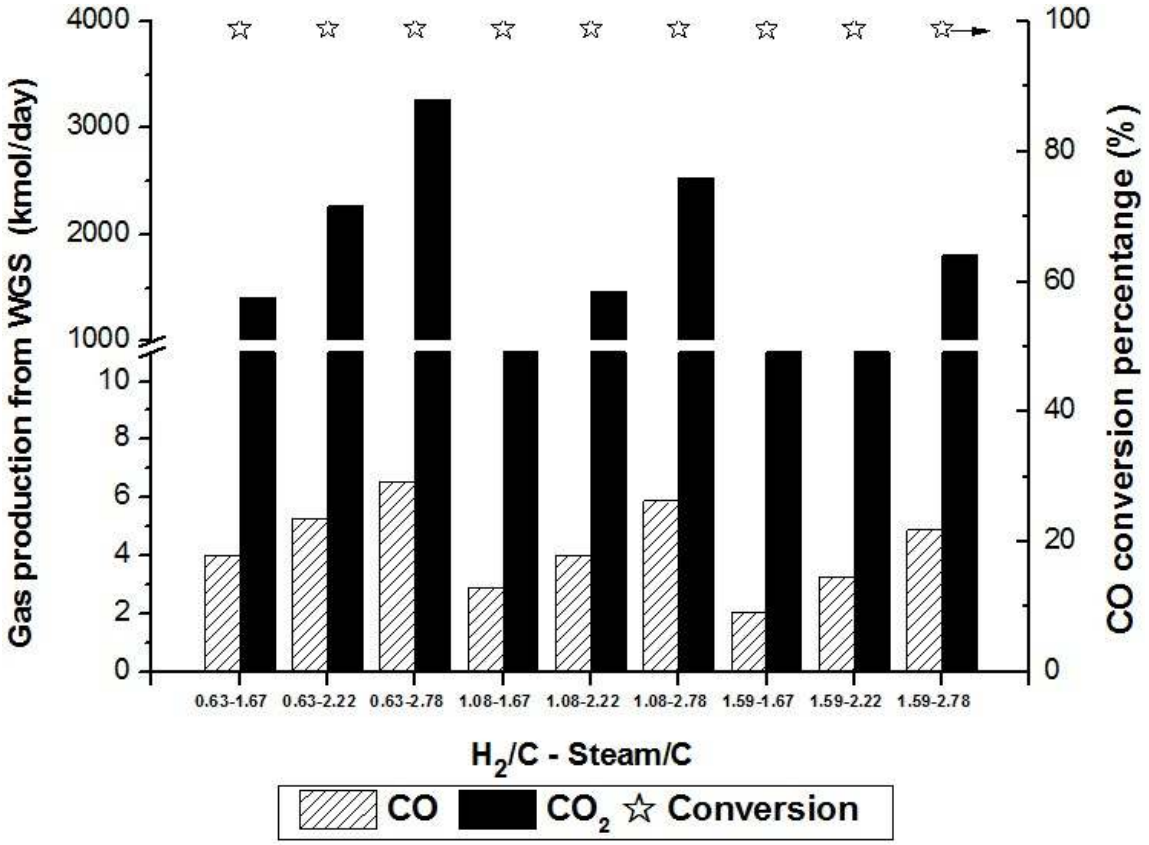

Fig.4.16 The production of CO and CO_2 with CO conversion percentage from WGS of SE-SHR based process for SNG production

The production of CO and CO_2 with conversion percentage from methanation of SE-SHR based process is shown in Fig.4.17. It can be seen that at each H_2/C the yield of CO and CO_2 was increased when the steam input was raised. However, the final yield of these two gases was extremely low and could be neglected in the SNG product. The conversion percentage of CO and CO_2 was very high due to two methanators in series.

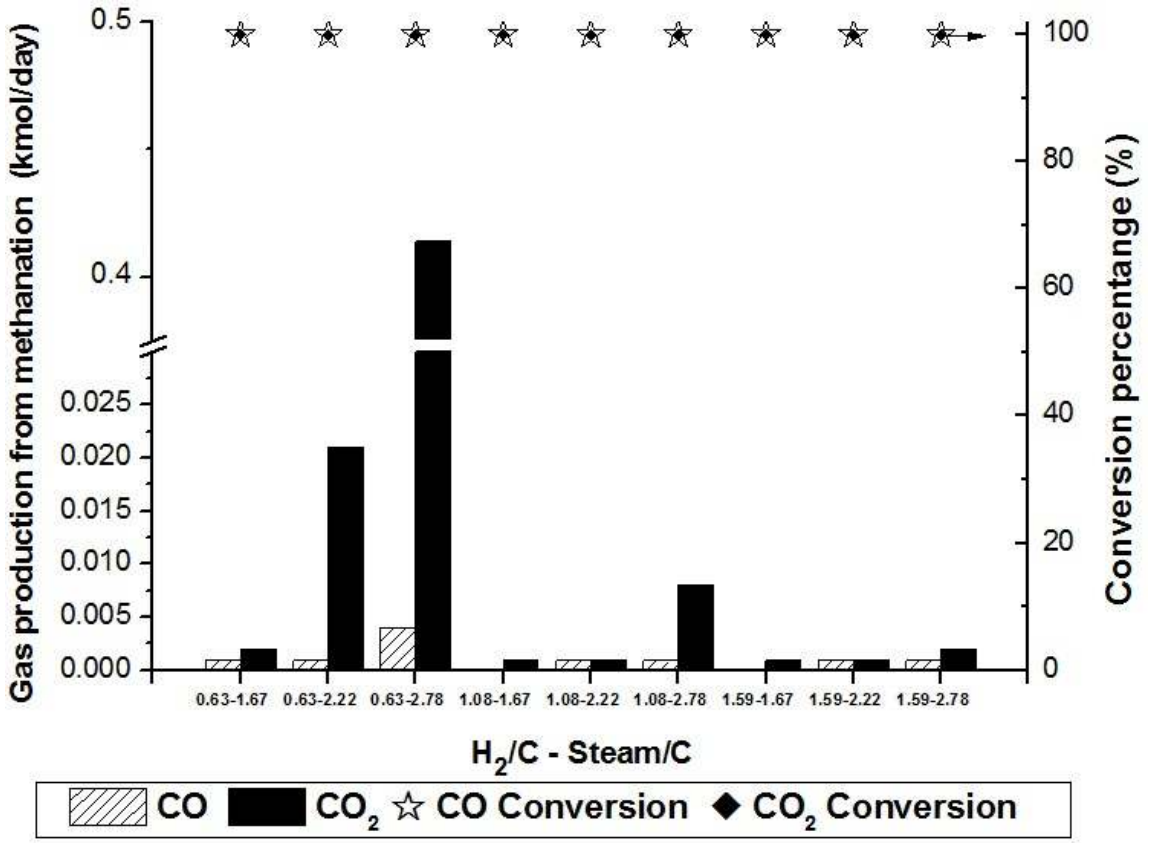

Fig.4.17 The production of CO and CO_2 with conversion percentage from methanation of SE-SHR based process for SNG production

The corresponding mass and heat analysis of above three optimum processes is depicted in Fig.4.18, Fig.4.19 and Fig.4.20. The mass balance of these processes is shown in Fig.4.18(a), Fig.4.19(a) and Fig.4.20(a), respectively. 4335kmol, 7779kmol and 6470kmol carbon was converted to CH_4 in the gasifier in the SHR-WGS based, SE-SHR-WGS based and SE-SHR-Methanation based processes, respectively. The carbon in the form of CO_2 released from the combustor or the regenerator in these three processes was 11720kmol, 11675kmol and 11993kmol, respectively. No more carbon was distributed to CH_4 after WGS for SHR-WGS based and SE-SHR-WGS based processes. But more

carbon was converted to CH_4 via methanation in the SE-SHR-Methanation based process. So the CH_4 production in the final SNG product was 7939kmol. Less CO entered the WGS reactor in the SE-SHR-WGS based process compared to the SE-SHR-WGS based process. It indicated the potential to reduce the WGS reactor size. Besides, 3869kmol CO_2 needed to be separated from the final product gas in the SHR-WGS based process. By contrast, only 476kmol CO_2 was required for separation in the SE-SHR-WGS based process and almost no CO_2 existed in the SNG of the SE-SHR-Methanation based process. This substantially reduced the cost for CO_2 separation.

The corresponding heat balance of three optimum processes is shown in Fig.4.18(b), Fig.4.19(b) and Fig.4.20(b). In SHR-WGS based process, the energy recovered from the combustor and the flue gas cooling was enough for the heat requirement of the gasifier, the air preheating and the pretreatment. Besides, there was more energy output from the cooling of gas cleanup and WGS. In the case of SE-SHR-WGS and SE-SHR-Methanation based processes, the energy from the flue gas cooling could supply all the heat required by the air pretreating, the regenerator and the gasifier. The heat from the cooling of gas cleanup section and the WGS/Methanation section could be used for the pretreatment. There was very limited net energy output from two SE-SHR based processes, though the heat demand and the heat supply could be paired. A bit of the final SNG product (e.g. 5%) could be used for extra heat supply if necessary. This would not affect the higher production.

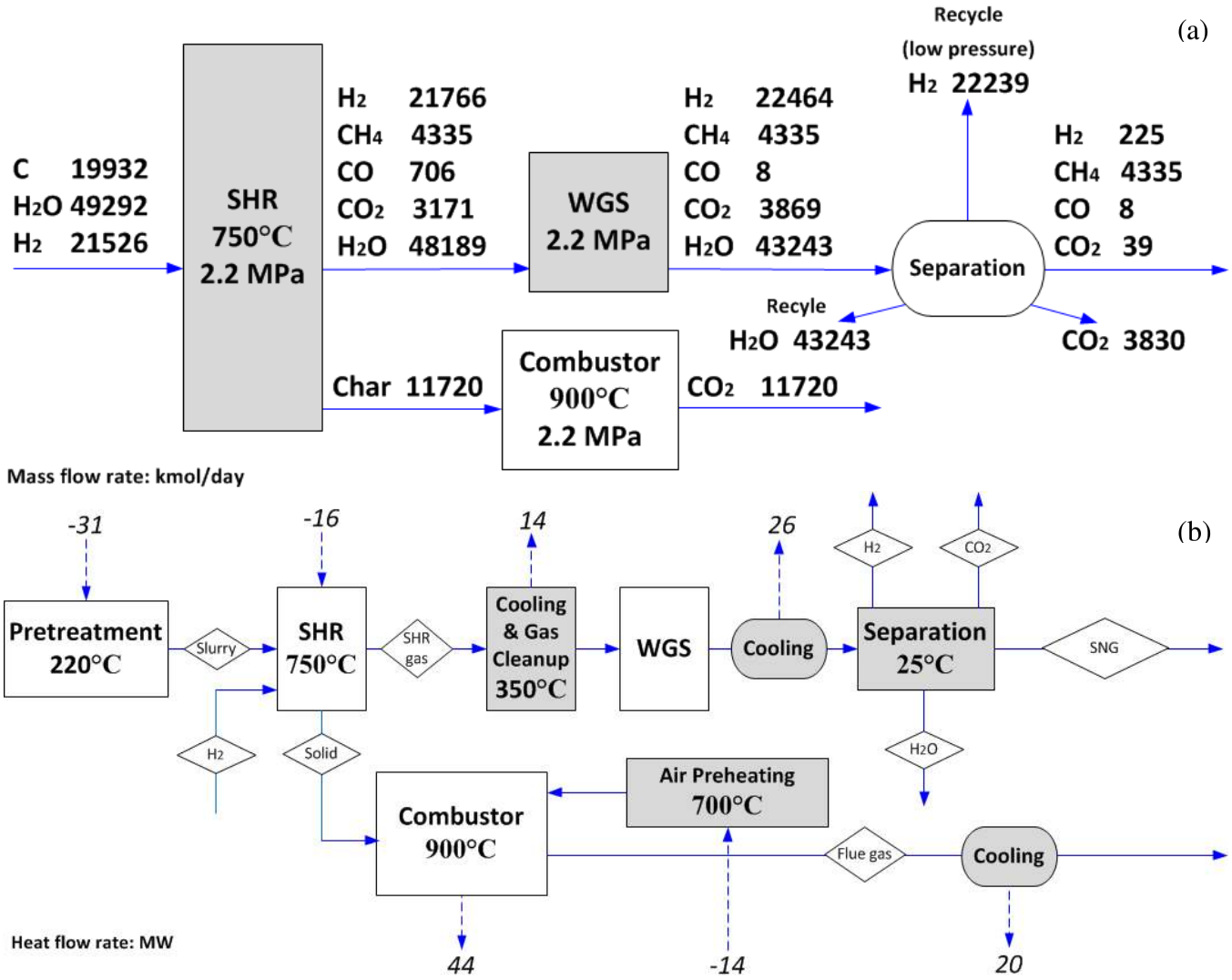

Fig.4.18 The mass and heat balance of main processing units of SHR-WGS based process for SNG production

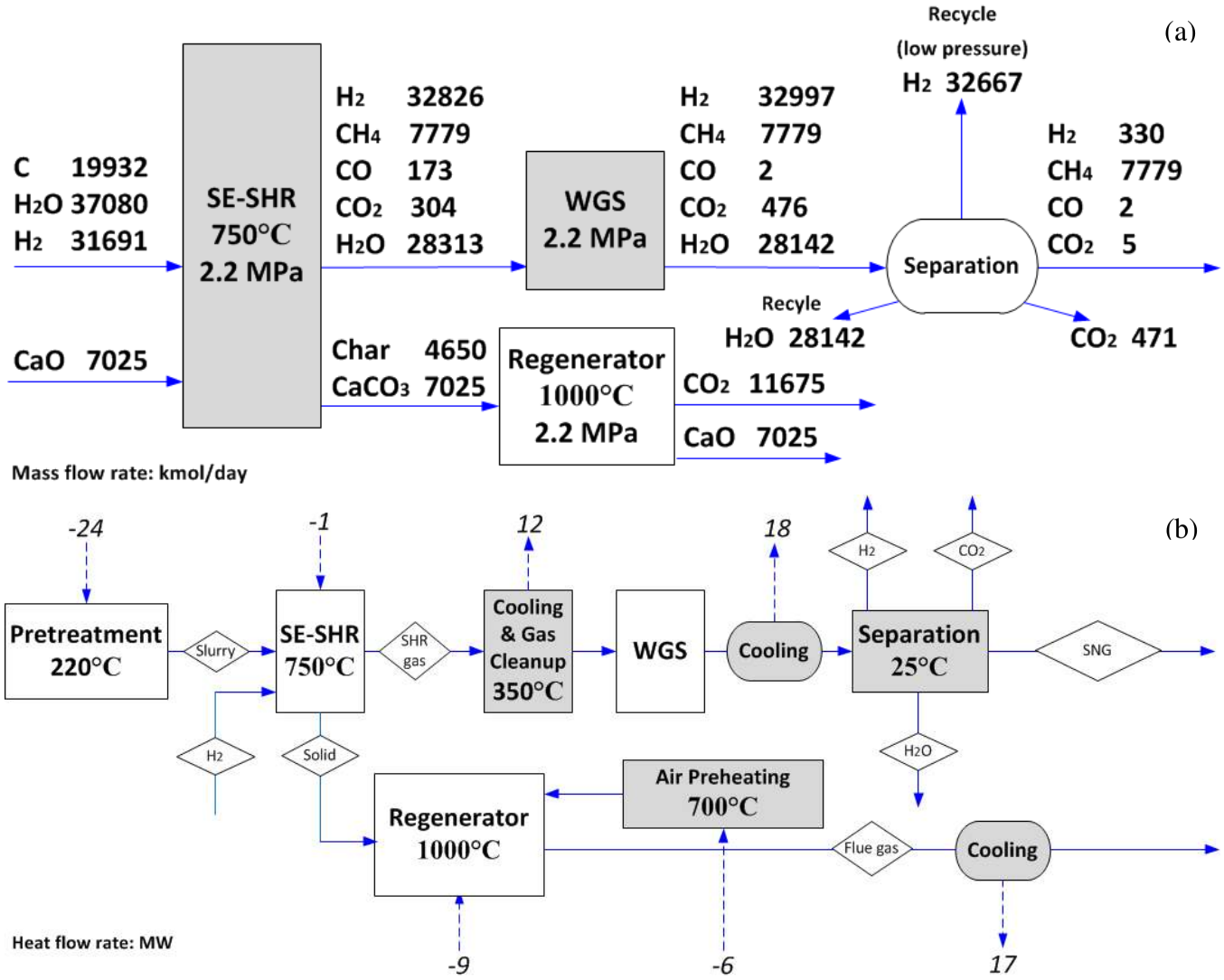

Fig.4.19 The mass and heat balance of main processing units of SE-SHR-WGS based process for SNG production

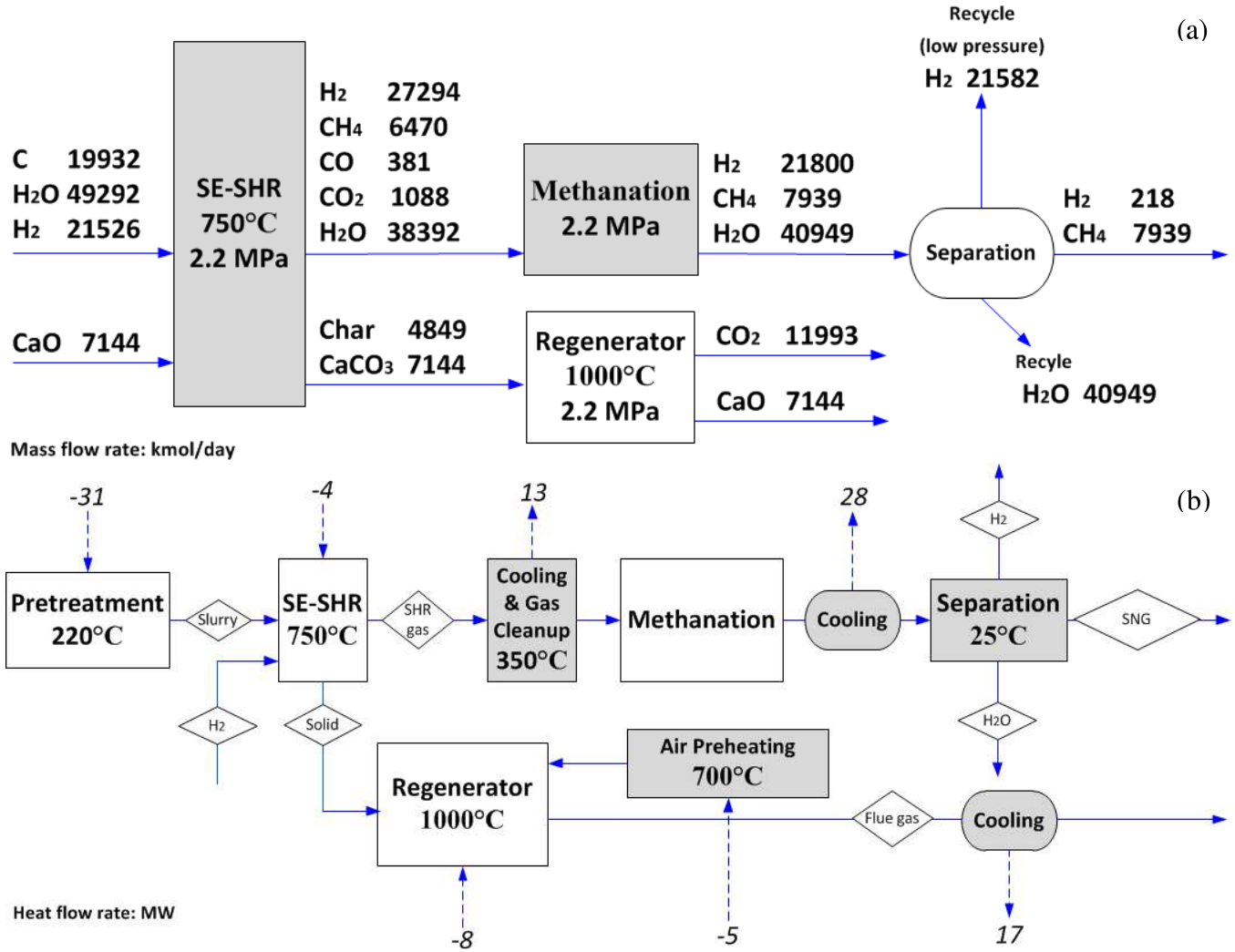

Fig.4.20 The mass and heat balance of main processing units of SE-SHR-Methanation based process for SNG production

The carbon balance of each process is depicted in Fig.4.21. It shows that about 60% carbon went to the combustor or the regenerator flue gas in these processes. Only 22% carbon was distributed to CH_4 in the SHR-WGS based process. By contrast, about 40% carbon was converted to CH_4 in the two SE-SHR based processes. In particular, SE-SHR-Methanation based process had almost zero carbon in the form of CO_2 in the end.

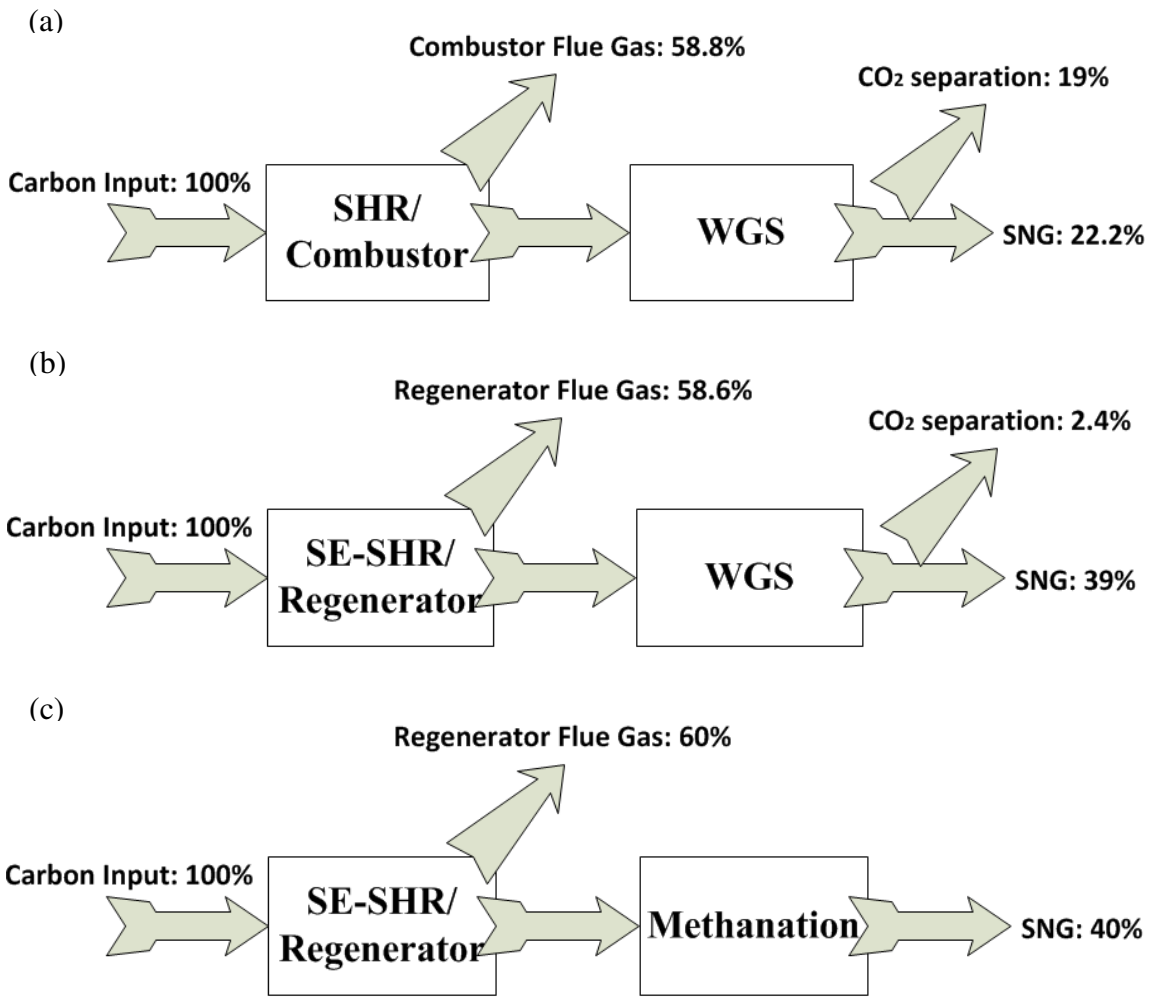

Fig.4.21 Carbon balance of SHR based and SE-SHR based processes for SNG production (a) based on SHR-WGS (b) based on SE-SHR-WGS (c) based on SE-SHR-Methanation

The comparison of SNG quality among SHR based and SE-SHR based processes is shown in Table 4.3.

Table 4.3 Comparison of SNG quality among SHR based and SE-SHR based processes

	SHR WGS	SE-SHR WGS	SE-SHR Methanation
CH_4 (vol%)	94.1	95.85	97.33
H_2 (vol%)	4.88	4.07	2.67
CO (vol%)	0.17	0.02	≈0
CO_2 (vol%)	0.85	0.06	≈0
Energy Efficiency%	38.02	67.99	69.06
CH_4 Conversion%	21.75	39.03	39.83
WI (MJ/Nm^3)	47.12	48.03	48.26

The table shows that SE-SHR-Methanation based process had comparatively higher CH_4% and lower CO_2%. The two SE-SHR based processes had much higher overall energy efficiency, which percentage was almost 70%. Additionally, the CH_4 conversion efficiency of the two SE-SHR based processes was almost two times higher than that of the SHR based process.

The absolute minimum and maximum number of WI in most United States cities are $44.8MJ/Nm^3$ and $52.9MJ/Nm^3$, respectively[126]. According to the Wobbe numbers in Table 4.3, these three SNG products could fit the standard range perfectly as a qualified interchangeable fuel. They could be burned satisfactorily in most appliances, boilers,

burners, power plants and turbines with negligible change in burner performance without the need for special adjustment.

4.4 Summary

The performance of SE-SHR based processes for both FT synfuel and SNG production was evaluated. The performance was compared to the conventional SHR based processes. The main results were summarized as below.

1. The optimum gasification condition (H_2/C-Steam/C) for FT synthetic fuel production using SHR based process and SE-SHR based process was 1.59-2.22 and 1.59-2.78, respectively.

2. The optimum SE-SHR based process for FT synthetic fuel production had comparatively lower total CO_2 emissions with higher FT product yield.

3. The optimum gasification condition (H_2/C-Steam/C) for SNG production using SHR-WGS based, SE-SHR-WGS based and SE-SHR-Methanation based processes was 1.08-2.22, 1.59-1.67 and 1.08-2.22, respectively.

4. The two optimum SE-SHR based processes for SNG production had much lower total CO_2 emissions with higher SNG yield compared to the SHR based process. The optimum SE-SHR-Methanation based process had the highest CH_4% with near zero CO_2% in the SNG.

5. The WGS reactor size in the SE-SHR-WGS based process could be reduced to save cost due to lower CO input compared to the SHR-WGS based process.

5. Conclusions and future work

5.1 Conclusions

The thesis is aimed to deal with energy-related CO_2 emissions with the increasing demand for energy. One unique CO_2 capture method, in-situ CO_2 capture technology, was used for SHR. This new concept was named sorption enhanced steam hydrogasification reaction. CO_2 was removed by the sorbent instantly in the gasifier as it formed, which changed the equilibrium to promote more energetic production. Thus, CO_2 emission minimization and energy production maximization could be achieved simultaneously.

It was found that the addition of sorbent could remove CO_2 and increase the production of H_2 and CH_4. In particular, the amount of H_2 increased dramatically and enough for recycle use over the CaO/C molar ratio of 0.29. Sorbent addition improved the H_2 production with CO_2 captured at different temperatures. Higher temperature favored higher energetic gas yield, but too high temperature (i.e. 800°C) would produce more CO_2. Besides, sorbent with different particle size had the same positive effect on CO_2 removal and H_2 enhancement.

When H_2/C was increased, the production of H_2 and CH_4 increased and that of CO and CO_2 decreased. This could be explained as hydrogasification was favored over steam gasification. When Steam/C was increased, the yield of H_2, CO and CO_2 was improved, because steam gasification was predominant. In particular, since more H_2 was produced during SE-SHR, the consumption of CH_4 was compensated by hydrogenation and its production had little change.

Moreover, the kinetics study showed that higher gasification temperature favored faster formation rates of CO_2, CO and CH_4 during both SE-SHR and SHR. The formation rates of CO_2 and CO at 650°C, 700°C and 750°C during SE-SHR were much lower than those during SHR. It was mainly due to the enhanced shift of WGS with sorbent addition, making more CO converted with simultaneous CO_2 capture. The activation energies of CO and CO_2 were increased accordingly. In addition, more sorbent loading could capture more CO_2, leading to slower CO_2 evolution. Better mixing between feedstock and sorbent could reduce CO_2 formation rate.

Lastly, SE-SHR was used for the production of FT fuel and SNG. The SE-SHR based processes were technically evaluated and compared to the conventional SHR based processes. The optimum gasification condition (H_2/C-Steam/C) for FT synthetic fuel production using SHR based process and SE-SHR based process was 1.59-2.22 and 1.59-2.78, respectively. The optimum SE-SHR based process had lower total CO_2 emissions with higher FT product yield. The optimum gasification condition (H_2/C-Steam/C) for SNG production using SHR-WGS based, SE-SHR-WGS based and SE-SHR-Methanation based processes was 1.08-2.22, 1.59-1.67 and 1.08-2.22, respectively. The two optimum SE-SHR based processes had much lower total CO_2 emissions with higher SNG yield compared to the SHR based process. The optimum SE-SHR-Methanation based process had the highest CH_4% with near zero CO_2% in the SNG. Besides, the WGS reactor size in the SE-SHR-WGS based process could be reduced to save cost due to lower CO input compared to the SHR-WGS based process

5.2 Future work

There are several concerns which should be addressed in the future application of sorption enhanced technology to the CE-CERT process. They are sorbent attrition issue, decay in CO_2 carrying capacity and economic feasibility.

Attrition inside the fluidized bed system makes sorbent into fine particles, which are prone to be elutriated from the reactor. Thus, the attrition rate of sorbent during SE-SHR should be investigated.

Some potential solutions were proposed to address the attrition problem, including optimum natural sorbent, pretreatment and artificial sorbent. First, attrition rate varies among limestones, thus, the optimum sorbent possessing best resistance should be selected. Also, attrition rate could be reduced by the improvement of mechanical stability via sorbent pretreatment. Last, artificial sorbent is an option, which could tolerate the attrition with more cycles. These solutions should be tested in the SE-SHR system.

Decay in CO_2 carrying capacity is another practical problem, which is mainly due to blockage and sintering. In general, after the first regeneration (calcination), the dispersed and porous CaO with high reactivity is formed. However, the following carbonation cannot be complete due to pore blocking and sintering. Sometimes, after 50 cycles, some pores are closed forever and a rigid backbone of sorbent with less reactivity is formed. Consequently, decay is a major barrier during the implementation of sorption enhanced technology.

There are two possible solutions to this issue, using dolomites and improvement by attrition. Calcined dolomites display superior long-term CO_2 uptake. It is mainly because

that the porosity is maintained by the unreacted MgO network. The carrying capacity of dolomites drops slowly upon further cycling. Therefore, dolomites should be evaluated in the SE-SHR system. Besides, as mentioned above, attrition makes sorbent break up, which makes pores reopen with higher capacity. The contribution from attrition should be also investigated.

Economic feasibility study is very crucial to evaluate the potential of commercializing a new process. The study will assist investors make right judgment. Economic analysis should be done based on the mass analysis of sorption enhanced CE-CERT processes. These processes should be on an IGCC basis for polygeneration including power, fuel and chemical. The cost of sorbent such as quicklime is not expensive, but the future work should consider the transportation cost, the reuse cycles and the disposal pathway, which could affect the final production cost.

References

1. U.S. Energy Information Administration, International Energy Outlook 2010, 2010.

2. http://www.esrl.noaa.gov/gmd/ccgg/trends/

3. U.S. Energy Information Administration, Emissions of Greenhouse Gases in the United States 2009, 2011.

4. http://en.wikipedia.org/wiki/Carbon_capture_and_storage

5. Johnson E. Goodbye to carbon neutral: Getting biomass footprints right. Environ Impact Asses. 2009; 29: 165-8.

6. Lemoine DM, Fuss S, Szolgayova, J, Obersteiner M, Kammen DM. The influence of negative emission technologies and technology policies on the optimal climate mitigation portfolio. Clim Chang. 2012; 113: 141-2.

7. Azar C, Lindgren K, Obersteiner M, Riahi K, van Vuuren DP, den Elzen, et al. The feasibility of low CO_2 concentration targets and the role of bio-energy with carbon capture and storage (BECCS). Clim Chang. 2010; 100: 195-2.

8. Kanniche M, Gros-Bonnivard R, Jaud P, Valle-Marcos J, Amann JM, Bouallou C. Pre-combustion, post-combustion and oxy-combustion in thermal power plant for CO_2 capture. Appl Therm Eng. 2010; 30: 53-2.

9. Li B, Duan Y, Luebke D, Morreale B. Advances in CO_2 capture technology: A patent review. Appl Energy. 2013; 102: 1439-7.

10. Wang Q, Luo J, Zhong Z, Borgna A. CO_2 capture by solid adsorbents and their applications: current status and new trends. Energ Environ Sci. 2011; 4: 42-5.

11. MacDowell N, Florin N, Buchard A, Hallett J, et al. An overview of CO_2 capture technologies. Energ Environ Sci. 2010; 3: 1645-9.

12. Manovic V, Anthony EJ. Lime-based sorbents for high-temperature CO_2 capture-a review of sorbent modification methods. Inter J Env Res Pub Heal. 2010; 7: 3129-0.

13. Liu W, An H, Qin C, Yin J, Wang G, et al. Performance enhancement of calcium oxide sorbents for cyclic CO_2 capture-a review. Energ Fuel. 2012; 26: 2751-7.

14. Yong Z, Mata V, Rodrigues AE. Adsorption of carbon dioxide at high temperature-a review. Sep Purif Technol. 2002; 26: 195-5.

15. Stanmore BR, Gilot P. Review-calcination and carbonation of limestone during thermal cycling for CO_2 sequestration. Fuel Process Technol. 2005; 86: 1707-3.

16. Weiss H. Rectisol wash for purification of partial oxidation gases. Gas Sep Purif. 1988; 2: 171-6.

17. http://www.co2crc.com.au/aboutccs/capture.html

18. Chen WH, Chen SM, Hung CI. Carbon dioxide capture by single droplet using Selexol, Rectisol and water as absorbents: A theoretical approach. Appl Energ. 2013; 111: 731-1.

19. http://en.wikipedia.org/wiki/Synthetic_fuel

20. Phillips J. Different types of gasifiers and their integration with gas turbines. Electric Power Research Institute. 2006.

21. Higman C, Van der Burgt M. Gasification. Gulf Professional Publishing. 2003.

22. Walker PL, Ruskino F, Austin LG. Gas reactions of carbon. Adv Catal. 1959; 11: 133-1.

23. Sudiro M, Bertucco A. Synthetic Natural Gas (SNG) from coal and biomass: a survey of existing process technologies, open issues and perspectives. In: Potocnik P, editor. Natural Gas, Rijeka: Sciyo; 2010, p.105-6.

24. Kopyscinski J, Schildhauer TJ, Biollaz S. Production of synthetic natural gas (SNG) from coal and dry biomass-A technology review from 1950 to 2009. Fuel. 2010; 89: 1763-3.

25. Mao X, Guo X, Chang Y, Peng Y. Improving air quality in large cities by substituting natural gas for coal in China: changing idea and incentive policy implications. Energ Policy. 2005; 33: 307-8.

26. Taoka N, Aoki T, Hanawa M, Onozaki M, Potential cases of coal-derived substitute natural gas to future Japanese market. In International Gas Union Research Conference 2008.

27. Hacatoglu K, McLellan PJ, Layzell DB. Production of bio-synthetic natural gas in Canada. Environ Sci Technol. 2010; 44: 2183-8.

28. Zwart RWR, Boerrigter H. High efficiency co-production of synthetic natural gas (SNG) and Fischer-Tropsch (FT) transportation fuels from biomass. Energ Fuel. 2005; 19: 591-7.

29. Bartone LM, White J. Industrial size gasification for syngas, substitute natural gas and power production. US DOE report (Report No.: DOE/NETL-401/040607).2007.

30. Lu XM, Norbeck JM, Park CS. Production of Fischer-Tropsch fuels and electricity from bituminous coal based on steam hydrogasification. Energy. 2012; 48: 525-1.

31. Swanson RM, Platon A, Satrio JA, Brown RC. Techno-economic analysis of biomass-to-liquids production based on gasification. Fuel. 2010; 89: S11-9.

32. Mantripragada HC, Rubin ES. Techno-economic evaluation of coal-to-liquids (CTL) plants with carbon capture and sequestration. Energ Policy. 2010; 39: 2808-6.

33. http://www.afdc.energy.gov/fuels/emerging_xtl_fuels.html

34. http://en.wikipedia.org/wiki/Fischer–Tropsch_process

35. Hamelinck CN, Faaij APC, Uil H, Boerrigter H. Production of FT transportation fuels from biomass; technical options, process analysis and optimisation, and development potential. Energy. 2004; 29: 1743-1.

36. Steynberg AP, Dry ME. Fischer-Tropsch Technology. Elsevier Science. 2004.

37. http://www.sasol.com/

38. Anastasi JL. Sasol: South Africa's oil from coal story-background for environmental assessment.US EPA report (Report No.: PB-80-148752). 1980.

39. De Klerk A. Fischer-Tropsch Refining. University of Pretoria. 2008.

40. Freide JJHMF, Gamlin TD, Hensman JR, Nay B, Sharp C. Development of a CO_2 tolerant Fischer-Tropsch catalyst: from laboratory to commercial-scale demonstration in Alaska. J. Nat. Gas Chem. 2004; 13: 1-9.

41. Lu Y, Lee T. Influence of the feed gas composition on the Fischer-Tropsch synthesis in commercial operations. J. Nat. Gas Chem. 2007; 16: 329-1.

42. Liu Y, Zhang CH, Wang Y, Li Y, Hao X, Bai L, etc. Effect of co-feeding carbon dioxide on Fischer-Tropsch synthesis over an iron-manganese catalyst in a spinning basket reactor. Fuel Process Technol. 2008; 89: 234-1.

43. Gnanamani MK, Shafer WD, Sparks DE, Davis BH. Fischer-Tropsch synthesis: Effect of CO_2 containing syngas over Pt promoted Co/γ-Al_2O_3 and K-promoted Fe catalysts. Catal. Commun. 2001; 12: 936-9.

44. Sudiro M, Bertucco A. Synthetic Natural Gas (SNG) from coal and biomass: a survey of existing process technologies, open issues and perspectives. In: Potocnik P, editor. Natural Gas, Rijeka: Sciyo; 2010, p.105-6.

45. Kopyscinski J, Schildhauer TJ, Biollaz S. Production of synthetic natural gas (SNG) from coal and dry biomass-A technology review from 1950 to 2009. Fuel. 2010; 89: 1763-3.

46.http://www.dakotagas.com/Miscellaneous/pdf/Safety_ByproductInfo/MSDS/Synthetic_Natural_Ga.pdf

47. http://www.docstoc.com/docs/73832821/Practical-Experience-Gained-During-the-First-Twenty-Years-of-Operation-of-the-Great-Plains-Gasifi-cation-Plant-and-Implications-for-Future-Projects

48. Jeon SK, Park CS, Hackett CE, Norbeck JM. Characteristics of steam hydrogasification of wood using a micro-batchreactor. Fuel. 2007; 86: 2817-3.

49. Raju ASK, Park CS, Norbeck JM. Synthesis gas production using steam hydrogasification and steam reforming. Fuel Process Technol. 2009; 90:330-6.

50. Jeon SK, Park CS, Kim SD, Song BH, Norbeck JM. Methane steam reforming for synthetic diesel fuel production from steam-hydrogasifier product gases. Korean J Chem Eng. 2008; 25: 1279-5.

51. Norbeck JM, Hackett CE. US patent application publication 20050032920A1.

52. Norbeck JM, Park CS. US patent application publication 7897649B2.

53. Norbeck JM, Park CS, Raju ASK. US patent application publication 20080021121A1.

54. Norbeck JM, Park CS, Raju ASK. US patent application publication 20110126458A1.

55. Lu XM. Development and application of advanced models for steam hydrogasification: process design and economic evaluation. University of California Riverside; 2012.

56. Rath L, Shelton W, Summers M, Winer J. Hydrogasification/F-T production with electricity & electricity only cases CERT-1 thru CERT-6, Conceptual Study. NETL Technical report (Report No.: DOE/NETL-401/CRADA). 2010.

57. He W, Park CS, Norbeck JM. Rheological study of comingled biomass and coal slurries with hydrothermal pretreatment. Energ Fuel. 2009; 23: 4763-7.

58. Park CS, Norbeck JM, He W. US patent application publication 20110162257A1.

59. Kim K, Park N. Removal of hydrogen sulfide from a steam-hydrogasifier product gas by zinc oxide sorbent: Effect of non-steam gas components. J Ind Eng Chem. 2010; 16: 967-2.

60. Kim K, Park N. Effect of non-steam component of steam-hydrogasifier product gas upon sulfidation of zinc oxide sorbent. Korean J Chem Eng. 2010; 27: 1715-7.

61. Kim K, Jeon SK, Vo C, Park CS, Norbeck JM. Removal of hydrogen sulfide from a steam-hydrogasifier product gas by zinc oxide sorbent. Ind Eng Chem Res. 2007; 46: 5848-4.

62. Luo Q. The development of warm gas cleanup technologies for the removal of sulfur containing species from steam hydrogasification. University of California Riverside; 2012.

63. Shah PP, Sturtvant GC, Gregor JH, Humbach MJ, Padrta FG, Steigleder KZ. Fischer–Tropsch wax characterization and upgrading: final report. US DOE report (Report No.: DOE/PC/80017-T1). 1998.

64. Selow ER, Cobden PD, Van den Brink RW, Hufton JR, Wright A. Carbon capture by sorption-enhanced water-gas shift reaction process using hydrotalcite-based material. Ind Eng Chem Res. 2009; 48: 4184-3.

65. Muller CR, Pacciani R, Bohn CD, Scott SA, Dennis JS. Investigation of the enhanced water gas shift reaction using natural and synthetic sorbents for the capture of CO_2. Ind Eng Chem Res. 2009; 48: 102841-1.

66. Bretado MAE, Vigil MDD, Gutierrez JS, Ortiz AL, Martinez VC. Hydrogen production by absorption enhanced water gas shift (AEWGS). Int J Hydrogen Energ. 2010; 35: 12083-0.

67. Ortiz AL, Harrison DP. Hydrogen production using sorption-enhanced reaction. Ind Eng Chem Res. 2001; 40: 5102-9.

68. Yi KB, Harrison DP. Low-pressure sorption-enhanced hydrogen production. Ind Eng Chem Res. 2005; 44: 1665-9.

69. He L, Berntsen H, Chen D. Approaching sustainable H_2 production: sorption enhanced steam reforming of ethanol. J Phys Chem A.2010; 114: 3834-4.

70. Chen ZX, Grace JR, Lim CJ. CO_2 capture and hydrogen production in an integrated fluidized bed reformer-regenerator system. Ind Eng Chem Res. 2011; 50: 4716-1.

71. Li ZS, Cai NS, Yang JB. Continuous production of hydrogen from sorption-enhanced steam methane reforming in two parallel fixed-bed reactors operated in a cyclic manner. Ind Eng Chem Res. 2006; 45: 8788-3.

72. Barelli L, Bidini G, Gallorini F, Servili S. Hydrogen production through sorption-enhanced steam methane reforming and membrane technology: A review. Energy. 2008; 33: 554-0.

73. Hildenbrand N, Readman J, Dahl IM, Blom R. Sorbent enhanced steam reforming (SESR) of methane using dolomite as internal carbon dioxide absorbent: Limitations due to $Ca(OH)_2$ formation. Appl Catal A-Gen. 2006; 303: 131-7.

74. Johnsen K, Ryu HJ, Grace JR, Lim CJ. Sorption-enhanced steam reforming of methane in a fluidized bed reactor with dolomite as CO_2-acceptor. Chem Eng Sci. 2006; 61: 1195-2.

75. Cobden PD, van Beurden P, Reijers HThJ, Elzinga GD, Kluiters SCA, Dijkstra JW, et al. Sorption-enhanced hydrogen production for pre-combustion CO_2 capture: Thermodynamic analysis and experimental results. Int J Greenh Gas Con. 2007; 1: 170-9.

76. Florin NH, Harris AT. Enhanced hydrogen production from biomass with in situ carbon dioxide capture using calcium oxide sorbents. Chem Eng Sci. 2008; 63: 287-6.

77. Qiao CZ, Xiao YH, Xu X, Zhao LF, Tian WD. Comparative analysis of hydrogen production systems from biomass based on different absorbent regeneration processes. Int J Hydrogen Energ. 2007; 32: 80-5.

78. Widyawati M, Church TL, Florin NH, Harris AT. Hydrogen synthesis from biomass pyrolysis with in situ carbon dioxide capture using calcium oxide. Int J Hydrogen Energ. 2011; 36: 4800-3.

79. Han L, Wang QH, Yang YK, Yu CJ, Fang MX, Luo ZY. Hydrogen production via CaO sorption enhanced anaerobic gasification of sawdust in a bubbling fluidized bed. Int J Hydrogen Energ. 2011; 36: 4820-9.

80. Acharya B, DuttaA, Basu P. An investigation into steam gasification of biomass for hydrogen enriched gas production in presence of CaO. Int J Hydrogen Energ. 2010; 35: 1582-9.

81. Koji K, Takeshi F, Yoshizo S, Hiroyuki H, Kazuhiro K, Ryo Y, et al. Coal gasification with a subcritical steam in the presence of a CO_2 sorbent: products and conversion under transient heating. Fuel Process Technol. 2003; 82: 61-3.

82. Mahishi MR, Sadrameli MS, Vijayaraghavan S, Goswami DY. A novel approach to enhance the hydrogen yield of biomass gasification using CO_2 sorbent. J Eng Gas Turb Power. 2008; 130: 1-8.

83. Soukup G, Pfeifer C, Kreuzeder A, Hofbauer H. In situ CO_2 capture in a dual fluidized bed biomass steam gasifier-bed material and fuel variation. Chem Eng Technol. 2009; 32: 348-4.

84. Toshiaki H, Takahiro Y, Shinji F, Kenji K,Michiaki H, Yoshizo S, et al. Hydrogen production from woody biomass by steam gasification using a CO_2 sorbent. Biomass Bioenerg. 2005; 28: 63-8.

85. Wei LG, Xu SP, Liu JG, Liu CG, Liu SQ. Hydrogen production in steam gasification of biomass with CaO as a CO_2 absorbent. Energ Fuel. 2008; 22: 1997-4.

86. Corujo A, Yerman L, Arizaga B, Brusoni M, Castiglioni J. Improved yield parameters in catalytic steam gasification of forestry residue; optimizing biomass feed rate and catalyst type. Biomass Bioenerg. 2010; 34: 1695-2.

87. Dou BL, Rickett GL, Dupont V, Williams PT, Chen HS, Ding YL, et al. Steam reforming of crude glycerol with in situ CO_2 sorption. Bioresource Technol. 2010; 101: 2436-2.

88. Hu GX, Huang H. Hydrogen rich fuel gas production by gasification of wet biomass using a CO_2 sorbent. Biomass Bioenerg. 2009; 33: 899-6.

89. Fermoso J, He L, Chen D. Production of high purity hydrogen by sorption enhanced steam reforming of crude glycerol. Int J Hydrogen Energ. 2012; 37: 14047-4.

90. Felice LD, Courson C, Jand N, Gallucci K, Foscolo PU, Kiennemann A. Catalytic biomass gasification: Simultaneous hydrocarbons steam reforming and CO_2 capture in a fluidised bed reactor. Chem Eng J. 2009; 154: 375-3.

91. Zhao M, Yang XS, Church TL, Harris AT. Interaction between a bimetallic Ni-Co catalyst and micrometer-sized CaO for enhanced H_2 production during cellulose decomposition. Int J Hydrogen Energ. 2011; 36: 421-1.

92. Satrio JA, Shanks BH, Wheelock TD. A combined catalyst and sorbent for enhancing hydrogen production from coal or biomass. Energ Fuel. 2007; 21: 322-6.

93. Mondal K, Piotrowski K, Dasgupta D, Hippo E, Wiltowski T. Hydrogen from coal in a single step. Ind Eng Chem Res. 2005; 44: 5508-7.

94. Guan YW, Luo SY, Liu SM, Xiao B, Cai L. Steam catalytic gasification of municipal solid waste for producing tar-free fuel gas. Int J Hydrogen Energ. 2009; 34: 9341-6.

95. Garcia XA, Alarcon NA, Gordon AL. Steam gasification of tars using a CaO catalyst. Fuel Process Technol. 1999; 58: 83-2.

96. Orio A, Corella J, Narvaez I. Performance of different dolomites on hot raw gas cleaning from biomass gasification with air. Ind Eng Chem Res. 1997; 36: 3800-8.

97. Corella J, Toledo JM, Padilla R. Olivine or dolomite as in-bed additive in biomass gasification with air in a fluidized bed: Which is better?. Energ Fuel. 2004; 18: 713-0.

98. Delgado J, Aznar MP. Biomass gasification with steam in fluidized bed: Effectiveness of CaO, MgO, and CaO-MgO for hot raw gas cleaning. Ind Eng Chem Res. 1997; 36: 1535-3.

99. Ansari AA, Singh GS, Lanza GR, Rast W. Eutrophication: causes, consequences and control. Springer; 2011.

100. Dymond JH, Marsh KN, Wilhoit RC. Virial coefficients of pure gases and mixtures. 1st ed. Springer; 2003.

101. Sun P, Grace JR, Lim CJ, Anthony EJ. Co-capture of H_2S and CO_2 in a pressurized-gasifier-based process. Energ Fuel. 2007; 21: 836-4.

102. Roberts DG, Harris DJ. A kinetic analysis of coal char gasification reactions at high pressures. Energ Fuel. 2006; 20: 2314-0.

103. Yang H, Chen H, Ju F, Yan R, Zhang S. Influence of pressure on coal pyrolysis and char gasification. Energ Fuel. 2007; 21: 3165-0.

104. Schmal M, Monteiro JLF, Castellan JL. Kinetics of coal gasification. Ind Eng Chem Process Des Dev. 1982; 21, 256-6.

105. Senneca O. Kinetics of pyrolysis, combustion and gasification of three biomass fuels. Fuel Process Technol. 2007; 88: 87-7.

106. Piatkowski N, Steinfeld A. Reaction kinetics of the combined pyrolysis and steam-gasification of carbonaceous waste materials. Fuel. 2010; 89: 1133-0.

107. Fushimi C, Araki K, Yamaguchi Y, Tsutsumi A. Effect of heating rate on steam gasification of biomass. 1. Reactivity of char. Ind Eng Chem Res. 2003; 42: 3922-8.

108. Barneto AG, CArmona JA, Conesa JA. Effects of the composting and the heating rate on biomass gasification. Energ Fuel. 2008; 23: 951-7.

109. Hüttinger KJ. Mechanism of water vapor gasification at high hydrogen levels. Carbon. 1988; 26: 79-7.

110. Gao C, Vejahati F, Katalambula H, Gupta R. Co-gasification of biomass with coal and oil sand coke in a drop tube furnace. Energ Fuel. 2009; 24: 232-0.

111. Fujimoto S, Yoshida T, Hanaoka T, Matsumura Y, Lin SY, Minowa T, Sasaki Y. A kinetic study of in situ CO_2 removal gasification of woody biomass for hydrogen production. Biomass Bioenerg. 2007; 31: 556-2.

112. Valkenburg C. Products and reaction kinetics using steam hydrogasification of various carbonaceous feedstocks. University of California Riverside; 2006.

113. Patel MJ. Design of an inverted reactor for studying the kinetics of the steam hydrogasification reaction. University of California Riverside; 2009.

114. http://www.thinksrs.com/downloads/PDFs/Manuals/RGAm.pdf

115. http://en.wikipedia.org/wiki/Hagen–Poiseuille_equation

116. Jüntgen H. Reactivities of carbon to steam and hydrogen and applications to technical gasification processes—A review. Carbon. 1981; 19: 167-3.

117. Encinar JM, Beltrán FJ, González JF, Moreno MJ. Pyrolysis of maize, sunflower, grape and tobacco residues. J. Chem. Technol. Biotechnol. 1997; 70: 400-0.

118. Yun MY, Bae DH, Park CS, Norbek JM. Development of circulating fluidized bed reactor for the steam hydrogasification of low ranked fuel. US-Korea Conference on Science, Technology and Entrepreneurship. 2012.

119. Spath PL, Dayton DC. Preliminary screening-technical and economic assessment of synthesis gas to fuels and chemicals with emphasis on the potential for biomass-derived syngas. NREL report (Report No.: NREL/TP-510-34929). 2003.

120. Werner S. Ultra-Low Temperature Water-Gas Shift Reaction with Supported Ionic Liquid Phase (SILP). Friedrich-Alexander-Universität Erlangen-Nürnberg. 2011.

121. Callaghan CA. Kinetics and catalysis of the water-gas-shift reaction: A microkinetic and graph theoretic approach. Worcester Polytechnic Institute. 2006.

122. Heyne S, Seemann M, Harvey S. Integration study for alternative methanation technologies for the production of synthetic natural gas from gasified biomass. In Chemical Engineering Transactions. 13th International Conference on Process Integration, PRES 2010; 21: 409-4.

123. Humphries KJ, Yarwood, TA. US Patent No. 3511624.

124. Rostrup-Nielsen JR, Pedersen K, Sehested J. High temperature methanation: Sintering and structure sensitivity. Appl. Catal., A. 2007; 330: 134-8.

125. Bader A, Bauersfeld S, Brunhuber C, Pardemann R, Meyer B, Siemens AG. Modelling of a chemical reactor for simulation of a methanisation plant. In Proceedings of the 8th International Modelica Conference, Dresden, Germany, March. 2011.

126. Klassen M. White paper on natural gas interchangeabiliy and non-combustion end use. NGC+Interchangeability Work Group. 2005.